Electronic Supplementary Material (ESI) for ChemComm.

Supplementary Information

Increasing the membrane permeability of carboxylic acid-containing drugs using synthetic transmembrane anion transporters

Rayhanus Salam, Surid Mohammad Chowdhury, Sarah R. Marshall, Hassan Gneid, Nathalie Busschaert*

Department of Chemistry, Tulane University, New Orleans, LA, United States

E-mail: nbusschaert@tulane.edu

Table of Contents

S1. General

Fluorescence spectra and kinetic studies were performed on an Agilent Cary Eclipse fluorescence spectrophotometer equipped with stirring function and Peltier temperature controller. 3 mL macrocuvettes (quartz or glass) were used and all solutions were stirred using a cuvette stir bar (Sigma-Aldrich #Z363545). HPLC traces were collected on a Thermo Fisher Scientific Vanquish Flex UHPLC with variable wavelength detector, using a Hypersil GOLD C18 column (150 mm length, 3.0 mm diameter, 3 µm particle size). Solvents, reagents, inorganic salt (NaCl, $NaNO_3$, K_2SO_4) and sodium salts of some drugs (carbenicillin, diatrizoate, diclofenac, ibuprofen, naproxen, penicillin G, sodium salicylate) were used as provided by the supplier. Ketorolac was used as the Tris salt, as provided by the supplier. Other drugs (amoxicillin, aspirin, bezafibrate, furosemide, gemfibrozil, ketoprofen, ramipril, valsartan) were converted to their sodium salt from the carboxylic acid by adding 1 equivalent NaOH to an aqueous solution of the acid, followed by lyophilization. For the valinomycin mediated uniport assay, potassium salicylate salt was prepared from salicylic acid and KOH. Buffers were prepared using fresh UltraPure water.

S2. Fluorescence quenching of lucigenin by carboxylate drugs

To a solution of 0.8 µM lucigenin in nitrate buffer (222 mM $NaNO_3$, 10 mM HEPES, pH 7.4), was added the sodium salt of the carboxylate drugs at various concentrations. The fluorescence spectrum (excitation 430 nm) was measured before and after the addition of the drug. The spectra were normalized by dividing the fluorescence intensity at any wavelength by the fluorescence intensity at 505 nm before the addition of drug. For the Stern-Volmer constant, the F_0/F value at 505 nm was calculated and plotted against the drug concentration. The Stern-Volmer constant, K_{SV}, is given by the slope of the linear fit (the intercept is fixed at a value of 1). The experiments were performed in triplicate and the results are shown in **Figure S1-Figure S19.** All drugs gave a good linear correlation ($R^2 > 0.99$).

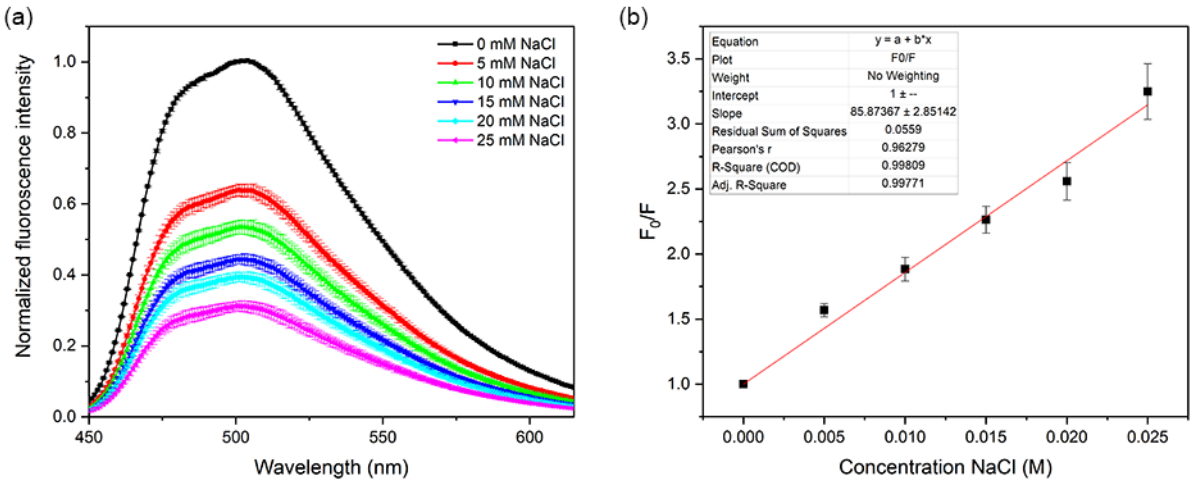

Figure S1. (a) Normalized fluorescence spectra of lucigenin in the presence of various concentrations of NaCl. The excitation wavelength was 430 nm. (b) Stern-Volmer plot of the quenching of lucigenin by various concentrations NaCl. Linear fits were performed for the range 0 – 0.025 M NaCl. Results are the average of 3 repeats and error bars represent standard deviations.

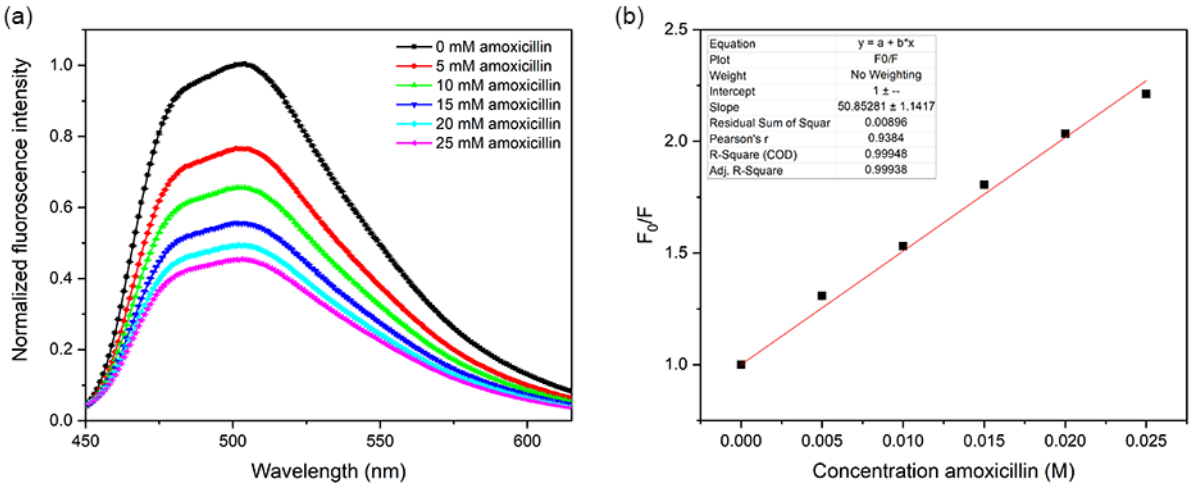

Figure S2. (a) Normalized fluorescence spectra of lucigenin in the presence of various concentrations of amoxicillin sodium. The excitation wavelength was 430 nm. (b) Stern-Volmer plot of the quenching of lucigenin by various concentrations amoxicillin sodium. Linear fits were performed for the range 0 – 0.025 M amoxicillin sodium. Results are the average of 3 repeats and error bars represent standard deviations.

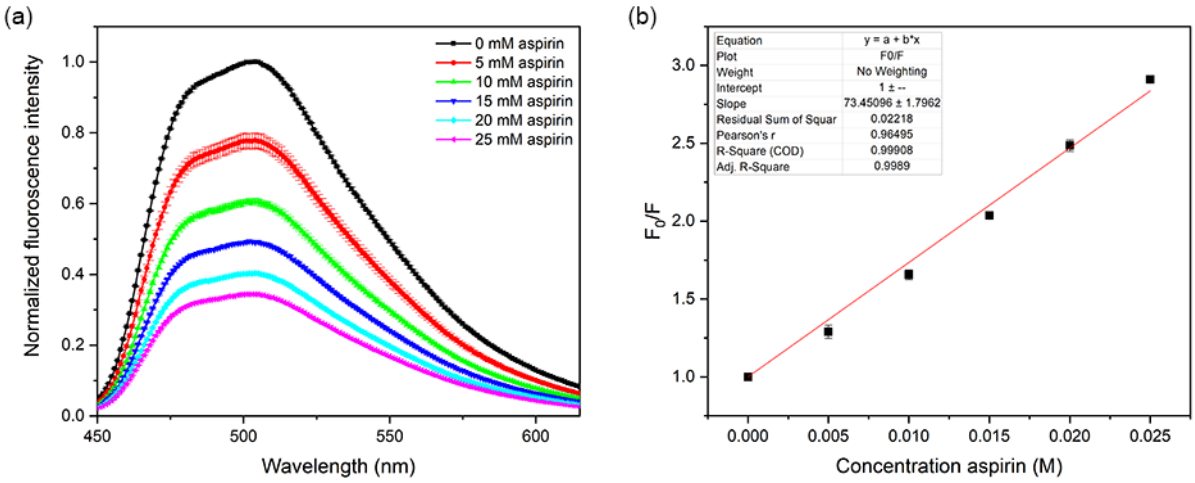

Figure S3. (a) Normalized fluorescence spectra of lucigenin in the presence of various concentrations of aspirin sodium. The excitation wavelength was 430 nm. (b) Stern-Volmer plot of the quenching of lucigenin by various concentrations aspirin sodium. Linear fits were performed for the range 0 – 0.025 M aspirin sodium. Results are the average of 3 repeats and error bars represent standard deviations.

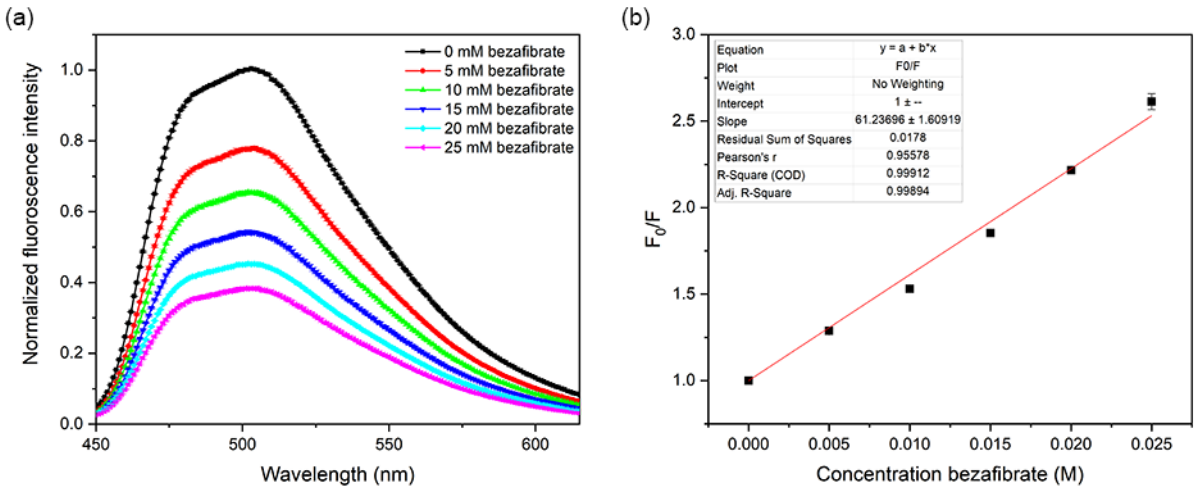

Figure S4. (a) Normalized fluorescence spectra of lucigenin in the presence of various concentrations of bezafibrate sodium. The excitation wavelength was 430 nm. (b) Stern-Volmer plot of the quenching of lucigenin by various concentrations bezafibrate sodium. Linear fits were performed for the range 0 – 0.025 M bezafibrate sodium. Results are the average of 3 repeats and error bars represent standard deviations.

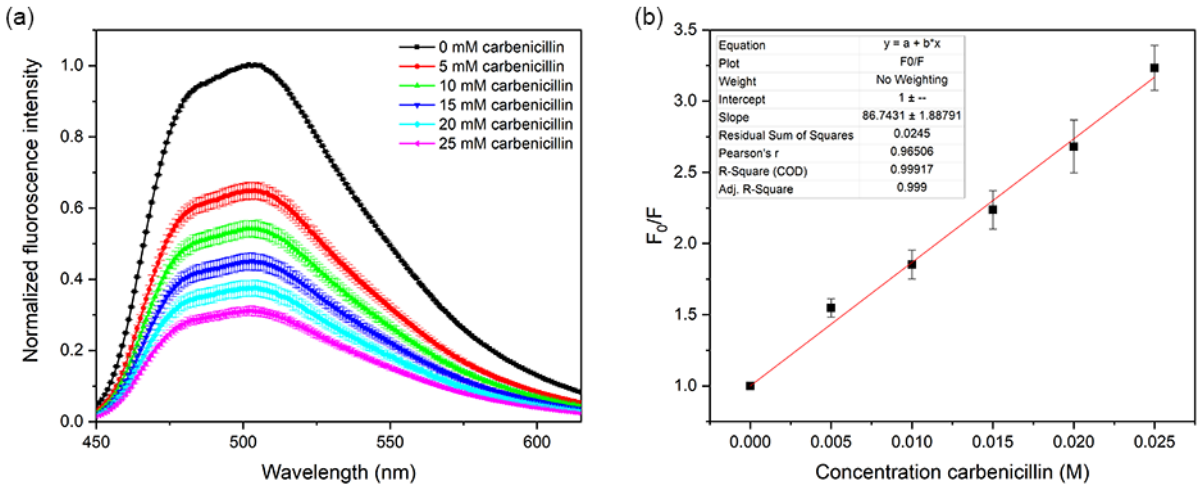

Figure S5. (a) Normalized fluorescence spectra of lucigenin in the presence of various concentrations of carbenicillin sodium. The excitation wavelength was 430 nm. (b) Stern-Volmer plot of the quenching of lucigenin by various concentrations carbenicillin sodium. Linear fits were performed for the range 0 – 0.025 M carbenicillin sodium. Results are the average of 3 repeats and error bars represent standard deviations.

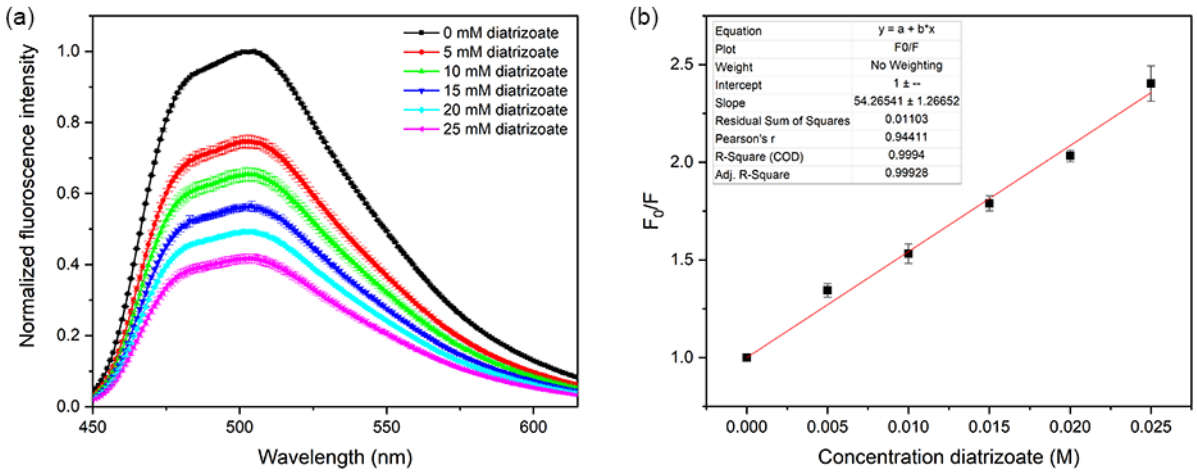

Figure S6. (a) Normalized fluorescence spectra of lucigenin in the presence of various concentrations of sodium diatrizoate. The excitation wavelength was 430 nm. (b) Stern-Volmer plot of the quenching of lucigenin by various concentrations sodium diatrizoate. Linear fits were performed for the range 0 – 0.025 M sodium diatrizoate. Results are the average of 3 repeats and error bars represent standard deviations.

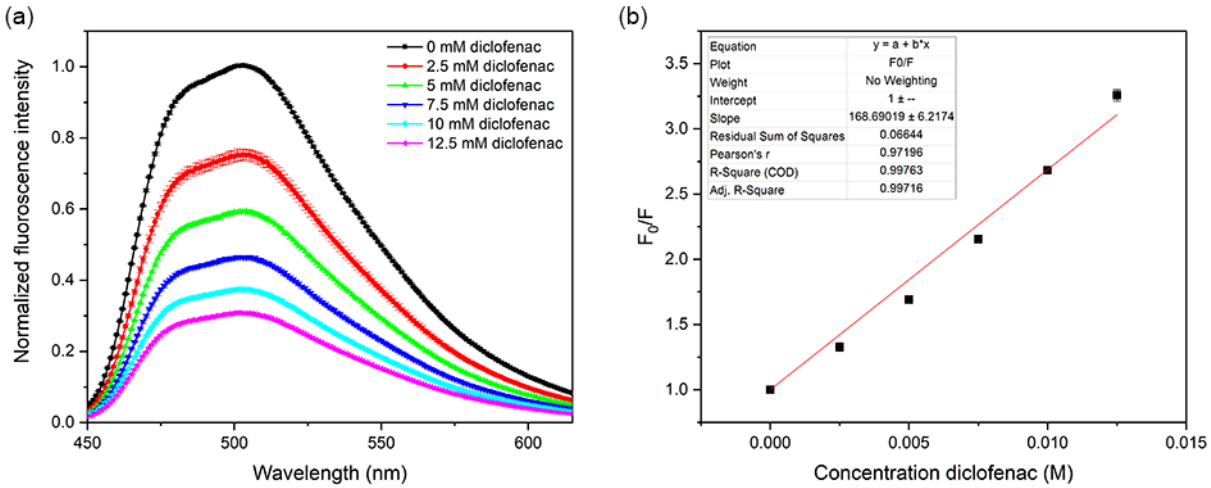

Figure S7. (a) Normalized fluorescence spectra of lucigenin in the presence of various concentrations of diclofenac sodium. The excitation wavelength was 430 nm. (b) Stern-Volmer plot of the quenching of lucigenin by various concentrations diclofenac sodium. Linear fits were performed for the range 0 – 0.0125 M diclofenac sodium. Results are the average of 3 repeats and error bars represent standard deviations.

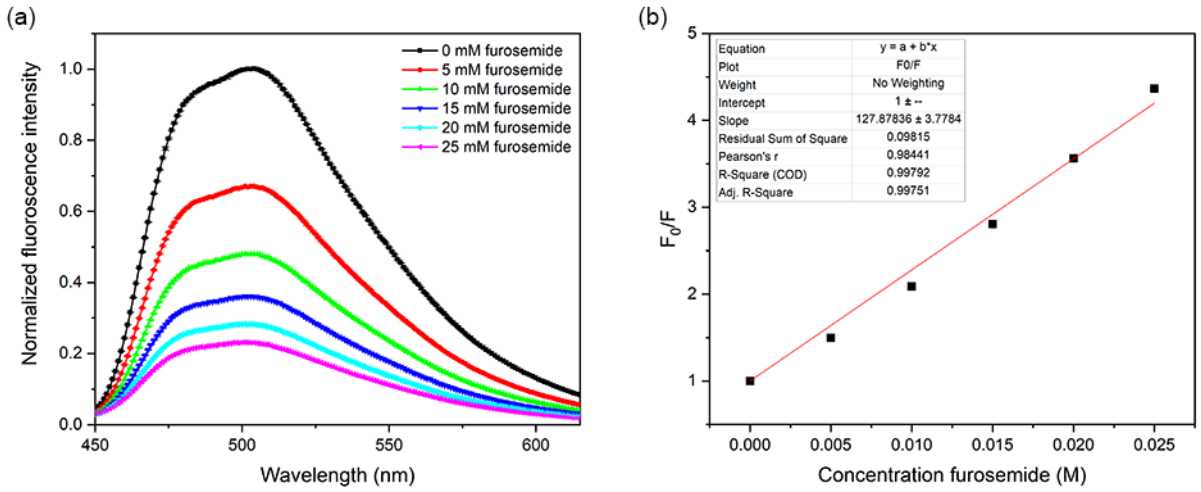

Figure S8. (a) Normalized fluorescence spectra of lucigenin in the presence of various concentrations of furosemide sodium. The excitation wavelength was 430 nm. (b) Stern-Volmer plot of the quenching of lucigenin by various concentrations furosemide sodium. Linear fits were performed for the range 0 – 0.025 M furosemide sodium. Results are the average of 3 repeats and error bars represent standard deviations.

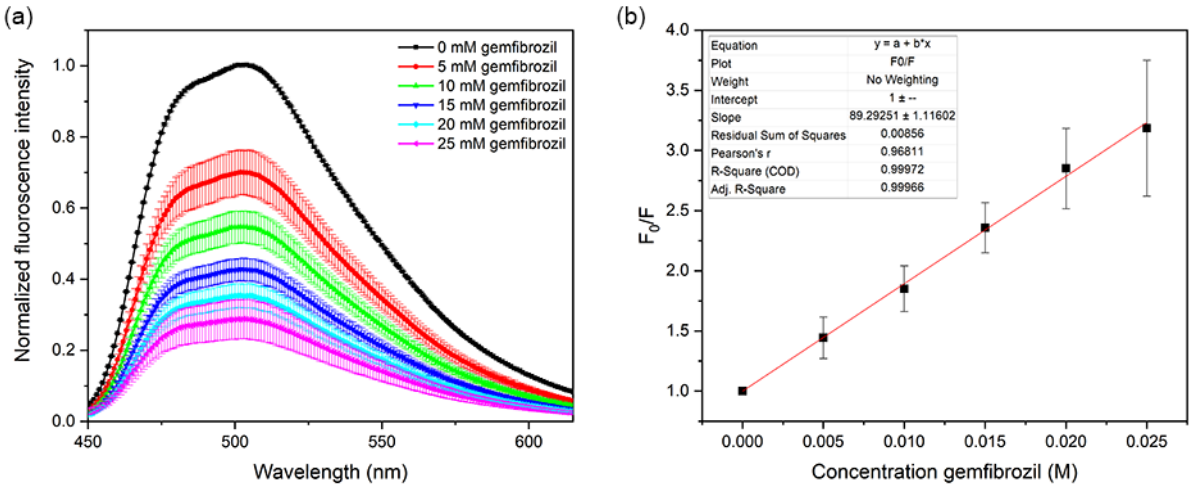

Figure S9. (a) Normalized fluorescence spectra of lucigenin in the presence of various concentrations of gemfibrozil sodium. The excitation wavelength was 430 nm. (b) Stern-Volmer plot of the quenching of lucigenin by various concentrations gemfibrozil sodium. Linear fits were performed for the range 0 – 0.025 M gemfibrozil sodium. Results are the average of 3 repeats and error bars represent standard deviations.

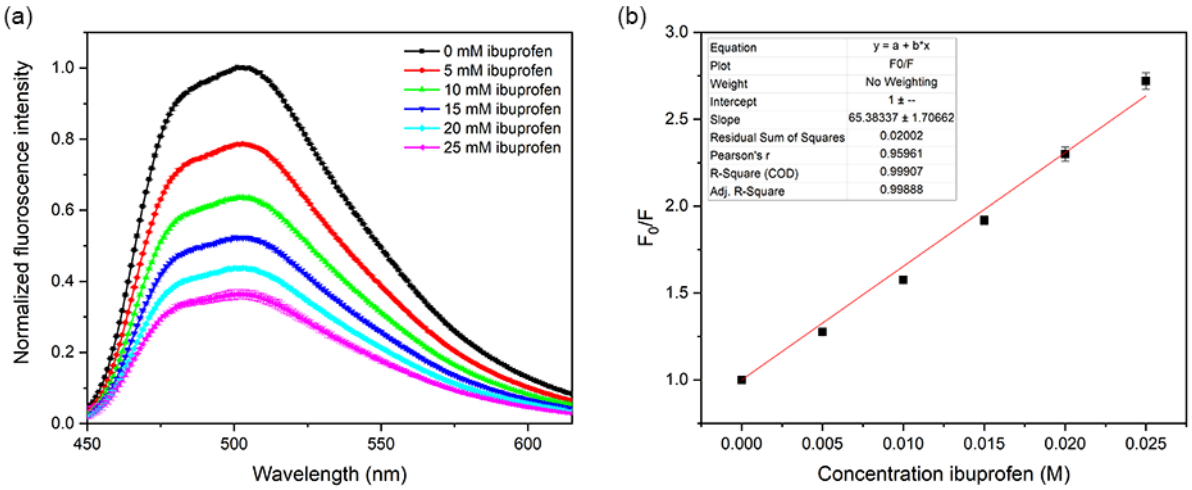

Figure S10. (a) Normalized fluorescence spectra of lucigenin in the presence of various concentrations of ibuprofen sodium. The excitation wavelength was 430 nm. (b) Stern-Volmer plot of the quenching of lucigenin by various concentrations ibuprofen sodium. Linear fits were performed for the range 0 – 0.025 M ibuprofen sodium. Results are the average of 3 repeats and error bars represent standard deviations.

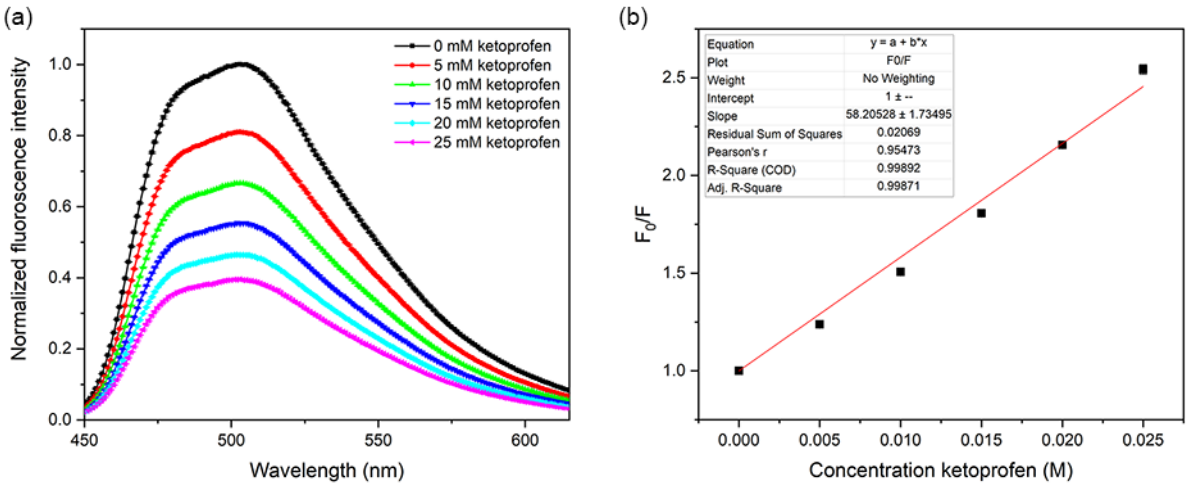

Figure S11. (a) Normalized fluorescence spectra of lucigenin in the presence of various concentrations of ketoprofen sodium. The excitation wavelength was 430 nm. (b) Stern-Volmer plot of the quenching of lucigenin by various concentrations ketoprofen sodium. Linear fits were performed for the range 0 – 0.025 M ketoprofen sodium. Results are the average of 3 repeats and error bars represent standard deviations.

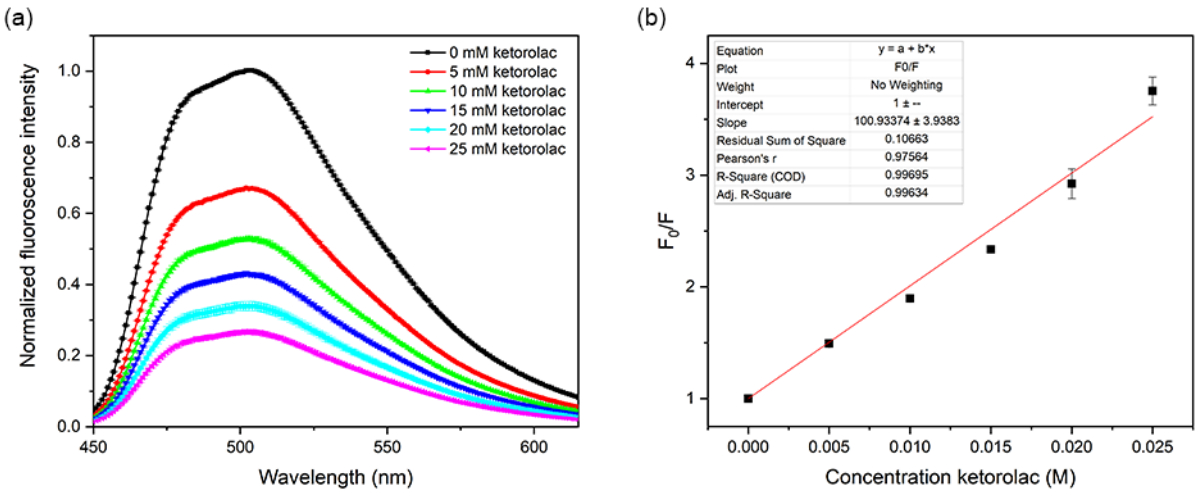

Figure S12. (a) Normalized fluorescence spectra of lucigenin in the presence of various concentrations of ketorolac tris salt. The excitation wavelength was 430 nm. (b) Stern-Volmer plot of the quenching of lucigenin by various concentrations ketorolac tris salt. Linear fits were performed for the range 0 – 0.025 M ketorolac tris salt. Results are the average of 3 repeats and error bars represent standard deviations.

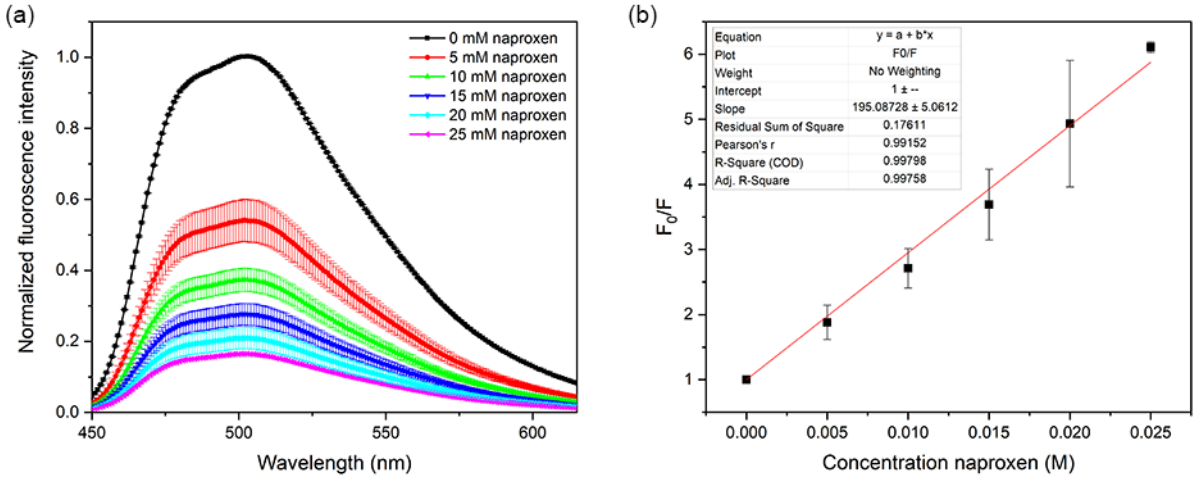

Figure S13. (a) Normalized fluorescence spectra of lucigenin in the presence of various concentrations of naproxen sodium. The excitation wavelength was 430 nm. (b) Stern-Volmer plot of the quenching of lucigenin by various concentrations naproxen sodium. Linear fits were performed for the range 0 – 0.025 M naproxen sodium. Results are the average of 3 repeats and error bars represent standard deviations.

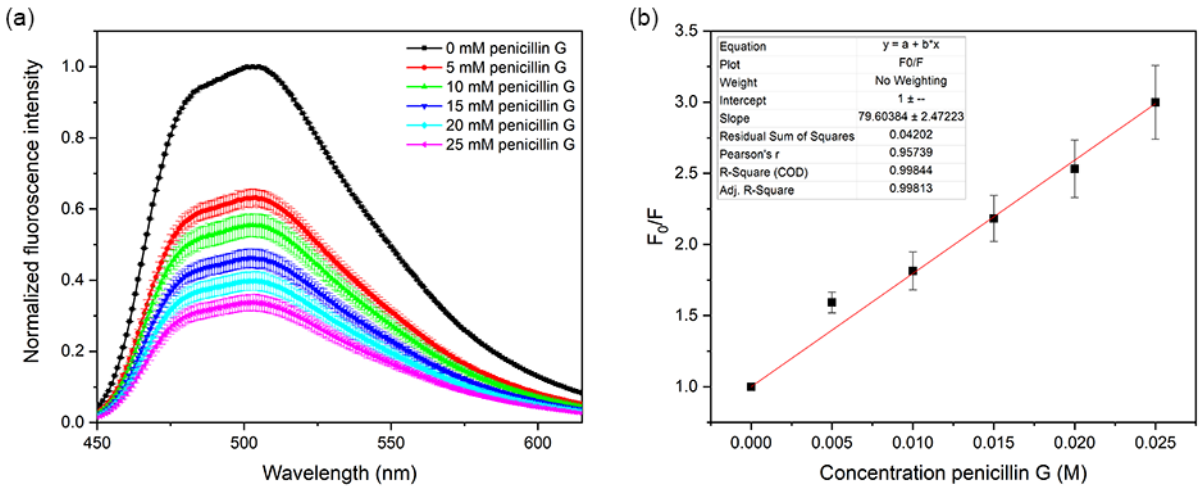

Figure S14. (a) Normalized fluorescence spectra of lucigenin in the presence of various concentrations of penicillin G sodium. The excitation wavelength was 430 nm. (b) Stern-Volmer plot of the quenching of lucigenin by various concentrations penicillin G sodium. Linear fits were performed for the range 0 – 0.025 M penicillin G sodium. Results are the average of 3 repeats and error bars represent standard deviations.

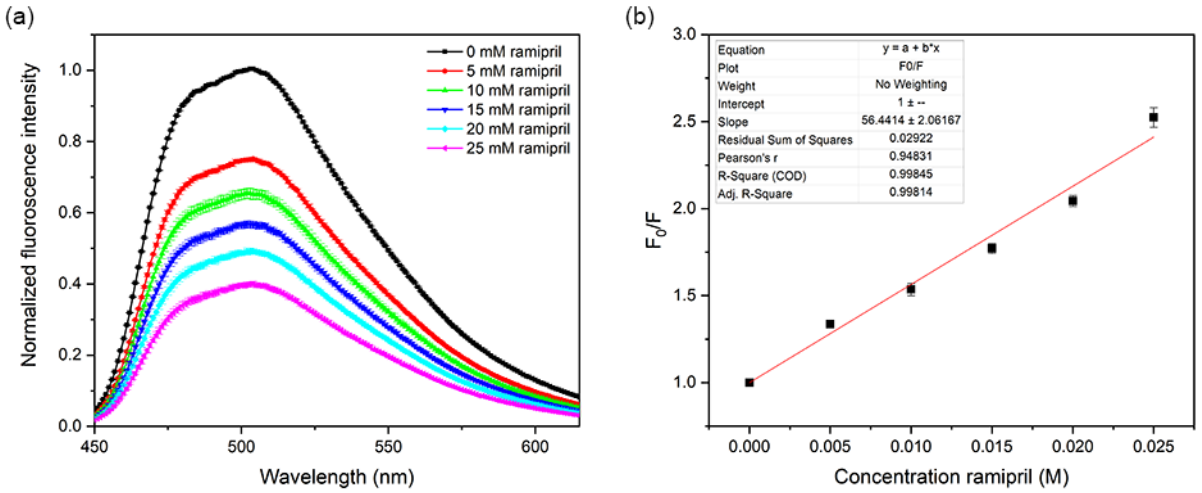

Figure S15. (a) Normalized fluorescence spectra of lucigenin in the presence of various concentrations of ramipril sodium. The excitation wavelength was 430 nm. (b) Stern-Volmer plot of the quenching of lucigenin by various concentrations ramipril sodium. Linear fits were performed for the range 0 – 0.025 M ramipril sodium. Results are the average of 3 repeats and error bars represent standard deviations.

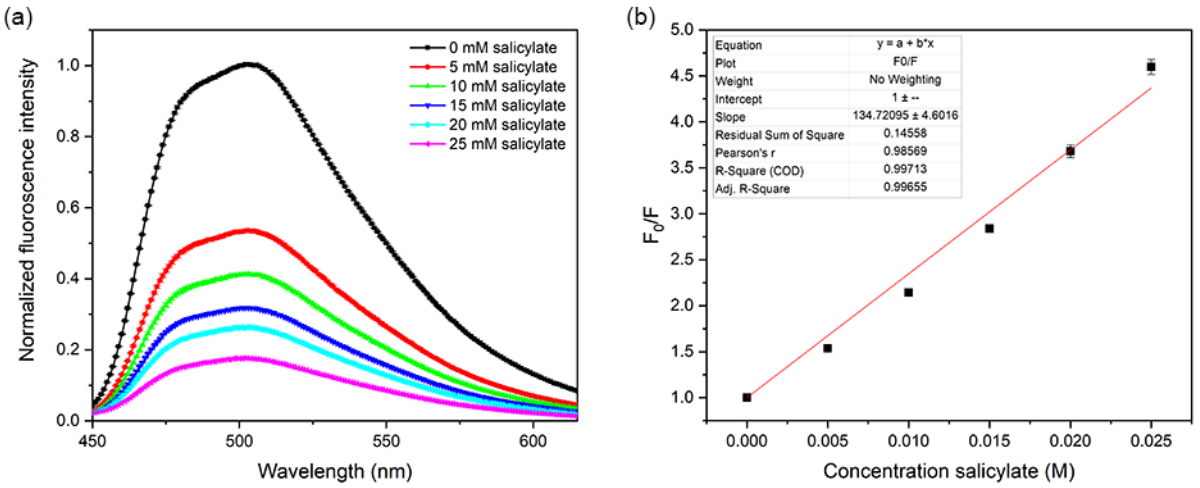

Figure S16. (a) Normalized fluorescence spectra of lucigenin in the presence of various concentrations of sodium salicylate. The excitation wavelength was 430 nm. (b) Stern-Volmer plot of the quenching of lucigenin by various concentrations sodium salicylate. Linear fits were performed for the range 0 – 0.025 M sodium salicylate. Results are the average of 3 repeats and error bars represent standard deviations.

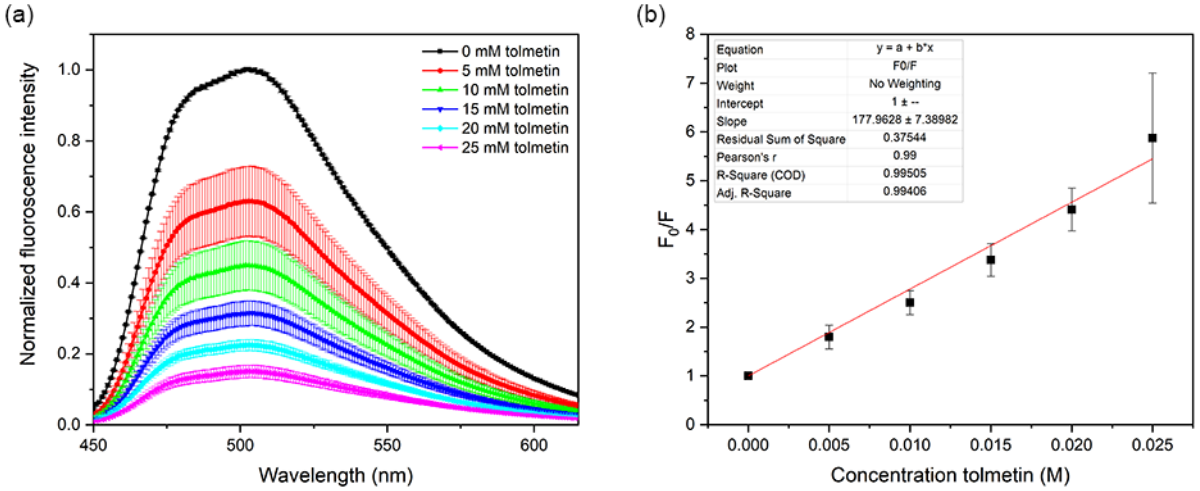

Figure S17. (a) Normalized fluorescence spectra of lucigenin in the presence of various concentrations of tolmetin sodium. The excitation wavelength was 430 nm. (b) Stern-Volmer plot of the quenching of lucigenin by various concentrations tolmetin sodium. Linear fits were performed for the range 0 – 0.025 M tolmetin sodium. Results are the average of 3 repeats and error bars represent standard deviations.

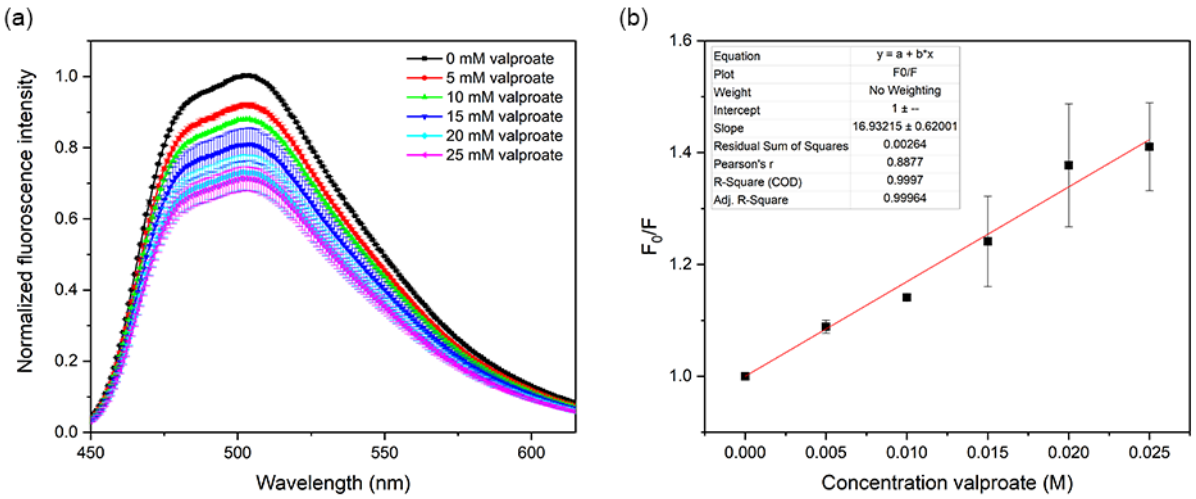

Figure S18. (A) Normalized fluorescence spectra of lucigenin in the presence of various concentrations of sodium valproate. The excitation wavelength was 430 nm. (B) Stern-Volmer plot of the quenching of lucigenin by various concentrations sodium valproate. Linear fits were performed for the range 0 – 0.025 M sodium valproate. Results are the average of 3 repeats and error bars represent standard deviations.

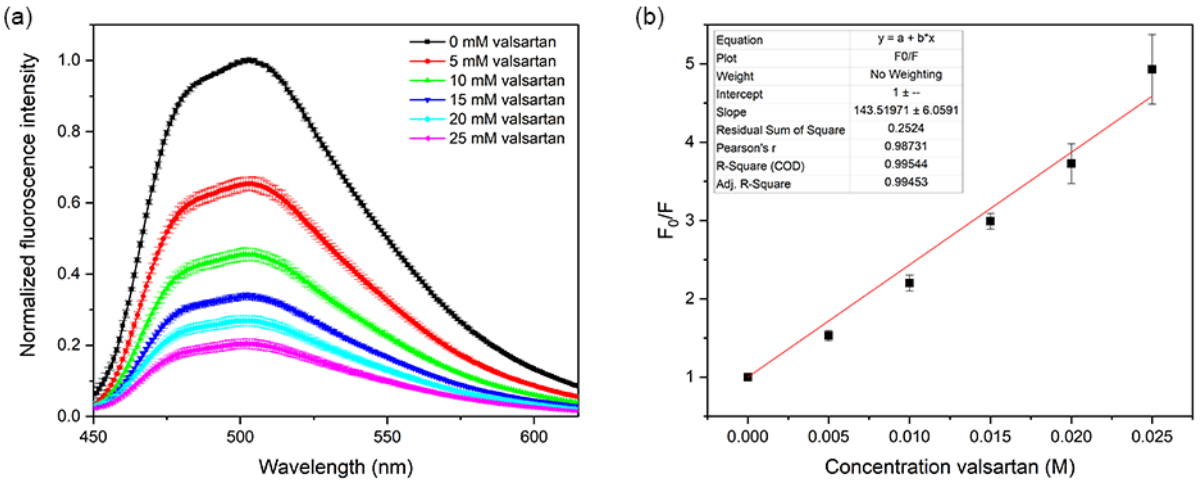

Figure S19. (a) Normalized fluorescence spectra of lucigenin in the presence of various concentrations of valsartan sodium. The excitation wavelength was 430 nm. (b) Stern-Volmer plot of the quenching of lucigenin by various concentrations valsartan sodium. Linear fits were performed for the range 0 – 0.025 M valsartan sodium. Results are the average of 3 repeats and error bars represent standard deviations.

S3. Kinetic drug permeability assay

The procedures for the various membrane transport assays mentioned in the article are described. The experiments are analogous to the standard lucigenin-based assay for transmembrane chloride transport.[1] EggPC (egg (chicken) phosphatidylcholine) was obtained from *Avanti Polar Lipids, Inc*. (catalog# 840051) and cholesterol was obtained from *VWR Life Science* (MDL# MFCD00003646). A combination of 70% eggPC and 30% cholesterol was used to mimic mammalian membrane composition.[2-4] The lipids were stored as a solution in chloroform at -20°C (28.63 mM eggPC and 12.27 mM cholesterol for a 7:3 mixture). Buffer was prepared with fresh UltraPure water following a recipe calculated using an online tool (https://www.biomol.net/en/tools/buffercalculator.htm) for a 10 mM HEPES buffer, pH 7.4, 25 ^{o}C, with an ionic strength of 225 mM. All drugs were used as sodium salt; either provided by the manufacturer or prepared by adding 1 equivalent NaOH to the carboxylic acid. Other salts and reagents were used as provided by the manufacturer. Stock solutions of transporters **1-5** were made in DMF at 400x the final concentration for the transport assay. Stock solutions of the analytes (drugs and NaCl) were prepared as 75 mM stock solutions in buffer; except amoxicillin sodium, furosemide sodium, ramipril sodium and valsartan sodium, which were prepared in 50 mM stock solutions for solubility reasons; and diclofenac and gemfibrozil, which were prepared in 25 mM stock solutions due to their low solubility. The pH of these drug stock solutions was adjusted to pH 7.4, if necessary, to avoid creating transmembrane pH gradients during the experiments. The kinetic assays were performed on an Agilent Cary Eclipse fluorometer using an excitation wavelength of 430 nm and emission wavelength of 505 nm.

S3.1. Preparation of large unilamellar vesicles

An aliquot of the lipid stock solution in chloroform was transferred to a small round bottom flask and dried via rotary evaporation. The lipid film was dried further on high vacuum for at least 5 hours prior to use. The lipid film was hydrated with the internal solution (1 mM lucigenin, 222 mM $NaNO_3$, 10 mM HEPES buffer at pH 7.4) and vortexed for about 5 minutes. The resulting suspension was subjected to seven freeze-thaw cycles, alternating between submersion in liquid nitrogen followed by thawing in mildly warm water (below 32 °C). The lipid suspension was allowed to rest at room temperature for 30 minutes before extruding 27 times through a 100 nm polycarbonate membrane (*Nucleopore*) using the Avanti mini extruder set (*Avanti Polar Lipids, Inc*.). The resulting uniform large unilamellar vesicles (LUVs) were separated from the unencapsulated lucigenin by size exclusion chromatography using a Sephadex column (G-50, medium). The obtained concentrated stock liposome solution was diluted in external buffer (222 mM $NaNO_3$, 10 mM HEPES buffer at pH 7.4) to afford a final total lipid concentration of 0.75 mM (1 mM stock total lipid solutions were used for experiments with low solubility drugs).

S3.2. Drug transport kinetic assays

1.0 mL of lucigenin-loaded liposomes (0.75 mM total lipid) were transferred to a 3 mL fluorescence cuvette and a small cuvette stir bar was added. A 3D printed block (9.5 mm × 12 mm × 12 mm) was taped to the bottom of the cuvette to lift the cuvette in an optimum height and reduce the total volume of the solution. The cuvette was placed in the fluorometer, stirring was started at maximum speed (stirring continued throughout the experiment) and data collection was started (λ_{ex}

= 430 nm, λ_{em} = 505 nm). At time t = 10 s, 3.75 µL transporter in DMF was added. The concentrations of transporter were chosen to minimize chloride transport[5]: 5 mol% **1**, 5 mol% **2**, 0.01 mol% **3**, 0.05 mol% **4**, and 5 mol% **5** (mol% with respect to total lipid concentration (eggPC+cholesterol)). At time t = 20 s, 500 µL NaCl or carboxylate drugs stock solution (75 mM) was added to achieve a final concentration of 25 mM drug and 0.5 mM lipid. Due to the large dilution occurring upon the addition of drug, a large drop in fluorescence intensity is observed, but this quickly stabilizes within 1 second of drug addition (see **Figure S20**). At time t = 330 s, detergent (10 µL of 10% Triton X-100) was added to fully lyse the membrane and observe maximum quenching.

In the case of drugs with low solubility (amoxicillin sodium, furosemide sodium, ramipril sodium, and valsartan sodium), 1.0 mL of lucigenin-loaded liposomes (1 mM total lipid) were transferred to a 3 mL fluorescence cuvette and a small cuvette stir bar was added. The cuvette was placed in the fluorometer, stirring was started at maximum speed (stirring continued throughout the experiment) and data collection was started (λ_{ex} = 430 nm, λ_{em} = 505 nm). At time t = 10 s, 3.75 µL transporter in DMF was added. At time t = 20 s, 1.0 mL carboxylate drugs stock solution (50 mM) was added to achieve a final concentration of 25 mM drug and 0.5 mM lipid. At time t = 330 s, detergent (10 µL of 10% Triton X-100) was added to fully lyse the membrane and observe maximum quenching.

In the case of drugs with extremely low solubility (diclofenac sodium and gemfibrozil sodium), 1.0 mL of lucigenin-loaded liposomes (1 mM total lipid) were transferred to a 3 mL fluorescence cuvette and a small cuvette stir bar was added. The cuvette was placed in the fluorometer, stirring was started at maximum speed (stirring continued throughout the experiment) and data collection was started (λ_{ex} = 430 nm, λ_{em} = 505 nm). At time t = 10 s, 3.75 µL transporter in DMF was added. At time t = 20 s, 1.0 mL carboxylate drugs stock solution (25 mM) was added to achieve a final concentration of 12.5 mM drug and 0.5 mM lipid. At time t = 330 s, detergent (10 µL of 10% Triton X-100) was added to fully lyse the membrane and observe maximum quenching.

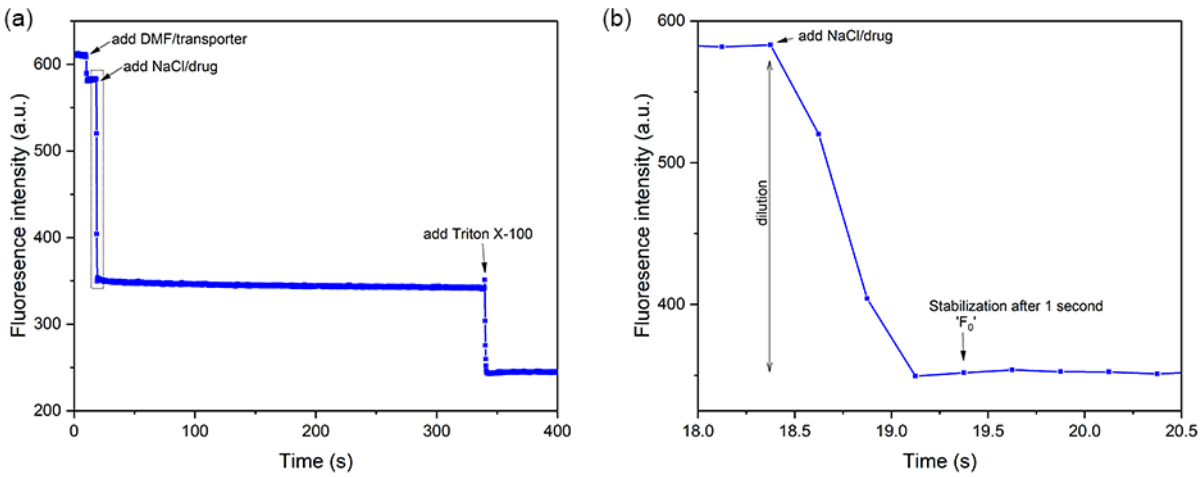

Figure S20. (a) Representative example of drug transport experiment (shown: addition of DMF at 10 s, and NaCl at 20 s). The addition of DMF leads to a small amount of quenching of lucigenin, while the addition of 0.5 mL NaCl stock to 1 mL lucigenin-encapsulated liposomes leads to a large reduction in fluorescence intensity due to dilution. The box shows the zoomed-in section of graph b (b) Zoomed-in section of graph a, showing that the dilution occurring upon the addition of NaCl stabilizes within 1 second (i.e., complete mixing is achieved within 1 second).

S3.3. Data work-up and results of kinetic assay

The time scale of the crude kinetic run was corrected to ensure that drug transport starts at time 0 (time 0 was taken as 1 second after the addition of NaCl or carboxylate drug, as shown in **Figure S20**). The corrected kinetic run was subsequently converted to 'normalized F_0/F', using the following equation (where F is the fluorescence intensity at any time, F_{final} is the fluorescence intensity after adding Triton X-100, and F_0 is the fluorescence intensity at time t = 0 s (1 second after the addition of NaCl or carboxylate drug, see **Figure S20**):

$$Normalized\ \frac{F_0}{F} = \frac{\frac{F_0}{F} - \frac{F_0}{F_0}}{\frac{F_0}{F_{final}} - \frac{F_0}{F_0}} = \frac{\frac{F_0}{F} - 1}{\frac{F_0}{F_{final}} - 1}$$

The calculation is valid because all drugs showed a linear correlation between lucigenin quenching (F_0/F) and drug concentration (see Section S2). By taking the value upon addition of Triton X-100 (F_{final}) as a reference point, the data is normalized and the error between experiments is reduced. By subtracting 1 in the formula, we ensure that values start at 0 and reach a maximum value of 1. The 'normalized F_0/F' data of 3-4 independent experiments conducted over at least 2 different sets of liposomes was averaged and the standard deviations were calculated. The results are shown in **Figure S21** - **Figure S35**. Diclofenac sodium, ibuprofen sodium, ketoprofen sodium and ramipril sodium displayed unusual transport profiles and are discussed in Section S3.5.

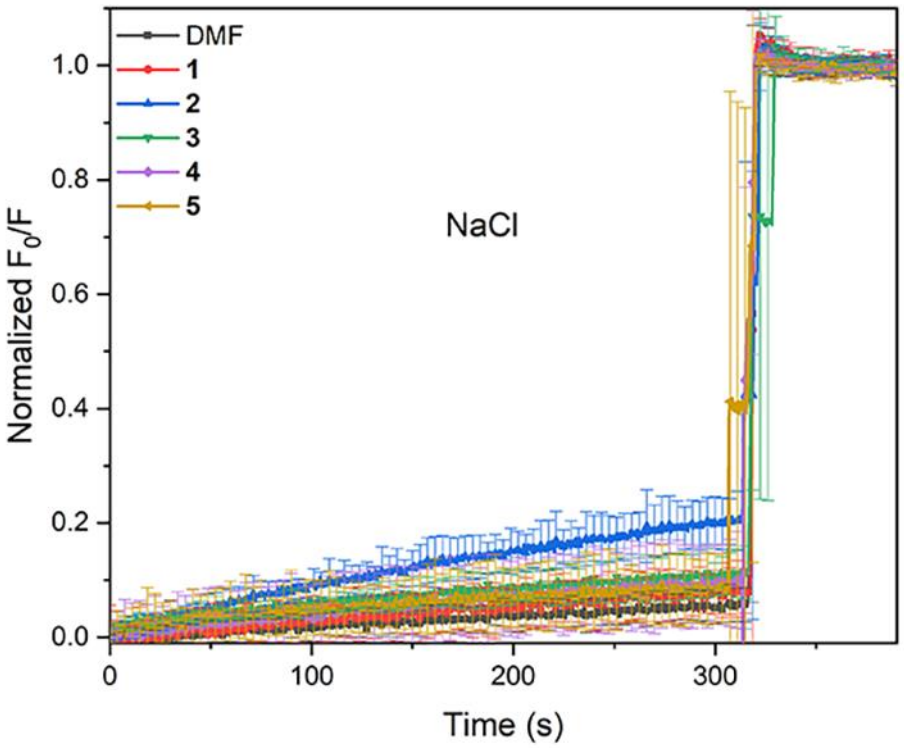

Figure S21. Chloride transport mediated by compounds **1**-**5**. Experiment was performed as described in Section S3, and is the average of a minimum of 3 repeats (error bars represent standard deviations). DMF was used as a blank run (no transporter added) to assess background chloride permeability. Detergent was added around 310 seconds.

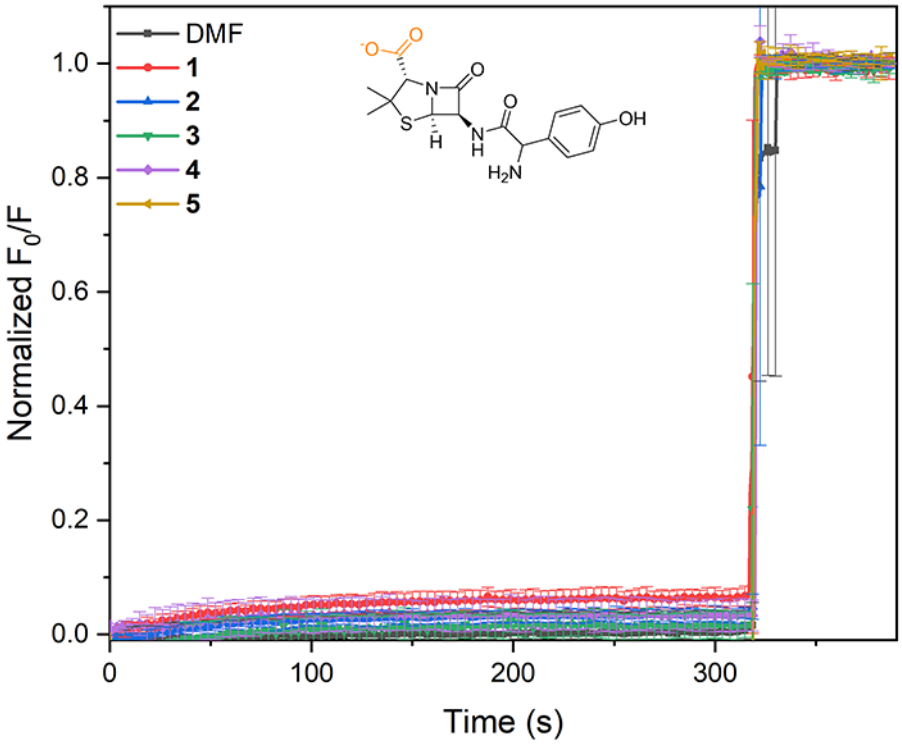

Figure S22. Amoxicillin transport mediated by compounds **1**-**5**. Experiment was performed as described in Section S3, and is the average of a minimum of 3 repeats (error bars represent standard deviations). DMF was used as a blank run (no transporter added) to assess background amoxicillin permeability. Detergent was added around 310 seconds.

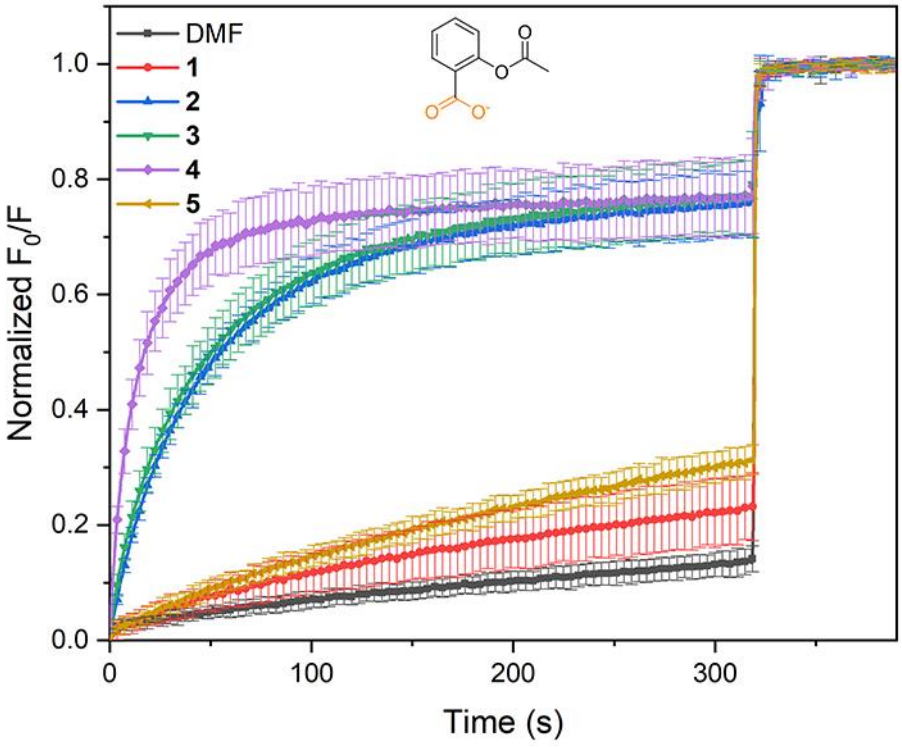

Figure S23. Aspirin transport mediated by compounds **1**-**5**. Experiment was performed as described in Section S3, and is the average of a minimum of 3 repeats (error bars represent standard deviations). DMF was used as a blank run (no transporter added) to assess background aspirin permeability. Detergent was added around 310 seconds.

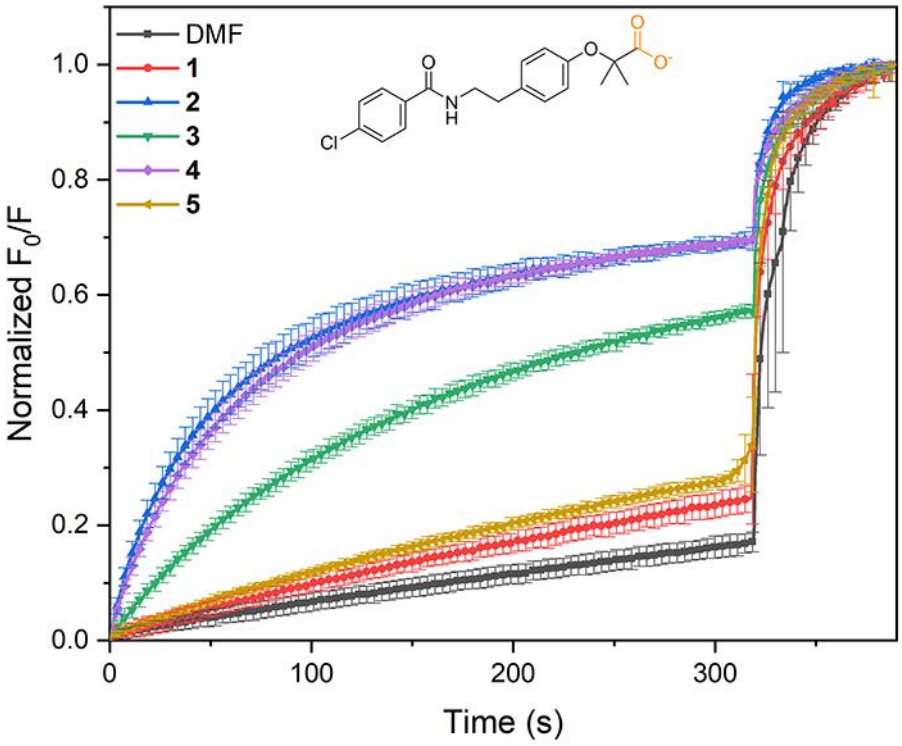

Figure S24. Bezafibrate transport mediated by compounds **1**-**5**. Experiment was performed as described in Section S3, and is the average of a minimum of 3 repeats (error bars represent standard deviations). DMF was used as a blank run (no transporter added) to assess background bezafibrate permeability. Detergent was added around 310 seconds.

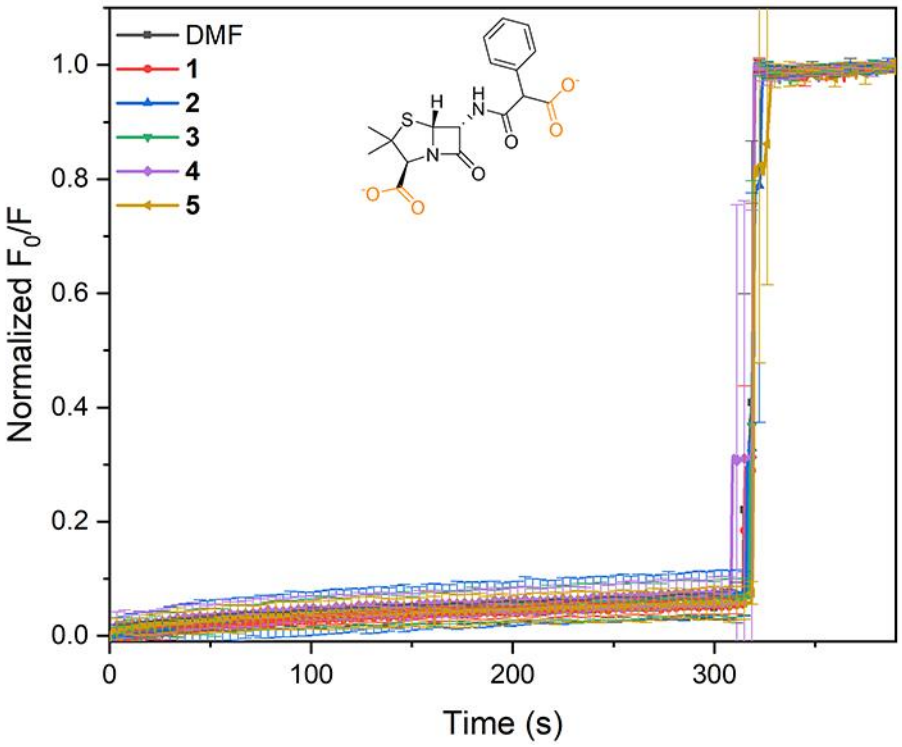

Figure S25. Carbenicillin transport mediated by compounds **1**-**5**. Experiment was performed as described in Section S3, and is the average of a minimum of 3 repeats (error bars represent standard deviations). DMF was used as a blank run (no transporter added) to assess background carbenicillin permeability. Detergent was added around 310 seconds.

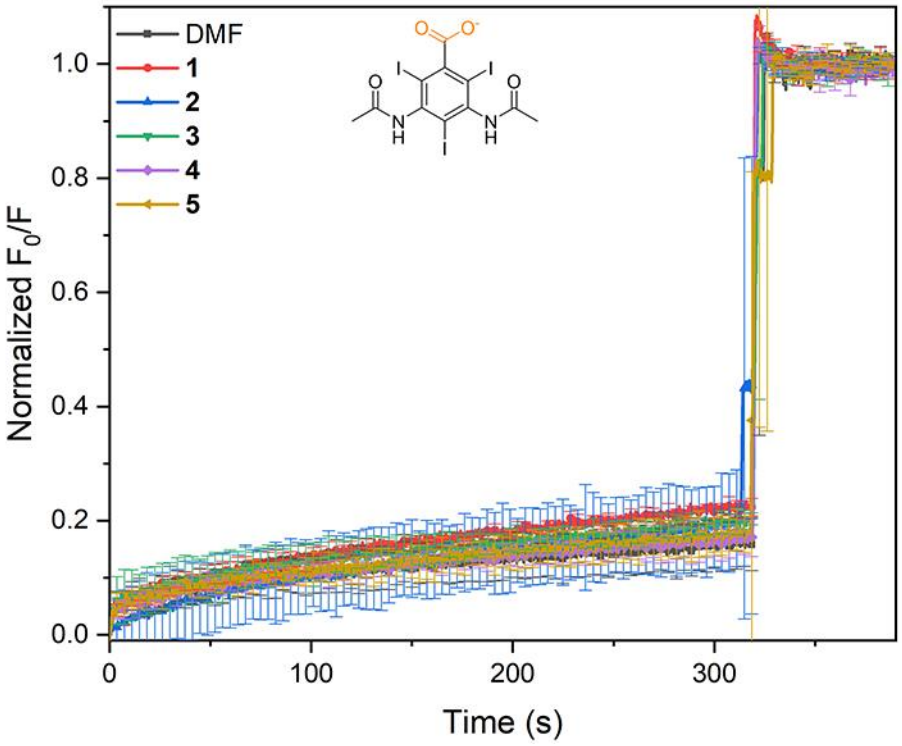

Figure S26. Diatrizoate transport mediated by compounds **1**-**5**. Experiment was performed as described in Section S3, and is the average of a minimum of 3 repeats (error bars represent standard deviations). DMF was used as a blank run (no transporter added) to assess background diatrizoate permeability. Detergent was added around 310 seconds.

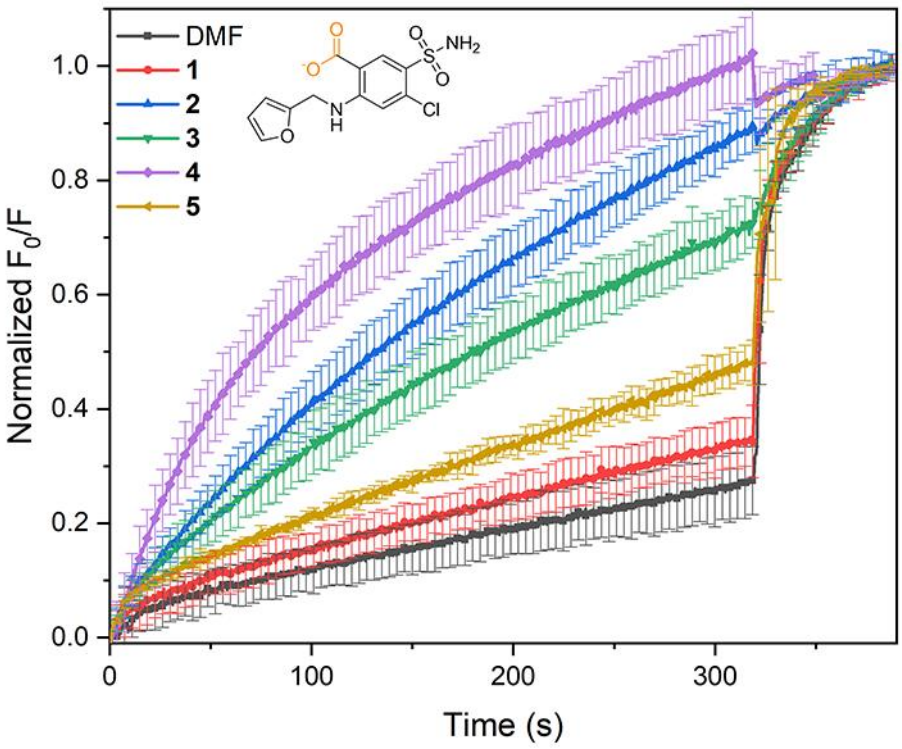

Figure S27. Furosemide transport mediated by compounds **1**-**5**. Experiment was performed as described in Section S3, and is the average of a minimum of 3 repeats (error bars represent standard deviations). DMF was used as a blank run (no transporter added) to assess background furosemide permeability. Detergent was added around 310 seconds.

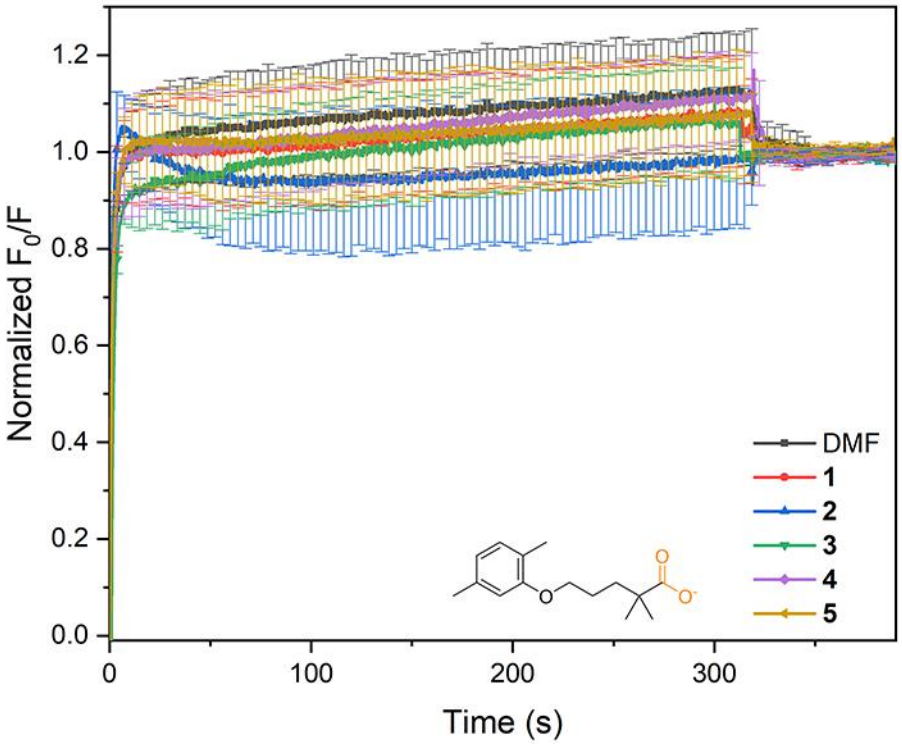

Figure S28. Gemfibrozil transport mediated by compounds **1**-**5**. Experiment was performed as described in Section S3, and is the average of a minimum of 3 repeats (error bars represent standard deviations). DMF was used as a blank run (no transporter added) to assess background gemfibrozil permeability. Detergent was added around 310 seconds.

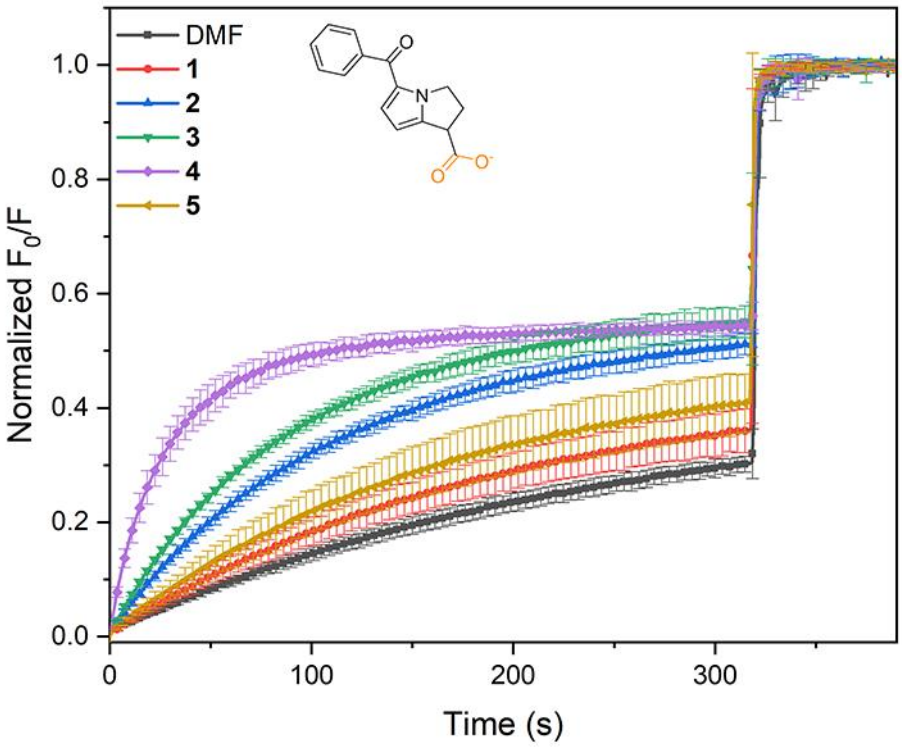

Figure S29. Ketorolac transport mediated by compounds **1**-**5**. Experiment was performed as described in Section S3, and is the average of a minimum of 3 repeats (error bars represent standard deviations). DMF was used as a blank run (no transporter added) to assess background ketorolac permeability. Detergent was added around 310 seconds.

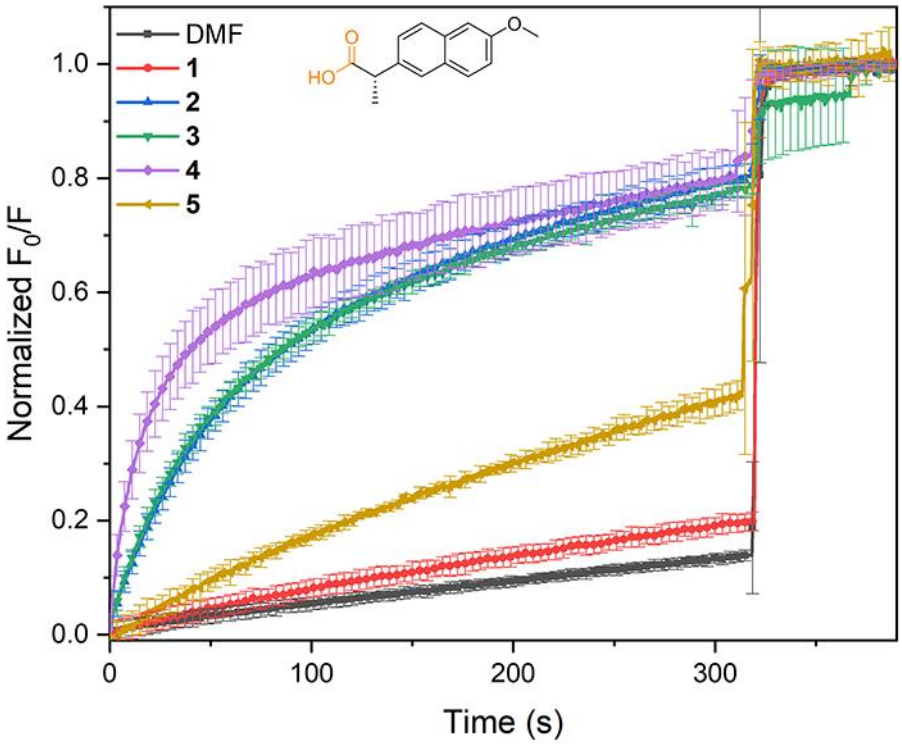

Figure S30. Naproxen transport mediated by compounds **1**-**5**. Experiment was performed as described in Section S3, and is the average of a minimum of 3 repeats (error bars represent standard deviations). DMF was used as a blank run (no transporter added) to assess background naproxen permeability. Detergent was added around 310 seconds.

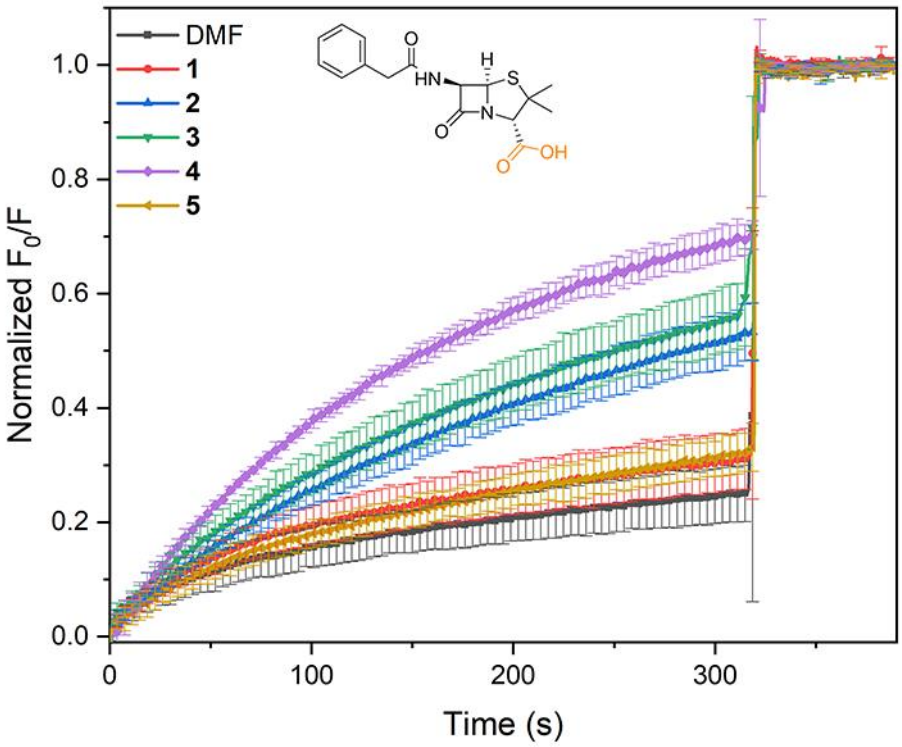

Figure S31. Penicillin G transport mediated by compounds **1**-**5**. Experiment was performed as described in Section S3, and is the average of a minimum of 3 repeats (error bars represent standard deviations). DMF was used as a blank run (no transporter added) to assess background penicillin G permeability. Detergent was added around 310 seconds.

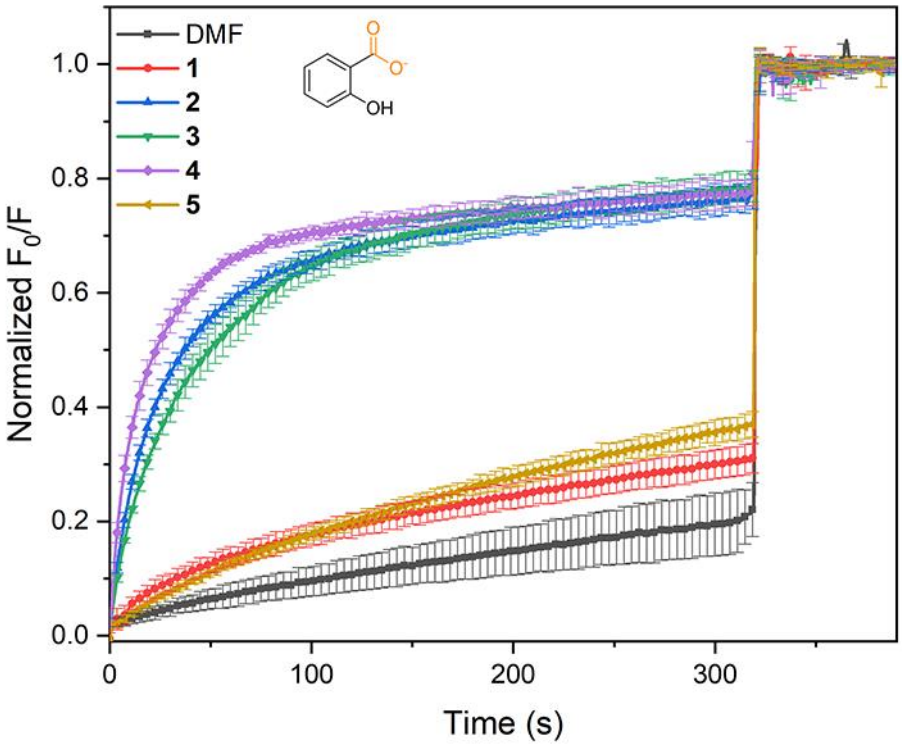

Figure S32. Salicylate transport mediated by compounds **1**-**5**. Experiment was performed as described in Section S3, and is the average of a minimum of 3 repeats (error bars represent standard deviations). DMF was used as a blank run (no transporter added) to assess background salicylate permeability. Detergent was added around 310 seconds.

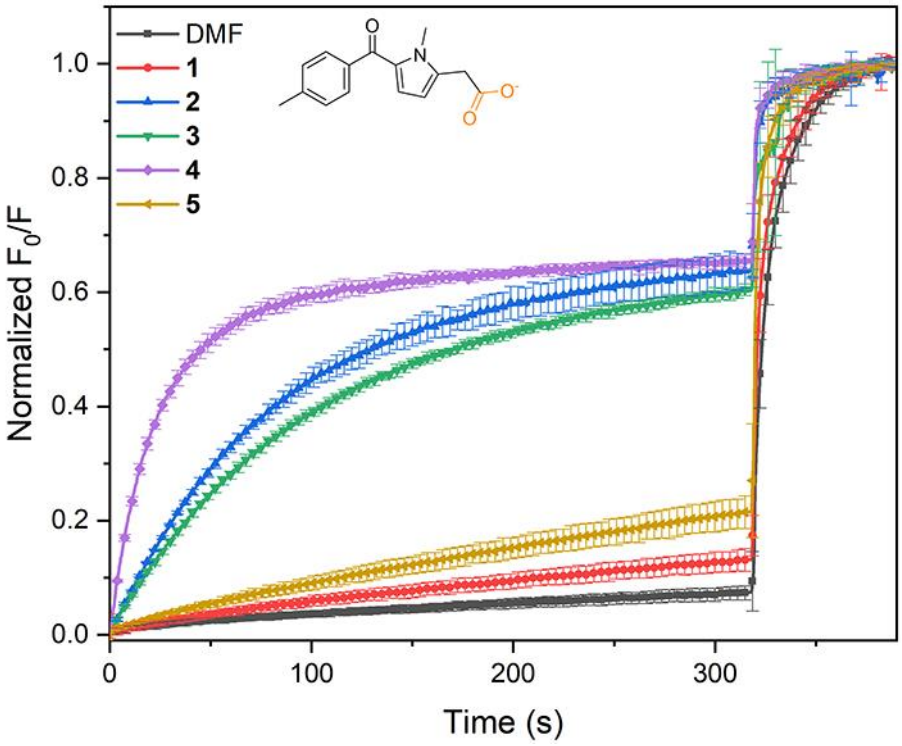

Figure S33. Tolmetin transport mediated by compounds **1**-**5**. Experiment was performed as described in Section S3, and is the average of a minimum of 3 repeats (error bars represent standard deviations). DMF was used as a blank run (no transporter added) to assess background tolmetin permeability. Detergent was added around 310 seconds.

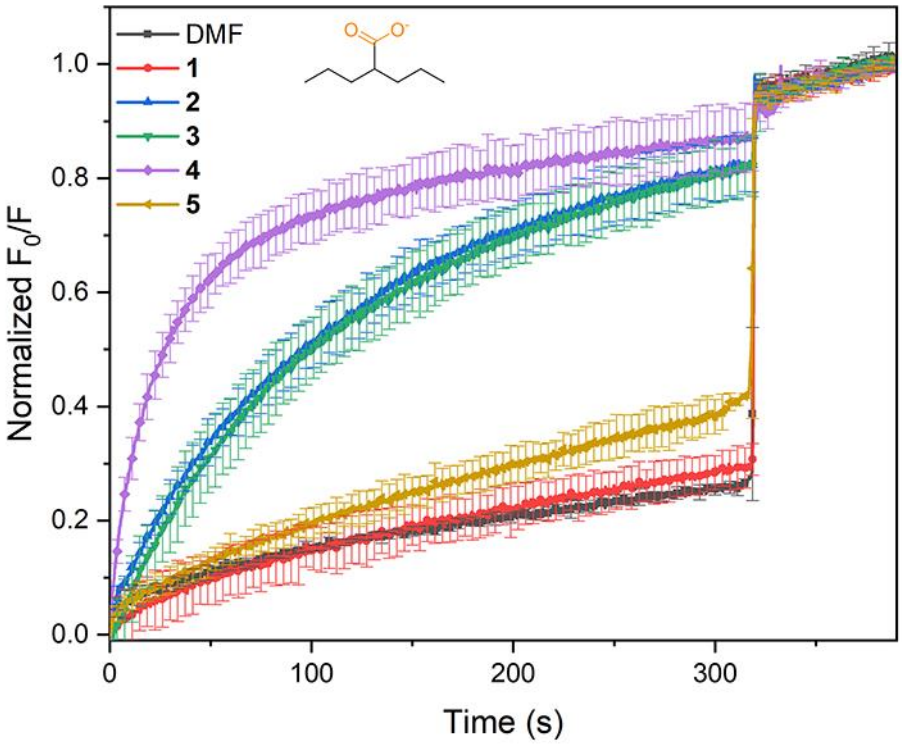

Figure S34. Valproate transport mediated by compounds **1**-**5**. Experiment was performed as described in Section S3, and is the average of a minimum of 3 repeats (error bars represent standard deviations). DMF was used as a blank run (no transporter added) to assess background valproate permeability. Detergent was added around 310 seconds.

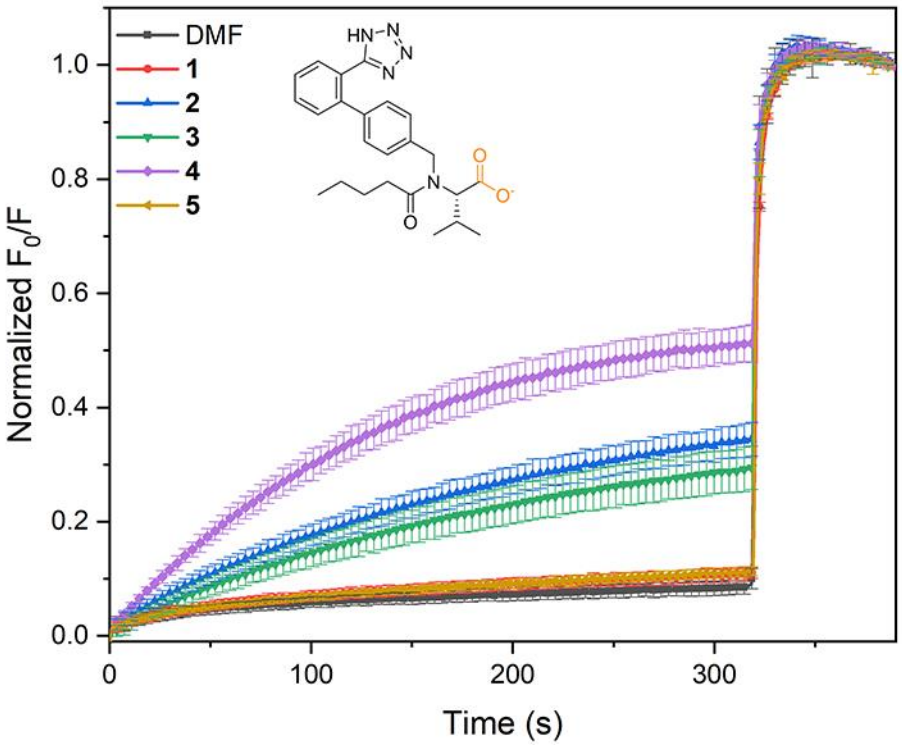

Figure S35. Valsartan transport mediated by compounds **1**-**5**. Experiment was performed as described in Section S3, and is the average of a minimum of 3 repeats (error bars represent standard deviations). DMF was used as a blank run (no transporter added) to assess background valsartan permeability. Detergent was added around 310 seconds.

S3.5. Calculation of permeability enhancement

The 'normalized F_0/F' versus time traces shown in **Figure S21-Figure S35** were subjected to an asymptotic fit using OriginPro 2019 ($y = a - bc^t$), and the absolute initial rate of transport was calculated from the first derivative at time t = 0 s ($k_{ini} = |b \cdot ln(c)|$). The permeability enhancement induced by the transporters is then given by the ratio of the initial rate of transport induced by compounds **1**-**5** (k_{ini}*(transporter)*) and the initial rate of transport observed in the absence of transporter (k_{ini}*(DMF)*):

$$permeability\ enhancement = \frac{k_{ini}(transporter)}{k_{ini}(DMF)}$$

To obtain the most accurate results, multiple DMF runs were performed per set of liposomes and their initial rates were averaged. Transporters tested on the same set of liposomes used the k_{ini}*(DMF)* average calculated for the blank run on the same set of liposomes. Data from at least two different sets of liposomes was used to ensure repeatability. The enhancement was calculated for each repeat separately, and then averaged and the standard deviation was calculated. For some drugs (sodium diatrizoate, amoxicillin sodium, and carbenicillin sodium), the permeability enhancement could not be accurately determined due to the very small amounts of membrane permeability of these drugs. In these cases, there was no visible transport in the presence or absence of compounds, and the permeability enhancement was therefore assumed to be '1'. An overview of the obtained permeability enhancement is given in **Table S1**. The results of the asymptotic fits are shown in **Figure S36** - **Figure S46**

Table S1. Permeability enhancement of a variety of carboxylate drugs induced by compounds **1**-**5**. The values are the average of at least 3 independent repeats and the errors represents standard deviations.

Drug	Compound 1	Compound 2	Compound 3	Compound 4	Compound 5
Amoxicillin sodium	1[a]	1[a]	1[a]	1[a]	1[a]
Aspirin sodium	2.14 ± 0.69	26.72 ± 0.70	24.7 ± 1.1	65.8 ± 4.8	2.67 ± 0.05
Bezafibrate sodium	1.82 ± 0.28	18.6 ± 4.2	7.4 ± 1.3	16.4 ± 3.5	2.11 ± 0.19
Carbenicillin sodium	1[a]	1[a]	1[a]	1[a]	1[a]
Sodium diatrizoate	1[a]	1[a]	1[a]	1[a]	1[a]
Furosemide sodium	1.13 ± 0.09	5.0 ± 1.4	4.11 ± 0.80	11.34 ± 0.76	2.24 ± 0.28
Gemfibrozil sodium	1.14 ± 0.56	1.48 ± 0.69	0.80 ± 0.80	1.06 ± 0.07	1.05 ± 0.33
Ketorolac Tris salt	1.39 ± 0.31	2.97 ± 0.39	3.84 ± 0.39	9.3 ± 1.1	1.74 ± 0.47
Naproxen sodium	1.96 ± 0.27	20.3 ± 3.3	21.4 ± 1.5	45 ± 10	4.63 ± 0.66
Penicillin G sodium	1.82 ± 0.41	1.77 ± 0.36	1.84 ± 0.45	3.02 ± 0.60	1.52 ± 0.17
Sodium salicylate	2.89 ± 0.42	24.2 ± 3.8	18.1 ± 1.3	32.3 ± 7.5	2.74 ± 0.40
Tolmetin sodium	2.25 ± 0.26	26.0 ± 5.5	20.5 ± 4.1	72 ± 19	3.12 ± 0.32
Sodium valproate	1.66 ± 0.66	6.1 ± 1.8	6.61 ± 0.89	17.2 ± 5.1	1.72 ± 0.46
Valsartan sodium	1.90 ± 0.08	3.76 ± 0.26	3.31 ± 0.44	6.86 ± 0.74	1.74 ± 0.11

[a] The enhancement was assumed to be '1' (i.e., no enhancement) because no transport was observed upon visual inspection of the graphs. The transport rates were too low to calculate an accurate enhancement factor.

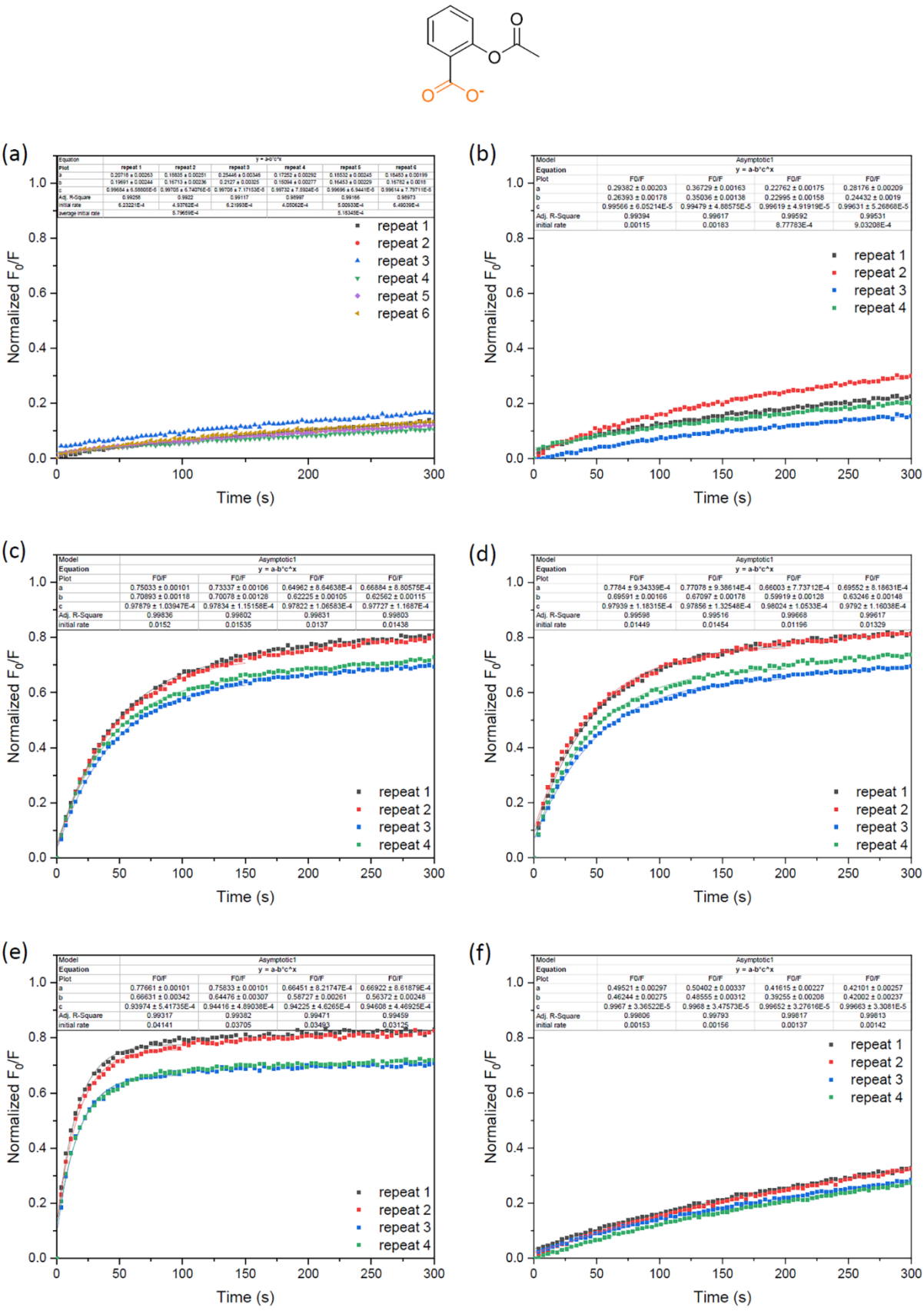

Figure S36. Aspirin transport mediated by compounds **1**-**5**. Experiment was performed as described in Section S3, and the graphs show the fitting of the data using OriginPro 2019 to determine the initial rate of transport and subsequently the enhancement factor. For clarity, only 1 in 15 data points are shown. The asymptotic fit is shown as solid lines. (a) DMF, (b) compound **1**, (c) compound **2**, (d) compound **3**, (e) compound **4**, (f) compound **5**.

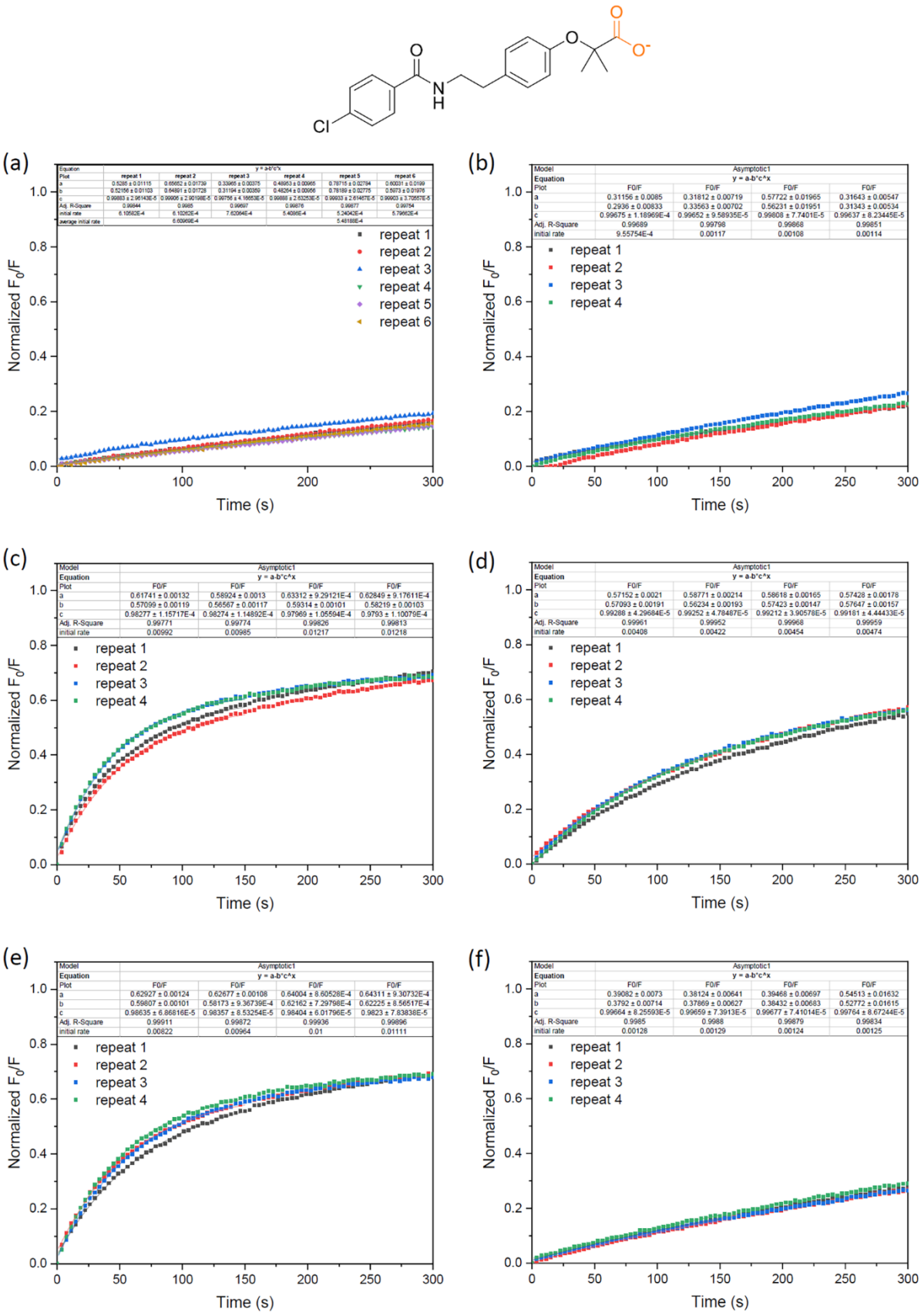

Figure S37. Bezafibrate transport mediated by compounds **1**-**5**. Experiment was performed as described in Section S3, and the graphs show the fitting of the data using OriginPro 2019 to determine the initial rate of transport and subsequently the enhancement factor. For clarity, only 1 in 15 data points are shown. The asymptotic fit is shown as solid lines. (a) DMF, (b) compound **1**, (c) compound **2**, (d) compound **3**, (e) compound **4**, (f) compound **5**.

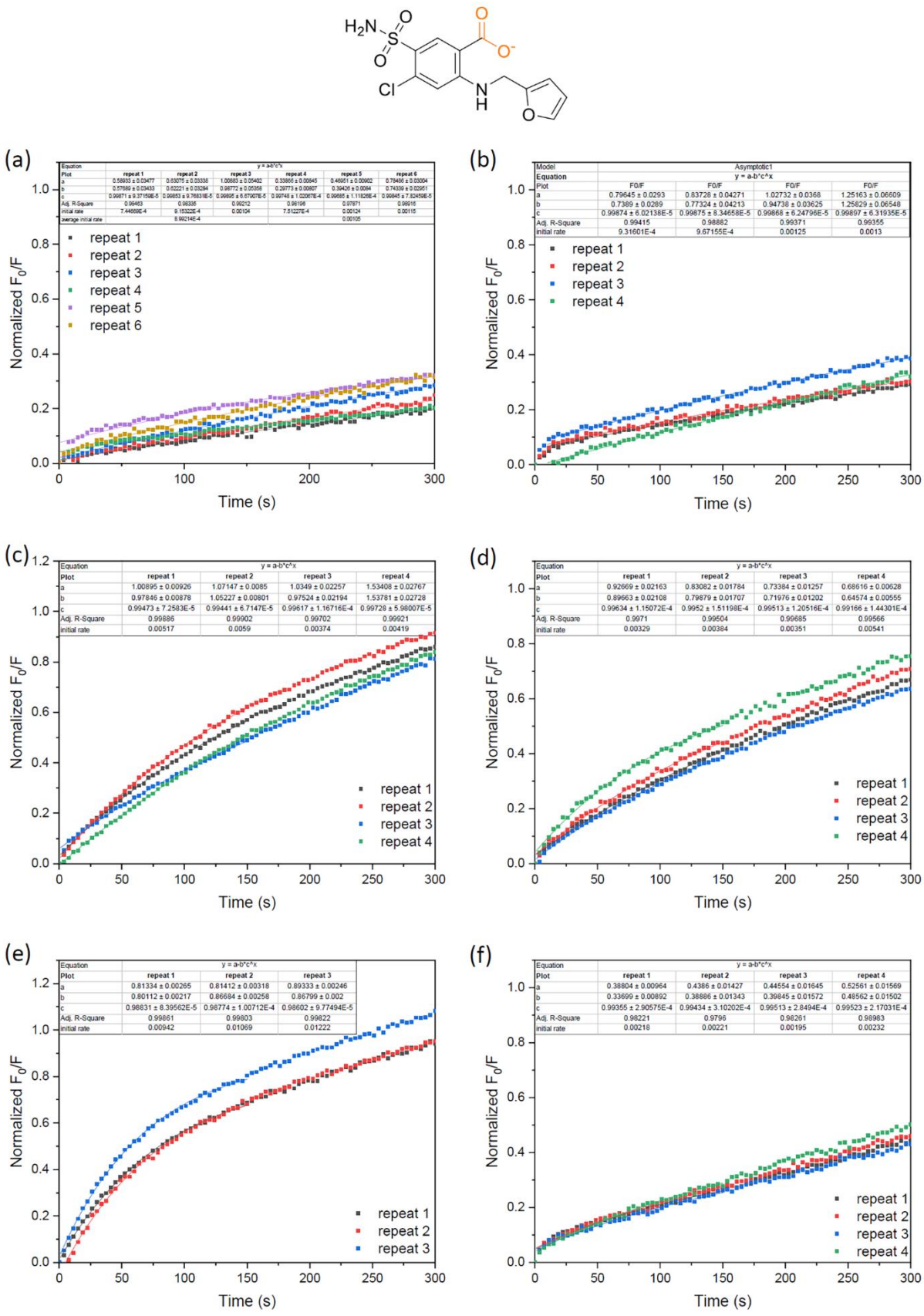

Figure S38. Furosemide transport mediated by compounds **1**-**5**. Experiment was performed as described in Section S3, and the graphs show the fitting of the data using OriginPro 2019 to determine the initial rate of transport and subsequently the enhancement factor. For clarity, only 1 in 15 data points are shown. The asymptotic fit is shown as solid lines. (a) DMF, (b) compound **1**, (c) compound **2**, (d) compound **3**, (e) compound **4**, (f) compound **5**.

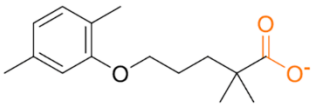

(a)

Model	Asymptotic1			
Equation	y = a-b*c^x			
Plot	F0/F	F0/F	F0/F	E
a	1.09656 ± 0.00319	1.02591 ± 0.00265	0.94519 ± 0.00269	0.9055 ± 0.00193
b	1.09673 ± 0.01068	1.01845 ± 0.0098	0.89702 ± 0.01309	0.87591 ± 0.01011
c	0.61158 ± 0.00547	0.57599 ± 0.00557	0.43637 ± 0.00914	0.3818 ± 0.00732
R-Square (COD)	0.99583	0.99801	0.99129	0.99453
initial rate	0.53027	0.56074	0.74387	0.84366
average rate	0.55001		0.79391	

(b)

Model	Asymptotic1			
Equation	y = a-b*c^x			
Plot	repeat 1	repeat 2	repeat 3	repeat 4
a	1.03518 ± 0.00288	1.04434 ± 0.00251	1.04845 ± 0.00273	0.84957 ± 0.00157
b	1.00349 ± 0.01046	0.83547 ± 0.01685	1.00452 ± 0.0173	0.83507 ± 0.00797
c	0.58209 ± 0.00599	0.64795 ± 0.00718	0.21279 ± 0.01007	0.40578 ± 0.00603
Adj. R-Square	0.99516	0.99271	0.98694	0.99613
initial rate	0.54302	0.36255	1.55444	0.75319

(c)

Model	Asymptotic1			
Equation	y = a-b*c^x			
Plot	repeat 1	repeat 2	repeat 3	repeat 4
a	1.13421 ± 0.00187	1.02883 ± 0.00289	1.13197 ± 0.0049	1.02434 ± 0.00235
b	1.11877 ± 0.00833	0.80007 ± 0.01647	1.13618 ± 0.01459	1.03182 ± 0.01059
c	0.48794 ± 0.00456	0.67108 ± 0.00748	0.20638 ± 0.00849	0.28714 ± 0.00665
Adj. R-Square	0.99762	0.99168	0.99711	0.99679
initial rate	0.80279	0.31912	1.79293	1.28749

(d)

Model	Asymptotic1		
Equation	y = a-b*c^x		
Plot	repeat 1	repeat 2	repeat 3
a	0.99075 ± 0.00367	0.8872 ± 0.00127	0.86328 ± 0.00174
b	0.93947 ± 0.01251	0.69444 ± 0.02651	0.84062 ± 0.00831
c	0.60528 ± 0.00752	0.45195 ± 0.01144	0.44884 ± 0.00616
Adj. R-Square	0.992	0.98677	0.99584
initial rate	0.47167	0.55151	0.67341

(e)

Model	Asymptotic1			
Equation	y = a-b*c^x			
Plot	repeat 1	repeat 2	repeat 3	repeat 4
a	1.03179 ± 0.00297	1.1334 ± 0.00146	0.93027 ± 0.00208	0.84662 ± 0.00201
b	0.99062 ± 0.01109	0.97061 ± 0.01971	0.90858 ± 0.01106	0.81039 ± 0.01059
c	0.5725 ± 0.00648	0.5312 ± 0.00661	0.37202 ± 0.00773	0.37978 ± 0.0083
Adj. R-Square	0.99446	0.99509	0.99371	0.99275
initial rate	0.55251	0.61402	0.89841	0.78459

(f)

Model	Asymptotic1			
Equation	y = a-b*c^x			
Plot	repeat 1	repeat 2	repeat 3	repeat 4
a	1.05058 ± 0.003	1.11307 ± 0.00245	0.92905 ± 0.00185	0.96634 ± 0.00139
b	1.01742 ± 0.01059	0.84185 ± 0.0193	0.89871 ± 0.00929	0.95546 ± 0.00816
c	0.59282 ± 0.00593	0.62354 ± 0.008	0.41186 ± 0.00653	0.28537 ± 0.00532
Adj. R-Square	0.99514	0.99142	0.99545	0.99684
initial rate	0.53197	0.39764	0.79722	1.19812

Figure S39. Gemfibrozil transport mediated by compounds **1**-**5**. Experiment was performed as described in Section S3, and the graphs show the fitting of the data using OriginPro 2019 to determine the initial rate of transport and subsequently the enhancement factor. Due to the fast permeability, only the first 50 seconds of the run is shown. The asymptotic fit is shown as solid lines. (a) DMF, (b) compound **1**, (c) compound **2**, (d) compound **3**, (e) compound **4**, (f) compound **5**.

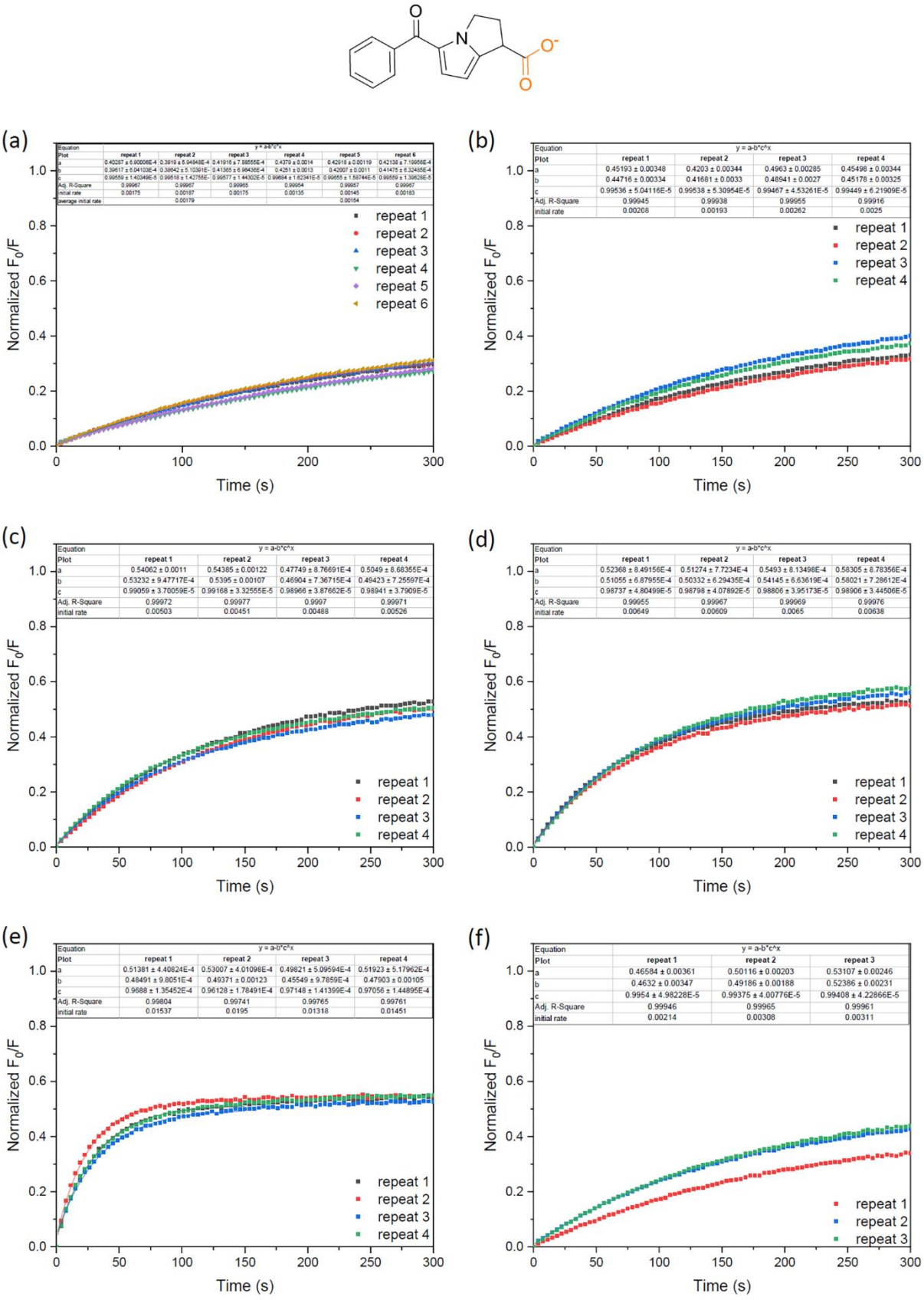

Figure S40. Ketorolac transport mediated by compounds **1**-**5**. Experiment was performed as described in Section S3, and the graphs show the fitting of the data using OriginPro 2019 to determine the initial rate of transport and subsequently the enhancement factor. For clarity, only 1 in 15 data points are shown. The asymptotic fit is shown as solid lines. (a) DMF, (b) compound **1**, (c) compound **2**, (d) compound **3**, (e) compound **4**, (f) compound **5**.

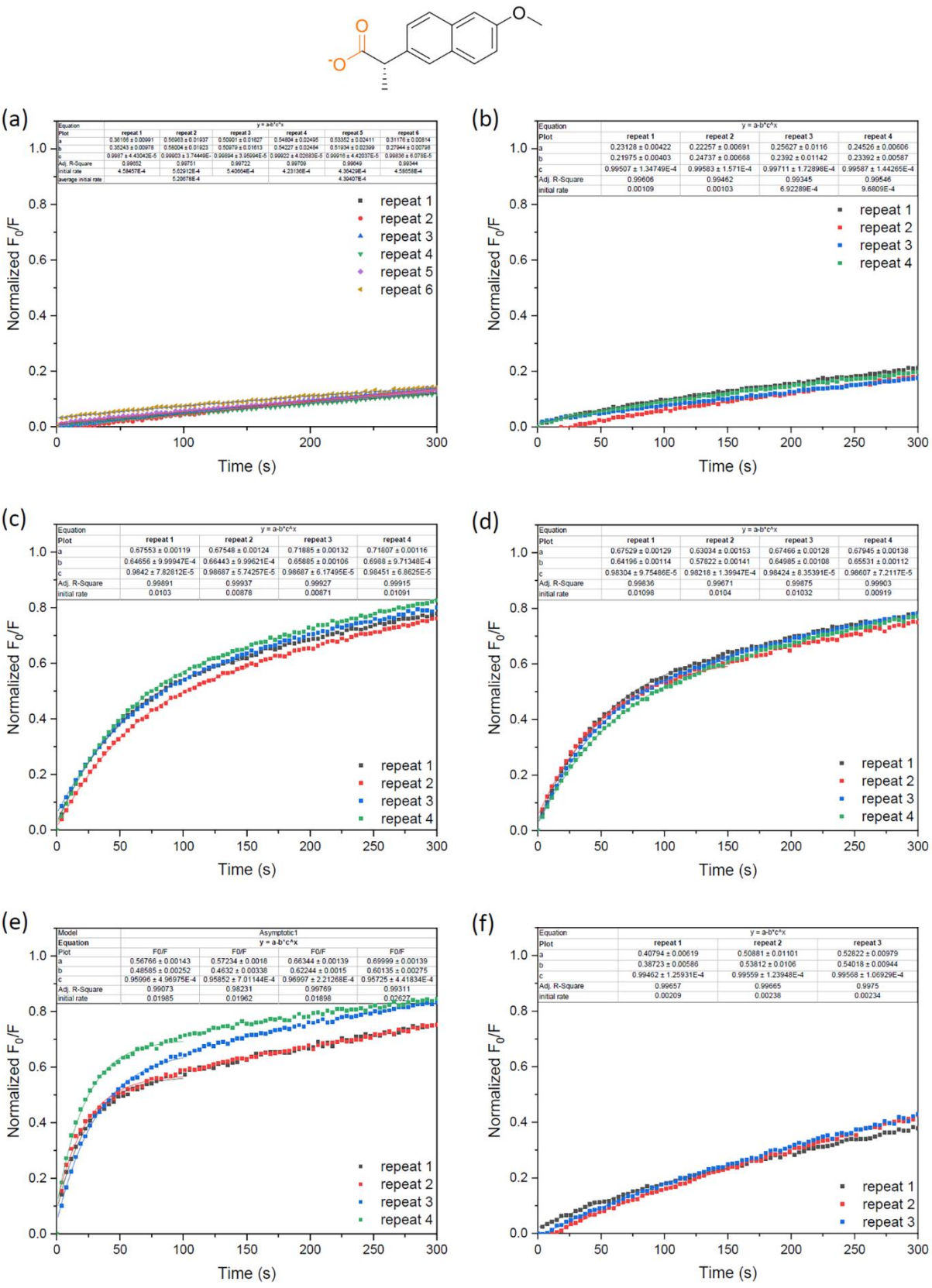

Figure S41. Naproxen transport mediated by compounds **1**-**5**. Experiment was performed as described in Section S3, and the graphs show the fitting of the data using OriginPro 2019 to determine the initial rate of transport and subsequently the enhancement factor. For clarity, only 1 in 15 data points are shown. The asymptotic fit is shown as solid lines. (a) DMF, (b) compound **1**, (c) compound **2**, (d) compound **3**, (e) compound **4**, (f) compound **5**.

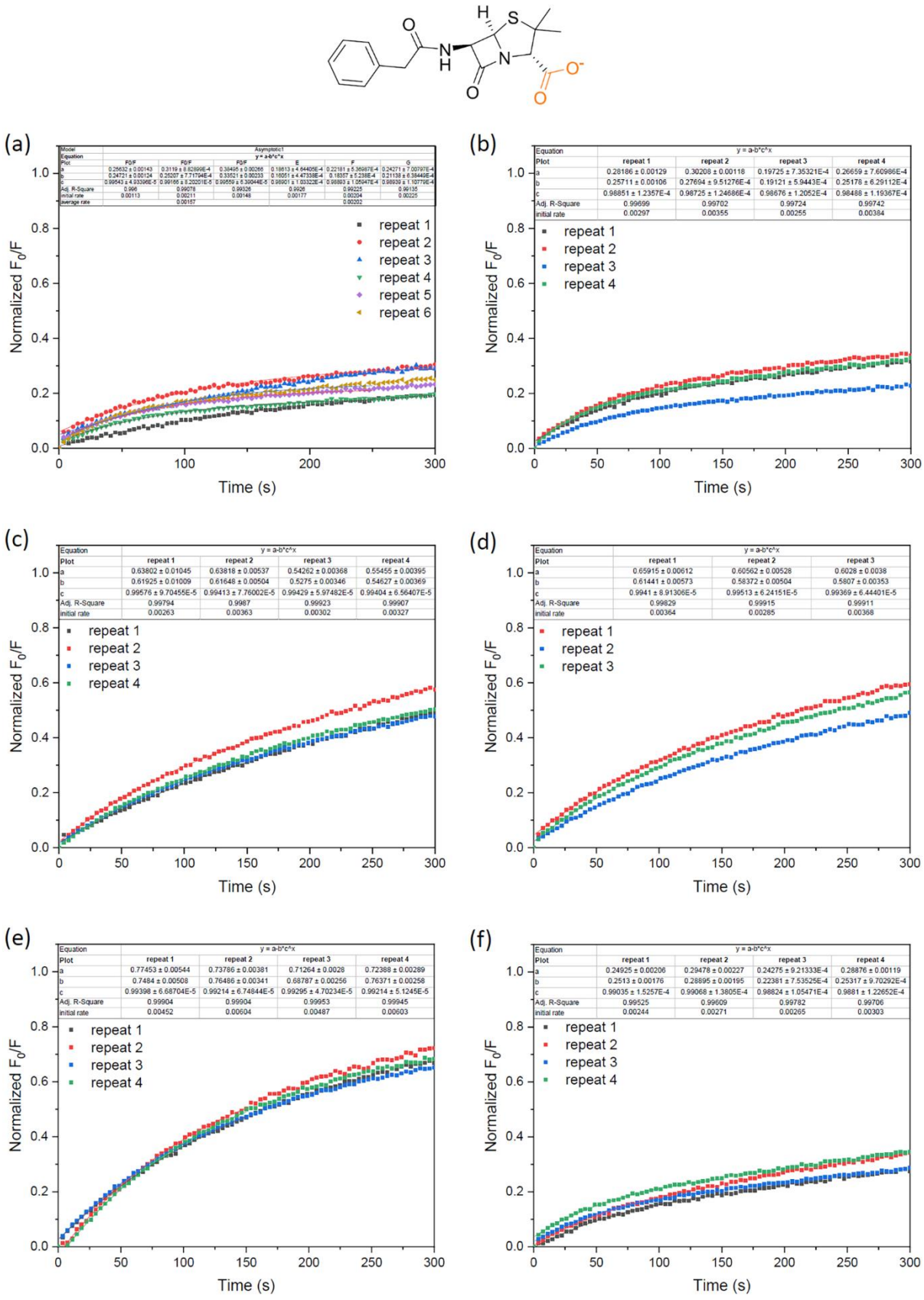

Figure S42. Penicillin G transport mediated by compounds **1**-**5**. Experiment was performed as described in Section S3, and the graphs show the fitting of the data using OriginPro 2019 to determine the initial rate of transport and subsequently the enhancement factor. For clarity, only 1 in 15 data points are shown. The asymptotic fit is shown as solid lines. (a) DMF, (b) compound **1**, (c) compound **2**, (d) compound **3**, (e) compound **4**, (f) compound **5**.

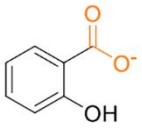

(a)

Equation	y = a-b*c^x					
Plot	repeat 1	repeat 2	repeat 3	repeat 4	repeat 5	repeat 6
a	0.54192 ± 0.02269	0.32084 ± 0.00354	0.31821 ± 0.00271	0.23388 ± 0.00201	0.32941 ± 0.00342	0.59525 ± 0.00553
b	0.51694 ± 0.0226	0.31126 ± 0.00337	0.28355 ± 0.00252	0.21992 ± 0.00187	0.30101 ± 0.00322	0.48292 ± 0.00527
c	0.99925 ± 3.67885E-5	0.99745 ± 4.1791E-5	0.99682 ± 4.78633E-5	0.99687 ± 4.61688E-5	0.99711 ± 4.94841E-5	0.99743 ± 4.24555E-5
Adj. R-Square	0.99759	0.99698	0.9961	0.9963	0.99574	0.99683
initial rate	3.8785E-4	7.94727E-4	9.03125E-4	6.61215E-4	8.71178E-4	0.00124
average initial rate		6.9034E-4			9.2503E-4	

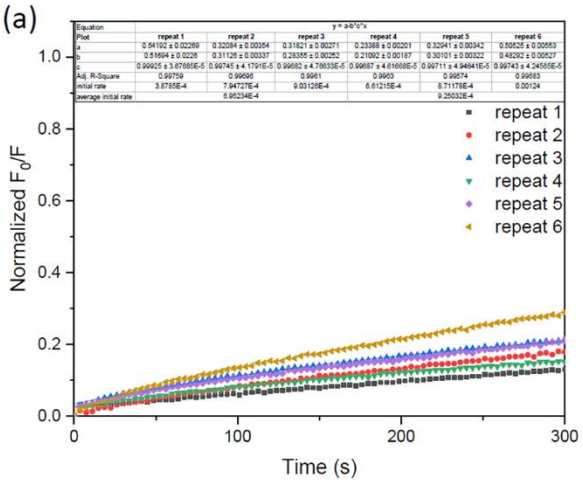

(b)

Equation	y = a-b*c^x			
Plot	F0/F	F0/F	F0/F	F0/F
a	0.24919 ± 0.00161	0.27688 ± 0.00157	0.23114 ± 0.00114	0.28321 ± 0.00121
b	0.19751 ± 0.00121	0.24261 ± 0.00135	0.21476 ± 9.65602E-4	0.24941 ± 0.00101
c	0.98946 ± 1.84956E-4	0.99051 ± 1.17369E-4	0.99002 ± 1.04093E-4	0.98927 ± 1.07245E-4
Adj. R-Square	0.99424	0.99718	0.9978	0.9977
initial rate	0.00209	0.00231	0.00215	0.00269

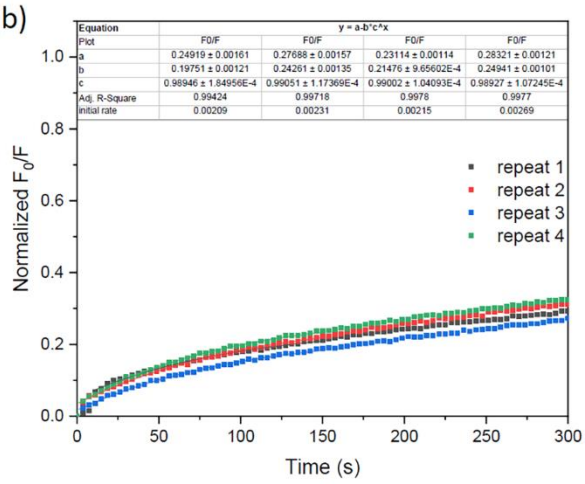

(c)

Equation	y = a-b*c^x			
Plot	repeat 1	repeat 2	repeat 3	repeat 4
a	0.66432 ± 8.61438E-4	0.68997 ± 0.001	0.69291 ± 9.15276E-4	0.71015 ± 9.75053E-4
b	0.59274 ± 0.00196	0.61505 ± 0.00215	0.61902 ± 0.00191	0.61819 ± 0.0022
c	0.96836 ± 2.22237E-4	0.96943 ± 2.33533E-4	0.97005 ± 2.04551E-4	0.96851 ± 2.3901E-4
Adj. R-Square	0.99482	0.99406	0.99533	0.99398
initial rate	0.01906	0.0191	0.01882	0.01978

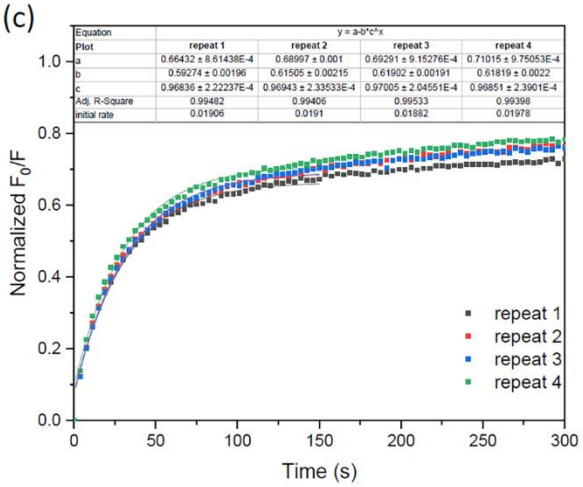

(d)

Equation	y = a-b*c^x			
Plot	repeat 1	repeat 2	repeat 3	repeat 4
a	0.67733 ± 0.00119	0.75498 ± 0.00257	0.70723 ± 0.00102	0.73482 ± 9.20671E-4
b	0.60718 ± 0.00153	0.66436 ± 0.00234	0.63889 ± 0.00158	0.68064 ± 0.00134
c	0.97745 ± 1.60523E-4	0.98247 ± 1.9921E-4	0.97491 ± 1.59346E-4	0.97581 ± 1.261E-4
Adj. R-Square	0.99627	0.9933	0.99663	0.99782
initial rate	0.01385	0.01175	0.01623	0.01667

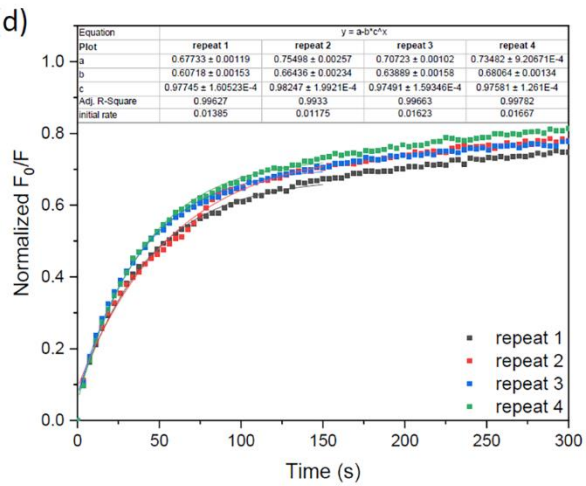

(e)

Equation	y = a-b*c^x			
Plot	repeat 1	repeat 2	repeat 3	repeat 4
a	0.69707 ± 8.1311E-4	0.71204 ± 8.56323E-4	0.71088 ± 8.08878E-4	0.74312 ± 9.14571E-4
b	0.57739 ± 0.00317	0.57238 ± 0.00312	0.60412 ± 0.0028	0.62643 ± 0.00237
c	0.95313 ± 4.32082E-4	0.95573 ± 4.15828E-4	0.9575 ± 3.4667E-4	0.96553 ± 2.6065E-4
Adj. R-Square	0.98867	0.98854	0.99151	0.99358
initial rate	0.02772	0.02592	0.02624	0.02197

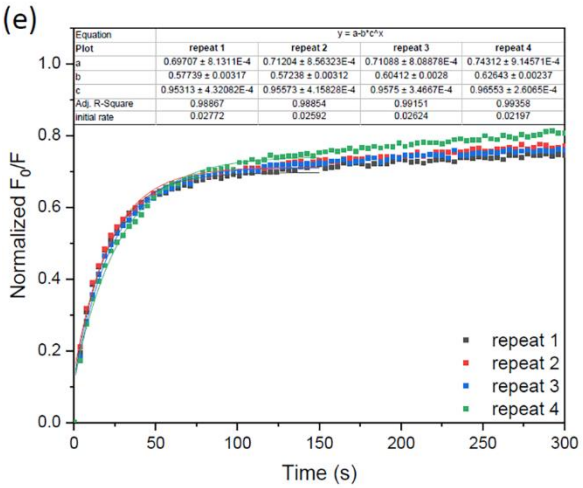

(f)

Equation	y = a-b*c^x			
Plot	repeat 1	repeat 2	repeat 3	repeat 4
a	0.36045 ± 0.00324	0.3681 ± 0.00333	0.3576 ± 0.00295	0.38475 ± 0.00271
b	0.34625 ± 0.00304	0.34546 ± 0.00309	0.33919 ± 0.00275	0.37537 ± 0.0025
c	0.99421 ± 8.17241E-5	0.99367 ± 9.53268E-5	0.99397 ± 8.01695E-5	0.99342 ± 7.53307E-5
Adj. R-Square	0.99856	0.99805	0.99862	0.99879
initial rate	0.00201	0.00219	0.00205	0.00248

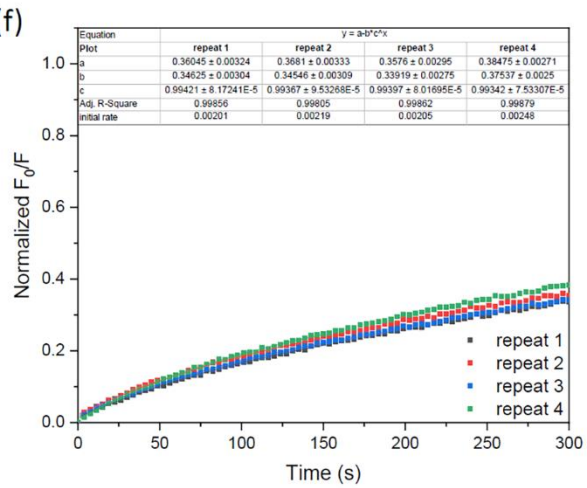

Figure S43. Salicylate transport mediated by compounds **1**-**5**. Experiment was performed as described in Section S3, and the graphs show the fitting of the data using OriginPro 2019 to determine the initial rate of transport and subsequently the enhancement factor. For clarity, only 1 in 15 data points are shown. The asymptotic fit is shown as solid lines. (a) DMF, (b) compound **1**, (c) compound **2**, (d) compound **3**, (e) compound **4**, (f) compound **5**.

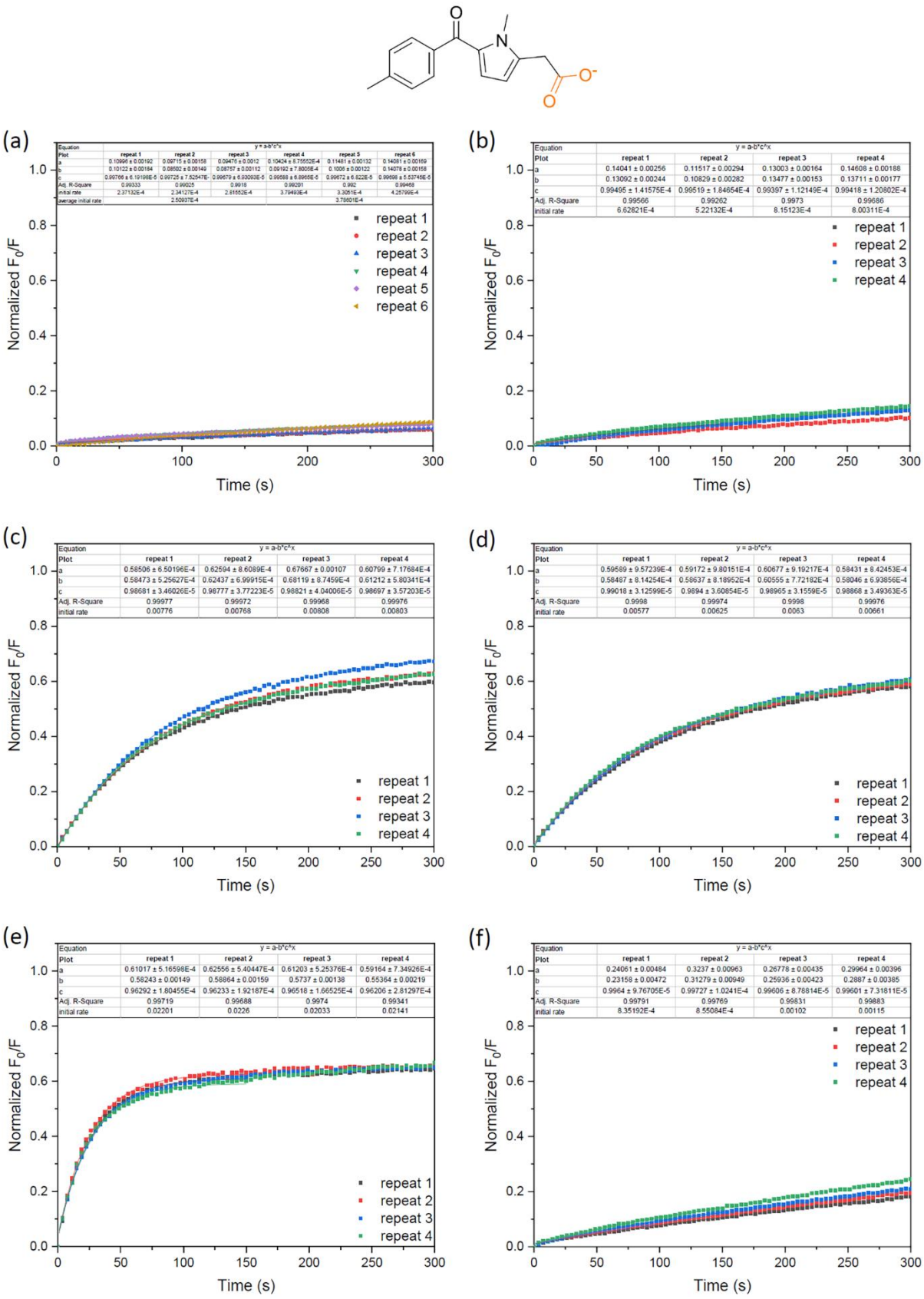

Figure S44. Tolmetin transport mediated by compounds **1**-**5**. Experiment was performed as described in Section S3, and the graphs show the fitting of the data using OriginPro 2019 to determine the initial rate of transport and subsequently the enhancement factor. For clarity, only 1 in 15 data points are shown. The asymptotic fit is shown as solid lines. (a) DMF, (b) compound **1**, (c) compound **2**, (d) compound **3**, (e) compound **4**, (f) compound **5**.

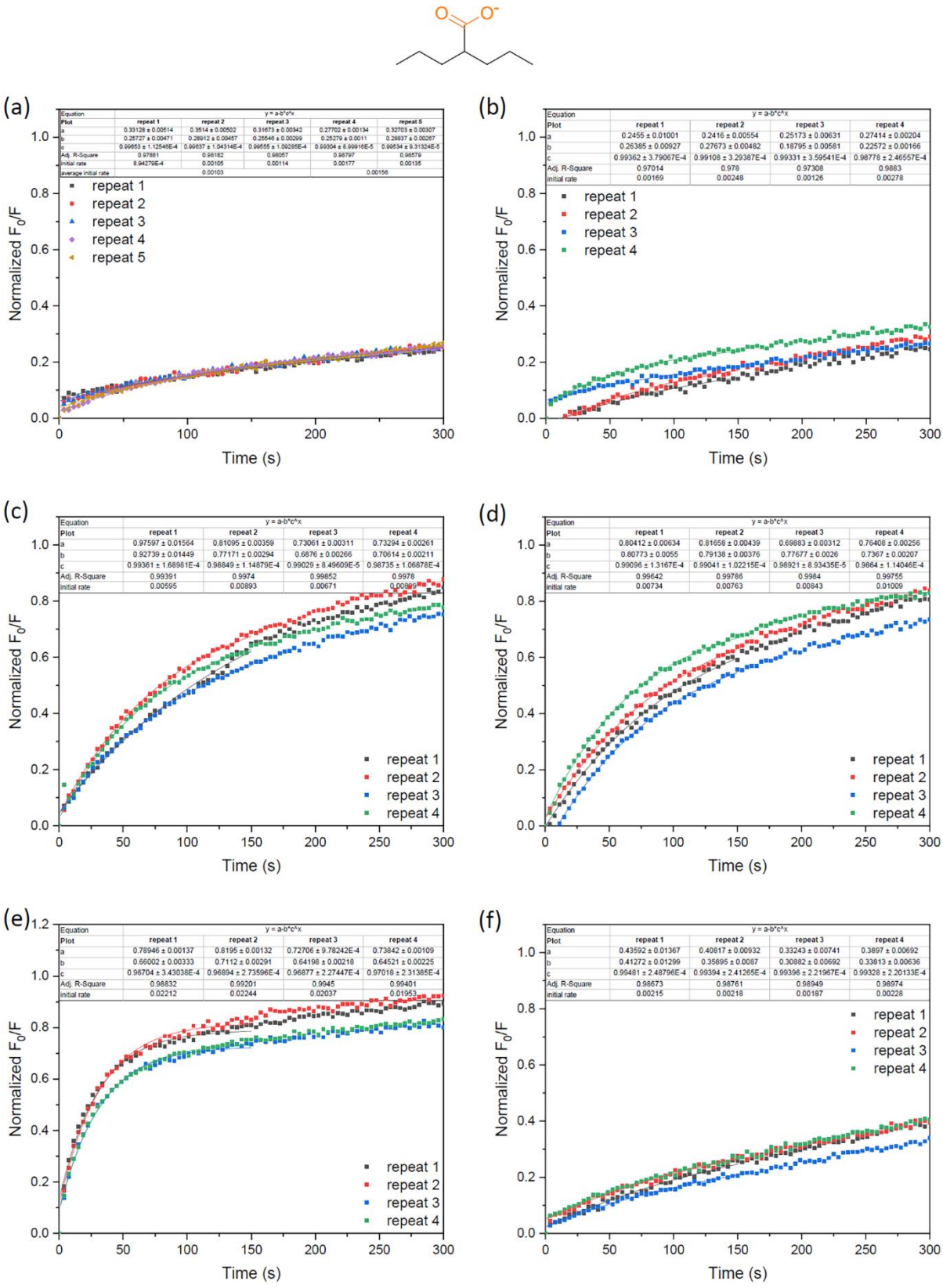

Figure S45. Valproate transport mediated by compounds **1**-**5**. Experiment was performed as described in Section S3, and the graphs show the fitting of the data using OriginPro 2019 to determine the initial rate of transport and subsequently the enhancement factor. For clarity, only 1 in 15 data points are shown. The asymptotic fit is shown as solid lines. (a) DMF, (b) compound **1**, (c) compound **2**, (d) compound **3**, (e) compound **4**, (f) compound **5**.

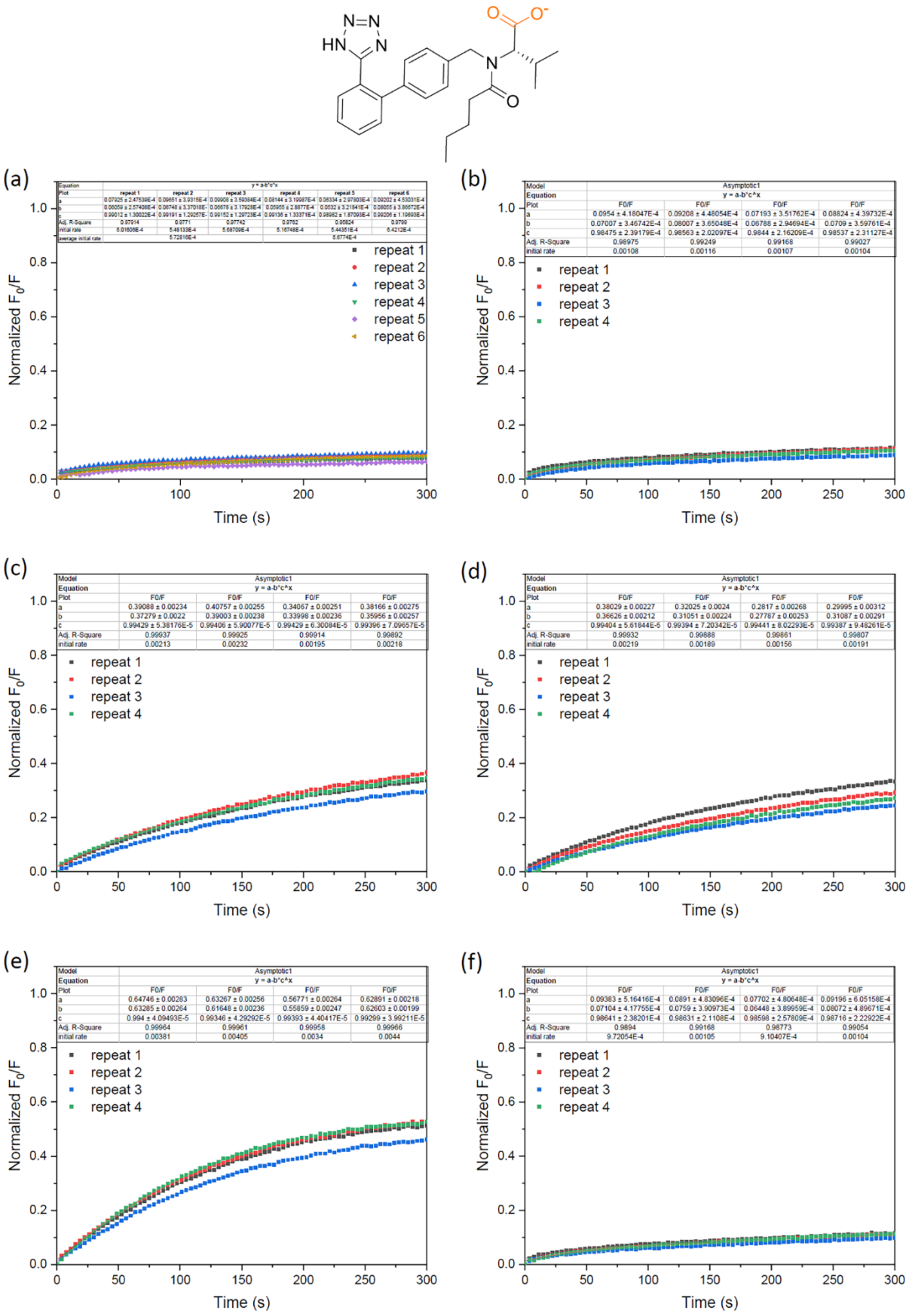

Figure S46. Valsartan transport mediated by compounds **1**-**5**. Experiment was performed as described in Section S3, and the graphs show the fitting of the data using OriginPro 2019 to determine the initial rate of transport and subsequently the enhancement factor. For clarity, only 1 in 15 data points are shown. The asymptotic fit is shown as solid lines. (a) DMF, (b) compound **1**, (c) compound **2**, (d) compound **3**, (e) compound **4**, (f) compound **5**.

S3.6. Drugs with unusual transport profiles

Four drugs (diclofenac, ibuprofen, ketoprofen and ramipril) showed unusual transport profiles in the kinetic transport assays. Although there is qualitatively a clear enhancement in permeability of these drugs in the presence of transporters **1-5**, the unusual transport profiles prohibit accurate determination of enhancement factors.

In the case of diclofenac (a very hydrophobic drug), the permeability in the absence of transporters did not show the usual asymptotic profile, but a bi-sigmoidal profile corresponding to very fast membrane permeability (see **Figure S47**). Consequently, the initial rate of transport could not be calculated. The reason for the unusual permeability profile is not clear, but might be related to the previously reported ability of diclofenac to interact with PC lipids.[6, 7]

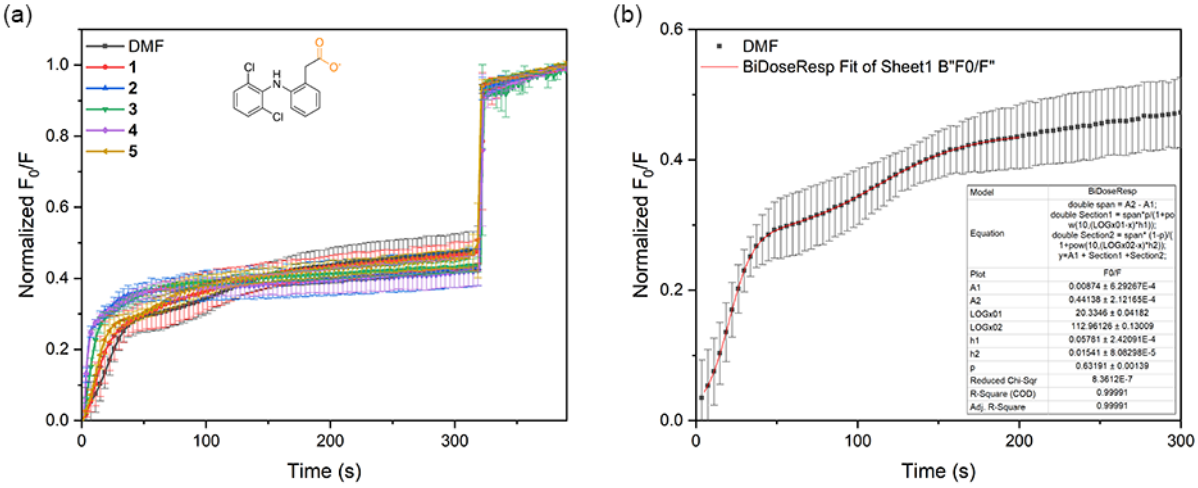

Figure S47. (a) Diclofenac transport mediated by compounds **1**-**5**. Experiment was performed as described in Section S3, and is the average of a minimum of 3 repeats (error bars represent standard deviations). DMF was used as a blank run (no transporter added) to assess background diclofenac permeability. Detergent was added around 310 seconds. (b) Graph showing the background permeability of diclofenac only (addition of DMF as a blank), indicating the bi-sigmoidal shape of the membrane permeability.

In the case of ibuprofen and ketoprofen, the addition of detergent did not lead to a stable F_0/F value. Instead, a continuous upwards drift is seen upon the addition of detergent (see **Figure S48**). A similar drift also appears to be present before the addition of detergent. To explain this observation, we conducted an experiment without liposomes. In this experiment, the fluorescence intensity (excitation 430 nm, emission 505 nm) of a solution of 0.8 µM lucigenin in nitrate buffer (222 mM $NaNO_3$, 10 mM HEPES, pH 7.4) was monitored for 400 seconds. After 10 seconds, sodium ibuprofen, sodium ketoprofen or sodium salicylate was added to achieve a final concentration of 25 mM drug; and after 200 seconds 10 µL Triton X-100 was added. The results are shown in **Figure S49**. It is normally expected that the fluorescence intensity upon the addition of carboxylate drug to lucigenin remains stable, as is observed in the case of sodium salicylate. There are no liposomes present and no kinetic events are expected (just quenching of lucigenin fluorescence). However, in the case of ibuprofen and ketoprofen, the fluorescence intensity is not stable, and shows a similar drift as observed during the transport experiments. The reason for this drift is not clear but could involve reactions between

ibuprofen/ketoprofen and lucigenin. Ibuprofen and ketoprofen can have photosensitization as a side effect due to their ability to photo-dissociate and generate radicals, which might explain the interaction with lucigenin.[8, 9] This unstable lucigenin reading in the presence of ketoprofen and ibuprofen prevents the calculation of accurate transport rates.

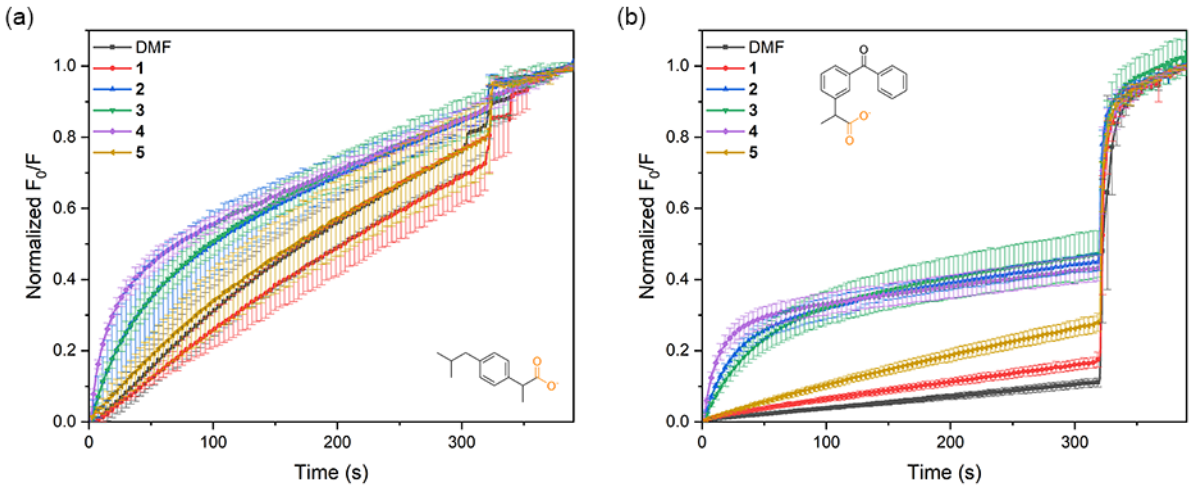

Figure S48. (a) Ibuprofen transport mediated by compounds **1**-**5**. Experiment was performed as described in Section S3, and is the average of a minimum of 3 repeats (error bars represent standard deviations). DMF was used as a blank run (no transporter added) to assess background ibuprofen permeability. (b) Ketoprofen transport mediated by compounds **1**-**5**. Experiment was performed as described in Section S3, and is the average of a minimum of 3 repeats (error bars represent standard deviations). DMF was used as a blank run (no transporter added) to assess background ketoprofen permeability. In both cases, detergent was added around 310 seconds and shows a 'drift' rather than a constant value.

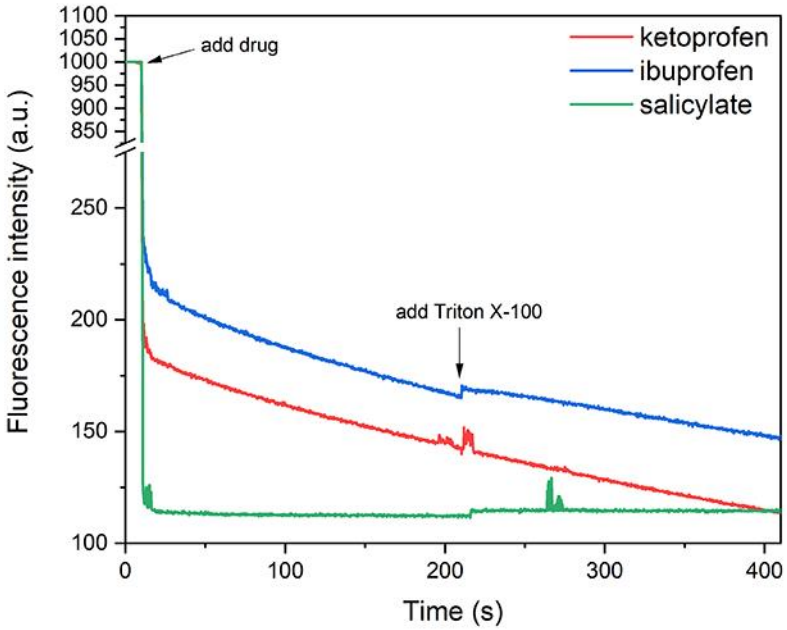

Figure S49. 'No liposome' experiment with ketoprofen, ibuprofen and salicylate. The fluorescence intensity (excitation 430 nm, emission 505 nm) of a solution of 0.8 µM lucigenin in nitrate buffer (222 mM $NaNO_3$, 10 mM HEPES, pH 7.4) was monitored for 400 seconds. After 10 seconds, sodium ibuprofen, sodium ketoprofen or sodium salicylate was added to achieve a final concentration of 25 mM drug; and after 200 seconds 10 µL Triton X-100 was added.

In the case of ramipril, a similar drift in the F_0/F value upon the addition of detergent was observed. In addition, normalized F_0/F values larger than 1 were observed for some of the transporters, which should not be possible (see **Figure S50a**). We therefore conducted the same 'no liposome' experiment as described for ibuprofen and ketoprofen. In this case, the fluorescence intensity upon the addition of ramipril is relatively stable, but starts to drift significantly when Triton X-100 is added to the solution (see **Figure S50b**). It is possible that this drift is due to partitioning of ramipril into the micelles generated by Triton X-100 (which can be a slow process). This might also explain the unusual transport profile of ramipril before the addition of detergent. It is possible that ramipril is quickly transported into the liposomes (resulting in a fast increase in normalized F_0/F), but then slowly partitions back into the membrane of the liposomes (resulting in a subsequent decrease in normalized F_0/F). Once again, these factors imply that accurate rates of transport cannot be obtained for ramipril.

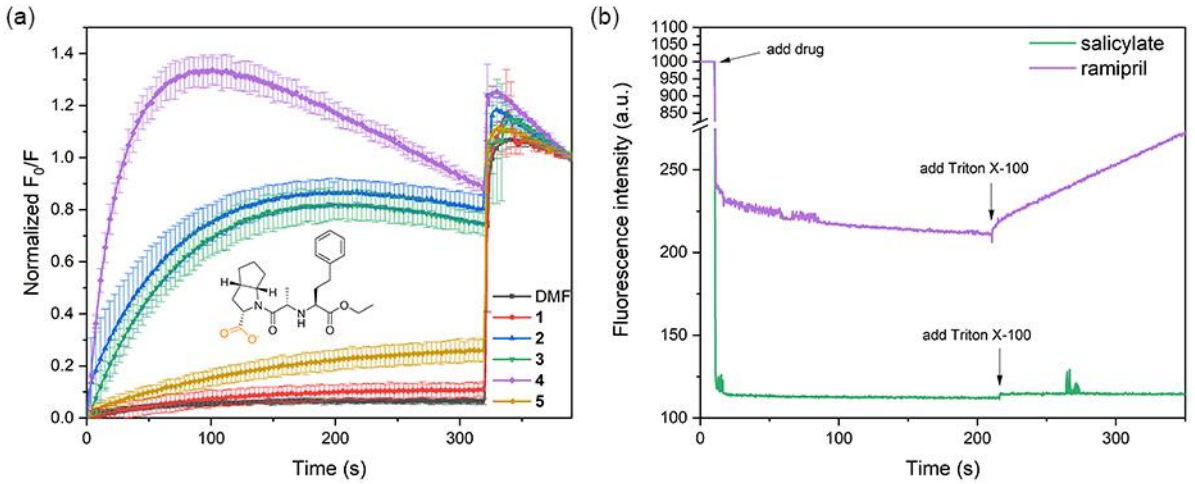

Figure S50. (a) Ramipril transport mediated by compounds **1**-**5**. Experiment was performed as described in Section S3, and is the average of a minimum of 3 repeats (error bars represent standard deviations). DMF was used as a blank run (no transporter added) to assess background diclofenac permeability. Detergent was added around 310 seconds. (b) 'No liposome' experiment with ramipril and salicylate. The fluorescence intensity (excitation 430 nm, emission 505 nm) of a solution of 0.8 µM lucigenin in nitrate buffer (222 mM $NaNO_3$, 10 mM HEPES, pH 7.4) was monitored for 400 seconds. After 10 seconds, sodium ramipril or sodium salicylate was added to achieve a final concentration of 25 mM drug; and after 200 seconds 10 µL Triton X-100 was added.

As a comparison, the 'no liposome' experiment was also repeated with all other drugs tested. As shown in **Figure S51**, most drugs show stable readings that remain constant throughout the experiment and do not show the extreme 'drifts' as seen for ibuprofen, ketoprofen and ramipril (ibuprofen, ketoprofen and ramipril are shown as bold lines, while all other drugs are shown as dotted lines).

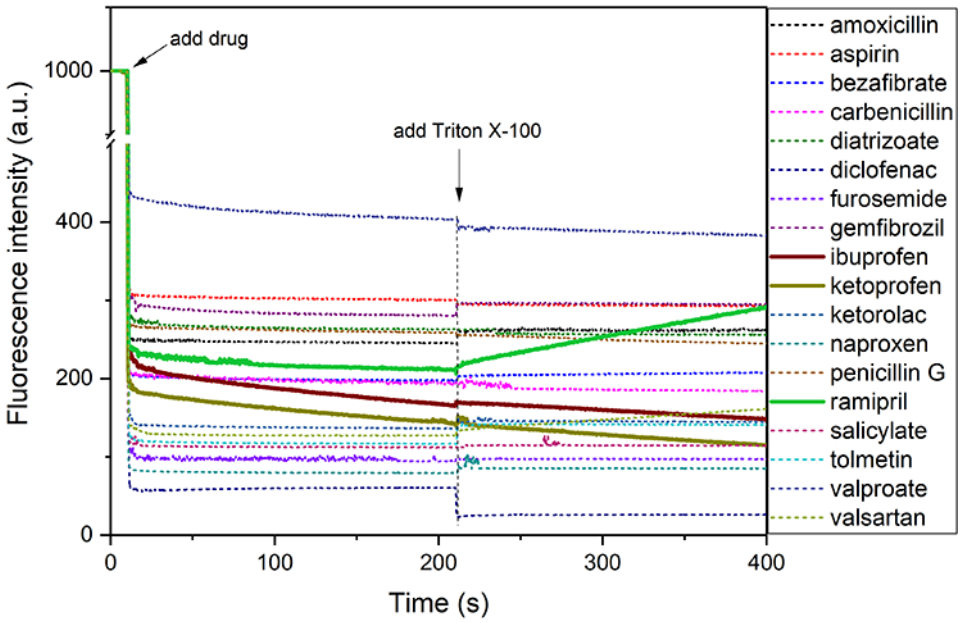

Figure S51. 'No liposome' experiment with all carboxylate drugs. The fluorescence intensity (excitation 430 nm, emission 505 nm) of a solution of 0.8 µM lucigenin in nitrate buffer (222 mM $NaNO_3$, 10 mM HEPES, pH 7.4) was monitored for 400 seconds. After 10 seconds, the sodium salt of the carboxylate drugs was added to achieve a final concentration of 25 mM drug; and after 200 seconds 35 µL Triton X-100 was added.

S4. HPLC traces and lipophilicity of drugs

HPLC traces were collected on a Thermo Fisher Scientific Vanquish Flex UHPLC with variable wavelength detector with ISQ EC Single Quadrupole Mass Spectrometer, using a Hypersil GOLD C18 column (150 mm length, 3.0 mm diameter, 3 µm particle size). 'Solvent A' was 0.1% (v/v) HCOOH in water and 'solvent B' was 0.1% (v/v) HCOOH in acetonitrile. Gradient was from 10% B to 90% B in 15 min, followed by 5 minutes at 90% B. The detection wavelength was set at 225 nm and the baseline was corrected by subtracting a blank solvent run. Valproic acid does not absorb at this wavelength, and the MS trace was used to determine the retention time. Drugs were dissolved in water before injecting into the UHPLC. Carbenicillin gives two peaks on HPLC, but MS indicated that both peaks correspond to carbenicillin (they are presumably the result of different protonation states, as carbenicillin is a di-carboxylic acid). The experiment was performed in triplicate and the obtained HPLC traces are shown in **Figure S52** - **Figure S69**. Experimental log*P* values could be found for some drugs on https://go.drugbank.com/.[10] These values correlate well with our HPLC retention times (**Figure S70**), and this plot was used to calculate semi-empirical log*P* values for all drugs using the equation *logP = -0.03157 + 0.37369*(retention time)*. The obtained values are summarized in **Table S2**.

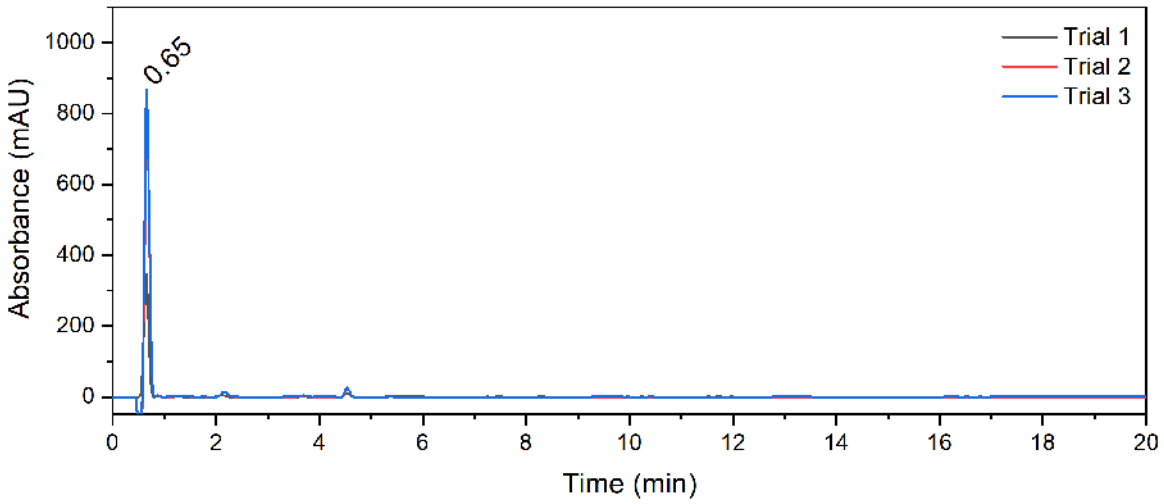

Figure S52. Reverse-phase HPLC of amoxicillin at 225 nm.

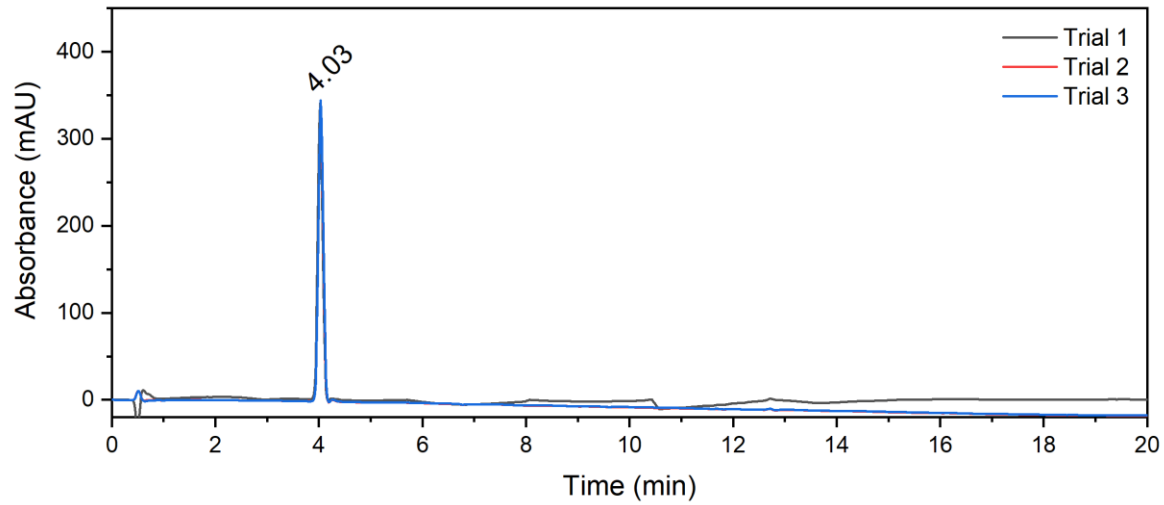

Figure S53. Reverse-phase HPLC of aspirin at 225 nm.

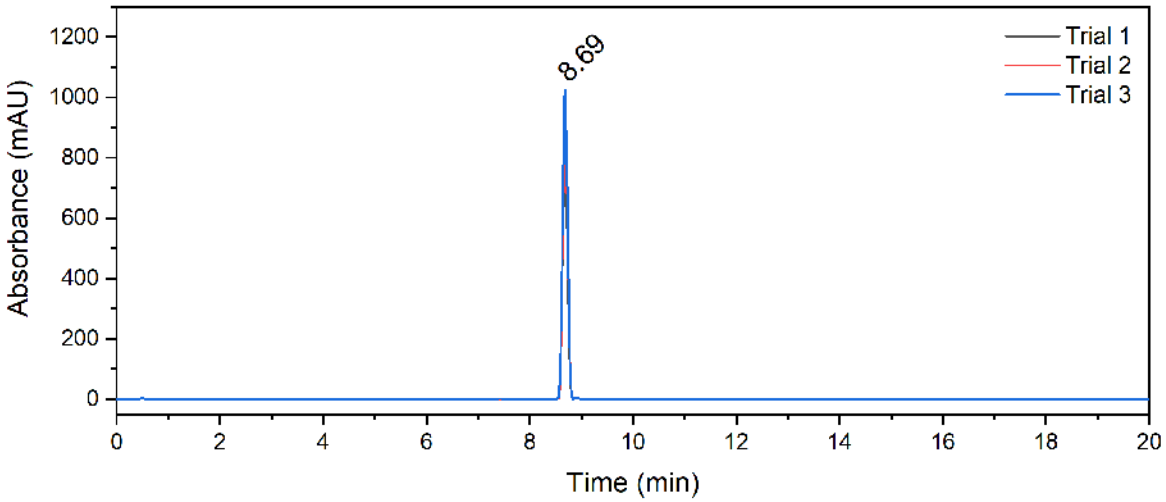

Figure S54. Reverse-phase HPLC of bezafibrate at 225 nm.

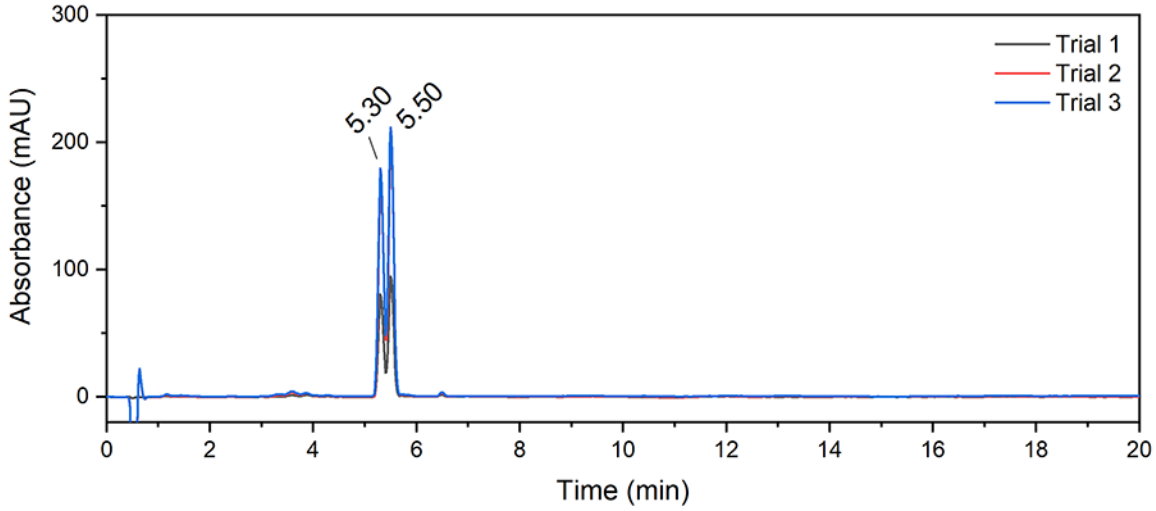

Figure S55. Reverse-phase HPLC of carbenicillin at 225 nm.

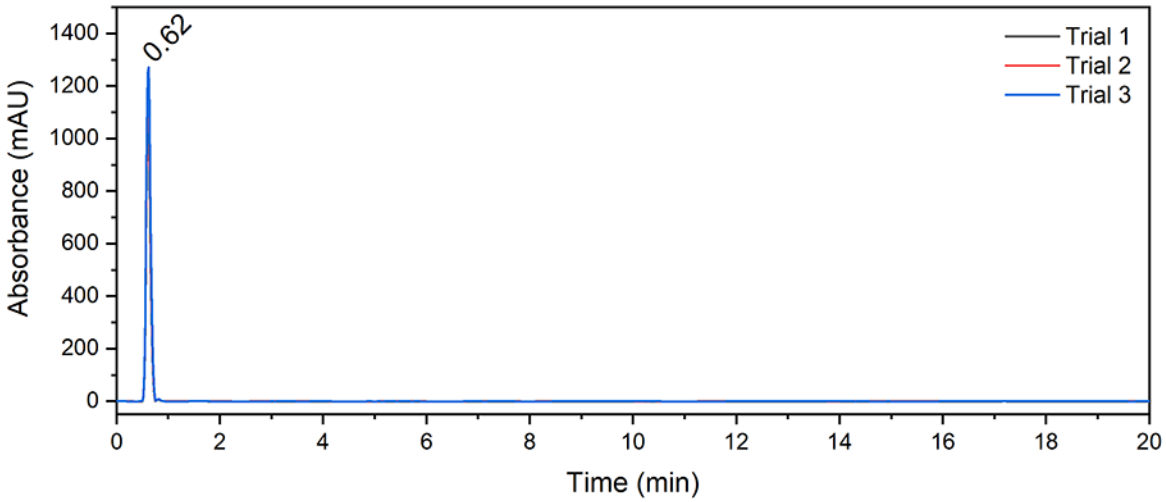

Figure S56. Reverse-phase HPLC of diatrizoate at 225 nm.

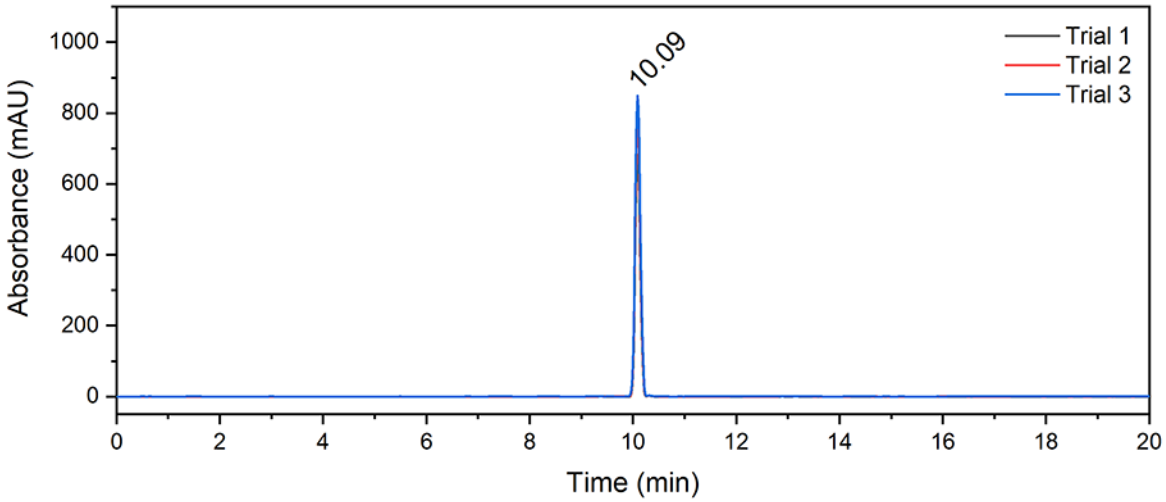

Figure S57. Reverse-phase HPLC of diclofenac at 225 nm.

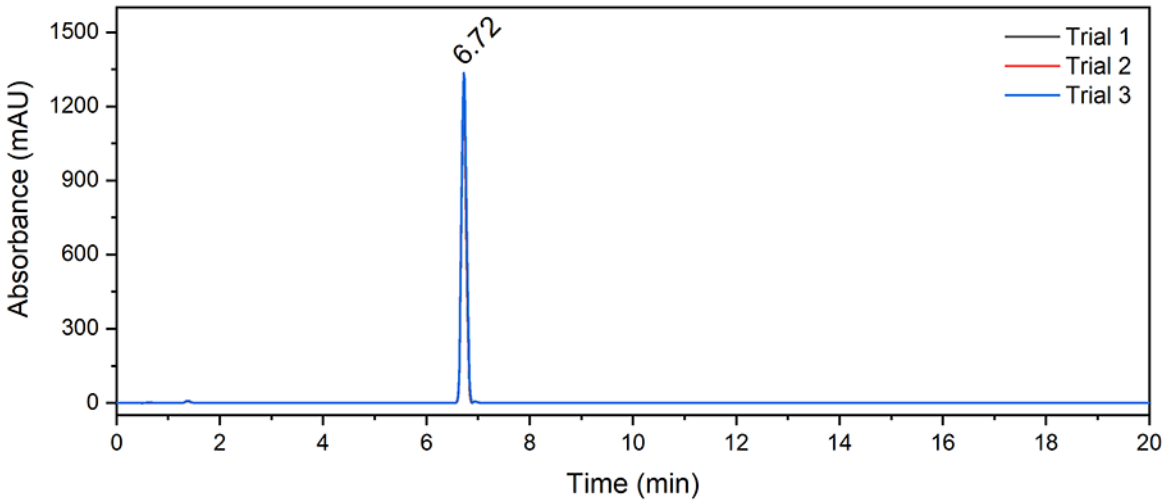

Figure S58. Reverse-phase HPLC of furosemide at 225 nm.

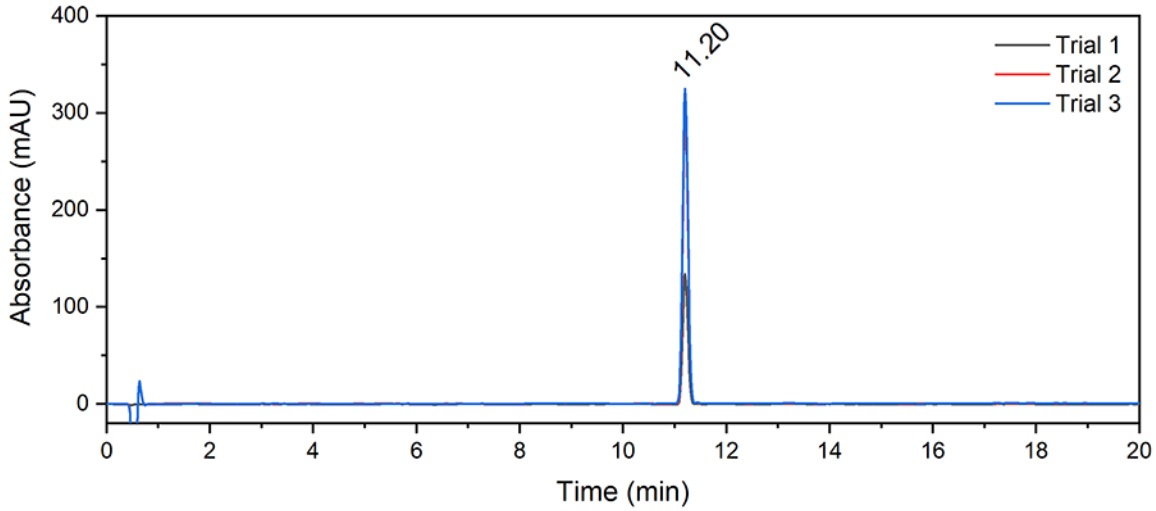

Figure S59. Reverse-phase HPLC of gemfibrozil at 225 nm.

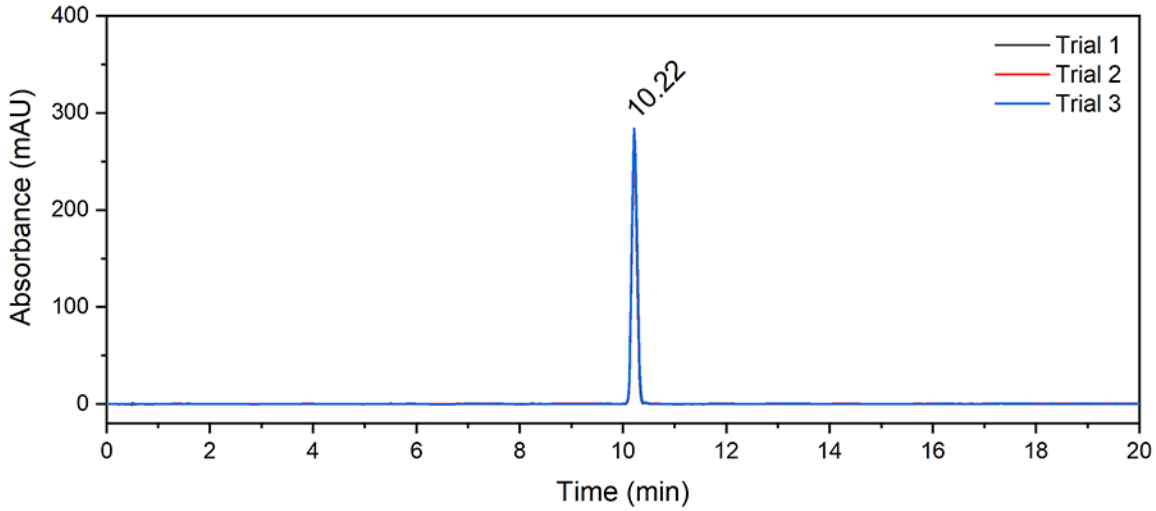

Figure S60. Reverse-phase HPLC of ibuprofen at 225 nm.

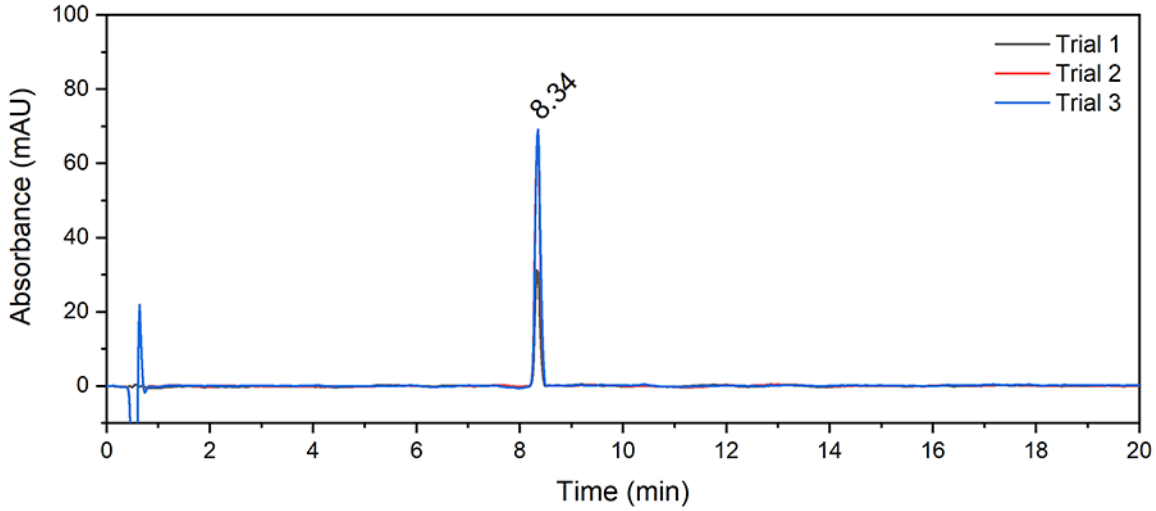

Figure S61. Reverse-phase HPLC of ketoprofen at 225 nm.

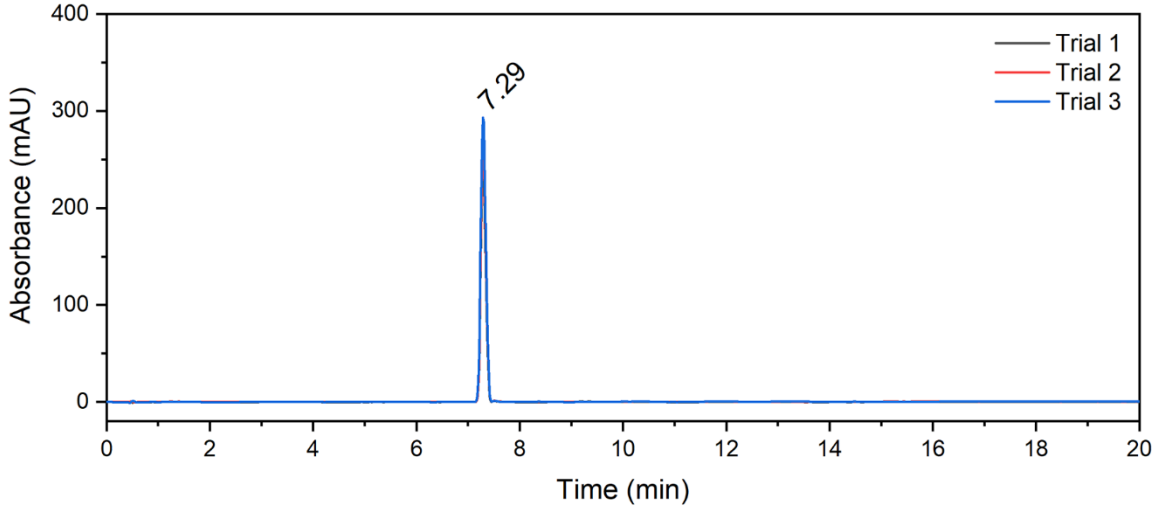

Figure S62. Reverse-phase HPLC of ketorolac at 225 nm.

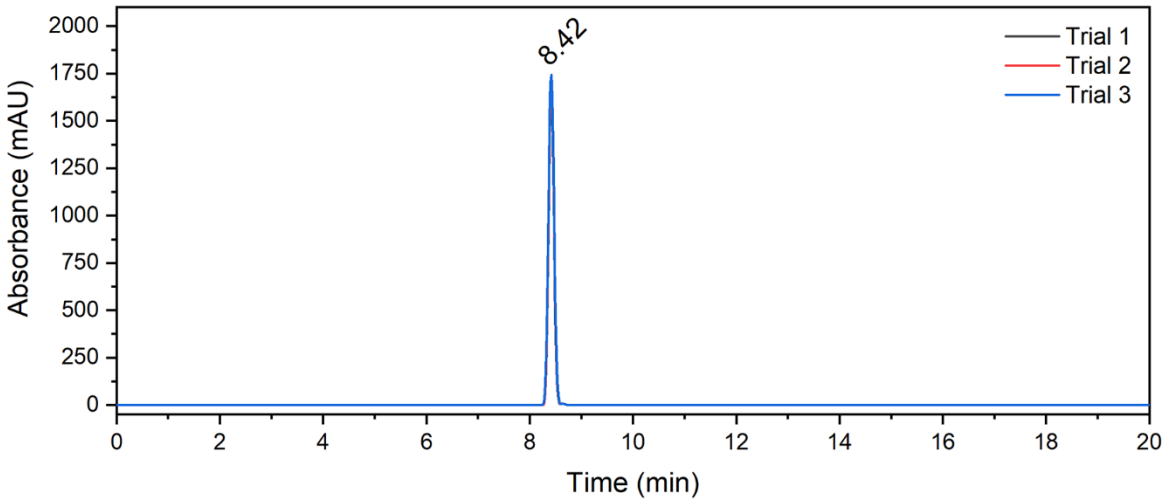

Figure S63. Reverse-phase HPLC of naproxen at 225 nm.

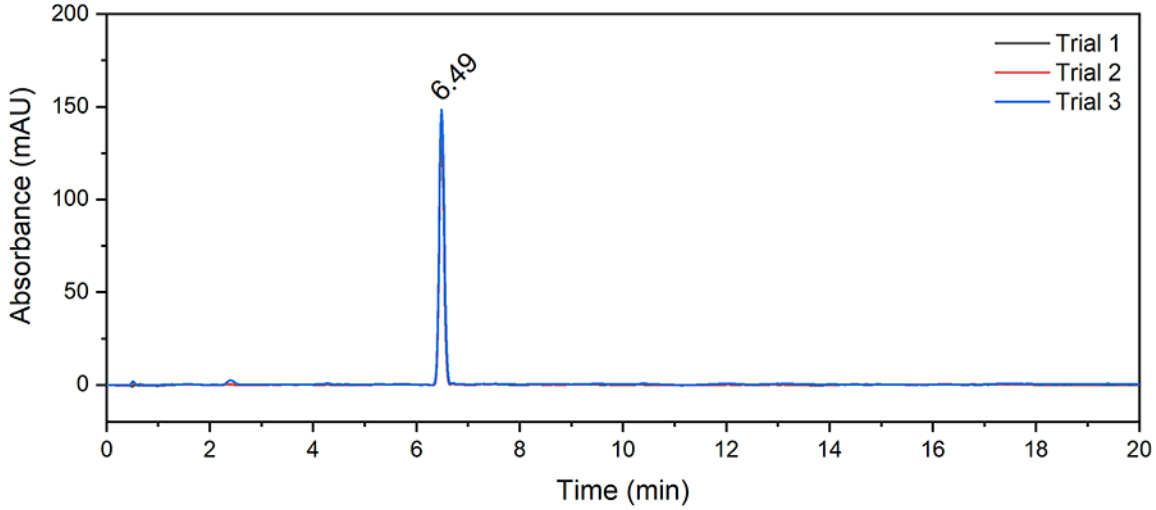

Figure S64. Reverse-phase HPLC of penicillin G at 225 nm.

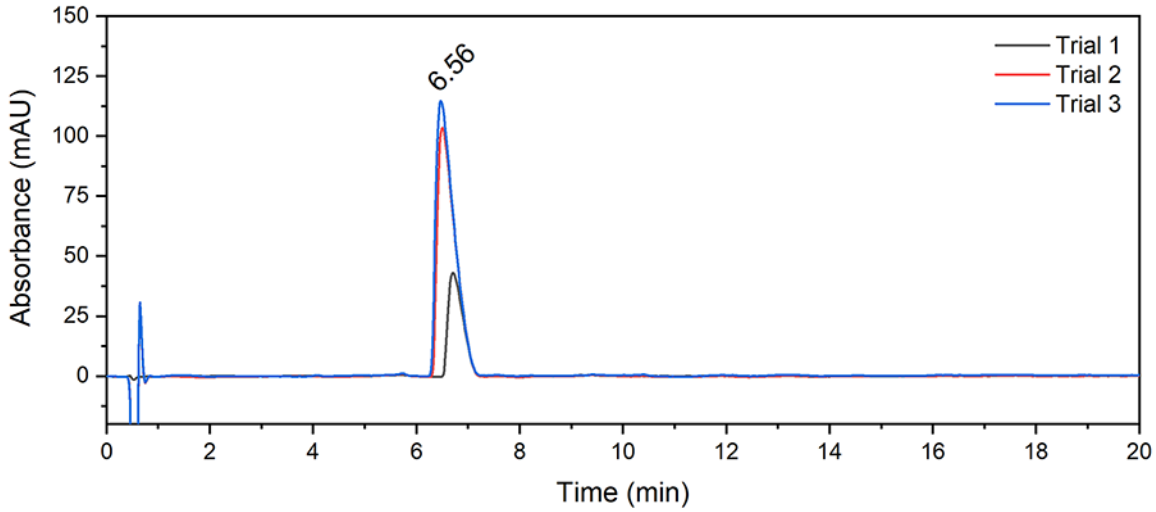

Figure S65. Reverse-phase HPLC of ramipril at 225 nm.

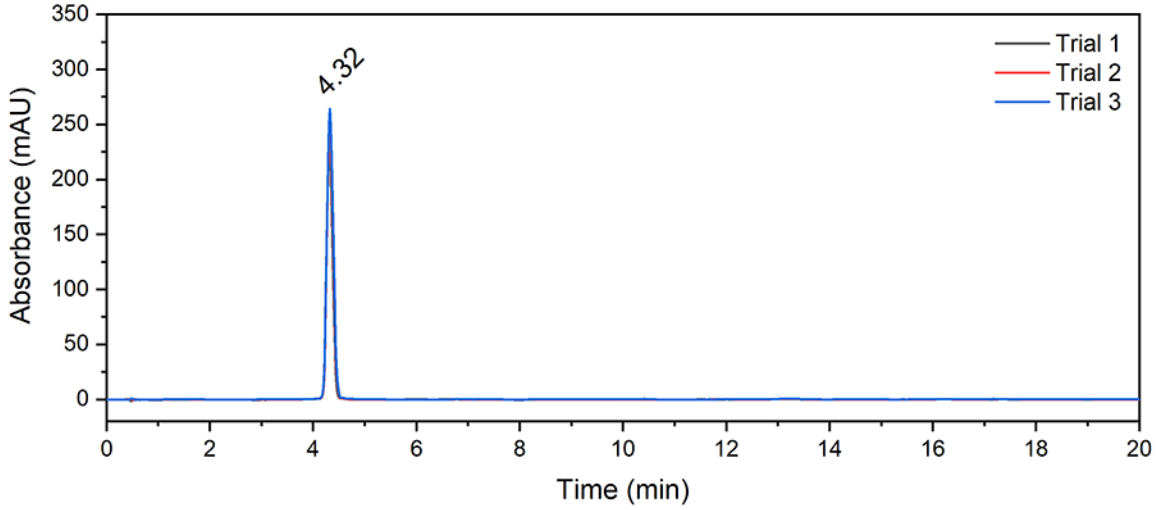

Figure S66. Reverse-phase HPLC of salicylate at 225 nm.

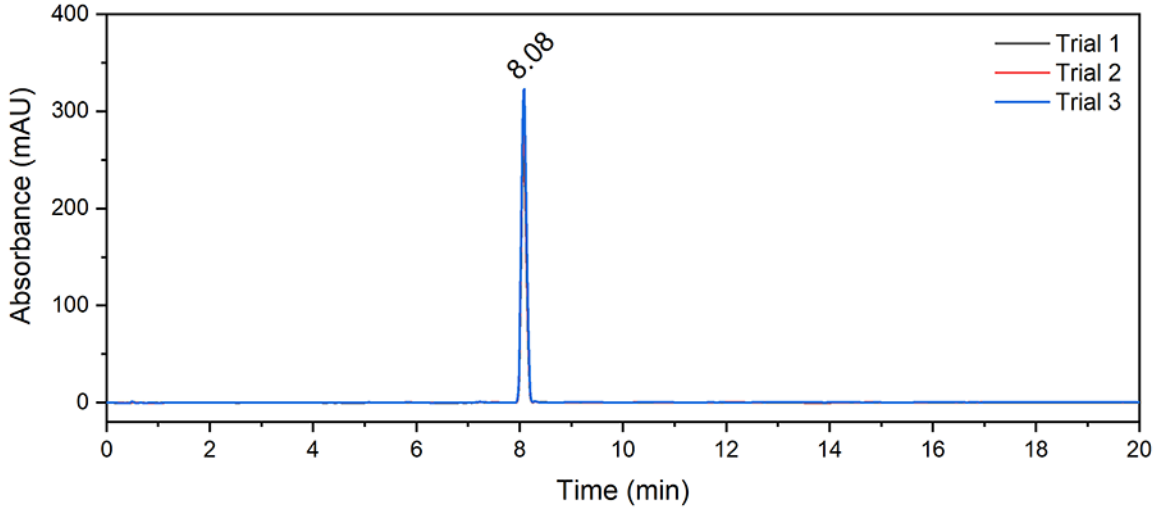

Figure S67. Reverse-phase HPLC of tolmetin at 225 nm.

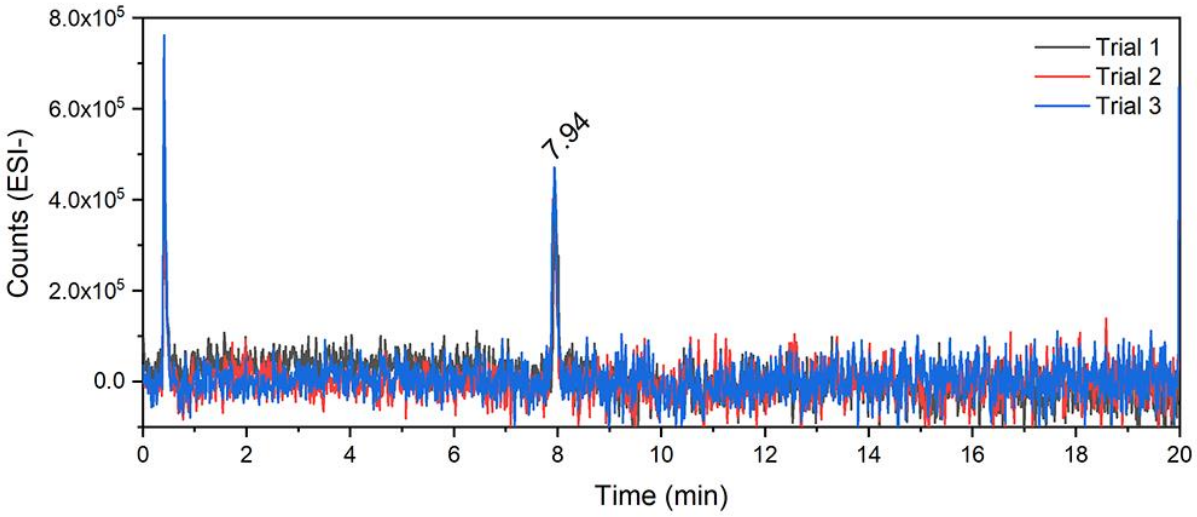

Figure S68. Reverse-phase HPLC of valproate, showing the MS (ESI-) trace.

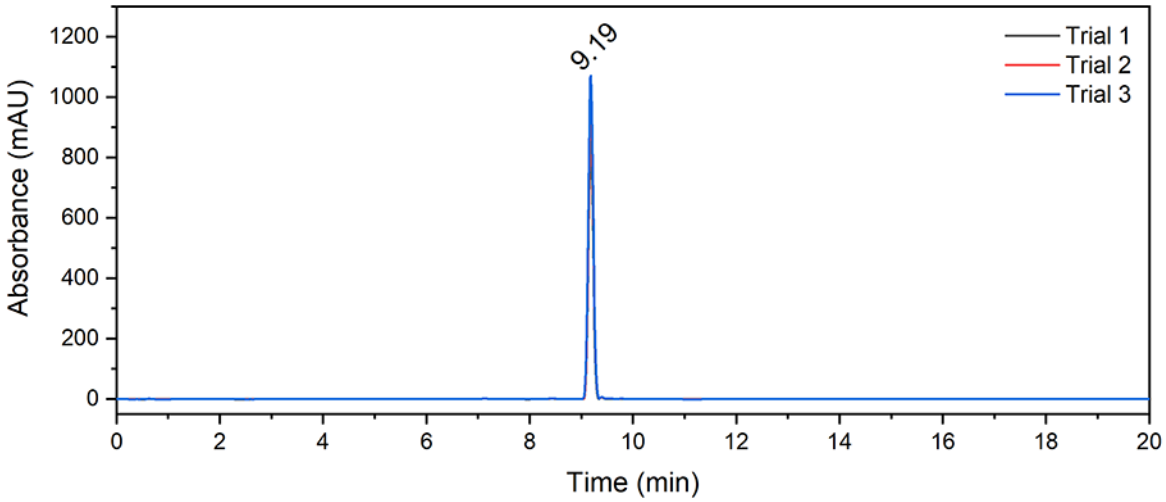

Figure S69. Reverse-phase HPLC of valsartan at 225 nm.

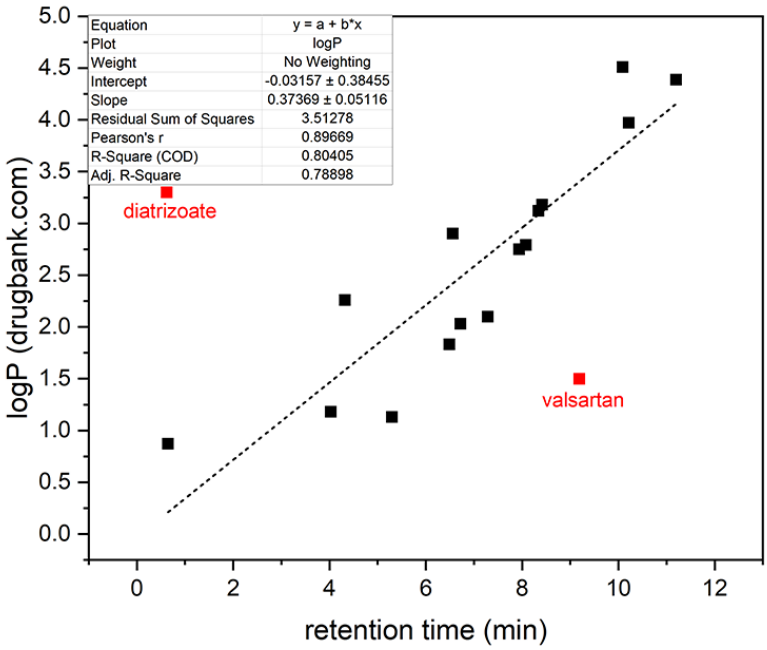

Figure S70. Experimental logP values for a selection of carboxylic acid containing drugs plotted against the experimental retention time on reverse-phase HPLC. The data points shown in red (diatrizoate and valsartan) were not included in the linear fit.

Table S2. Overview of the retention time on reverse-phase HPLC, experimental log*P* values obtained from Drugbank.com, and semi-empirical log*P* values calculated from the HPLC retention times.

Drug	HPLC retention time	log*P* (drugbank.com)	log*P* (semi-empirical)[a]
Amoxicillin	0.65	0.87	0.21
Aspirin	4.03	1.18	1.48
Bezafibrate	8.69	n/a[b]	3.21
Carbenicillin	5.3	1.13	1.95
Diatrizoate	0.62	3.3	0.20
Diclofenac	10.09	4.51	3.74
Furosemide	6.72	2.03	2.48
Gemfibrozil	11.2	4.387	4.16
Ibuprofen	10.22	3.97	3.79
Ketoprofen	8.34	3.12	3.09
Ketorolac	7.29	2.1	2.69
Naproxen	8.42	3.18	3.12
Penicillin G	6.49	1.83	2.39
Ramipril	6.56	2.9	2.42
Salicylate	4.32	2.26	1.58
Tolmetin	8.08	2.79	2.99
Valproate	7.94	2.75	2.94
Valsartan	9.19	1.499	3.40

[a] Semi-empirical logP values were calculated from the HPLC retention times using the equation obtained in ***Figure S70****. [b] No experimental logP value available on Drugbank.com.*

S5. Correlation of permeability enhancement and lipophilicity

The permeability enhancement induced by each transporter, was compared to the lipophilicity of the carboxylate drugs by plotting the semi-experimental log*P* value (see Section S4) against the permeability enhancement of the drug. The obtained graphs are given in **Figure S71-Figure S75**.

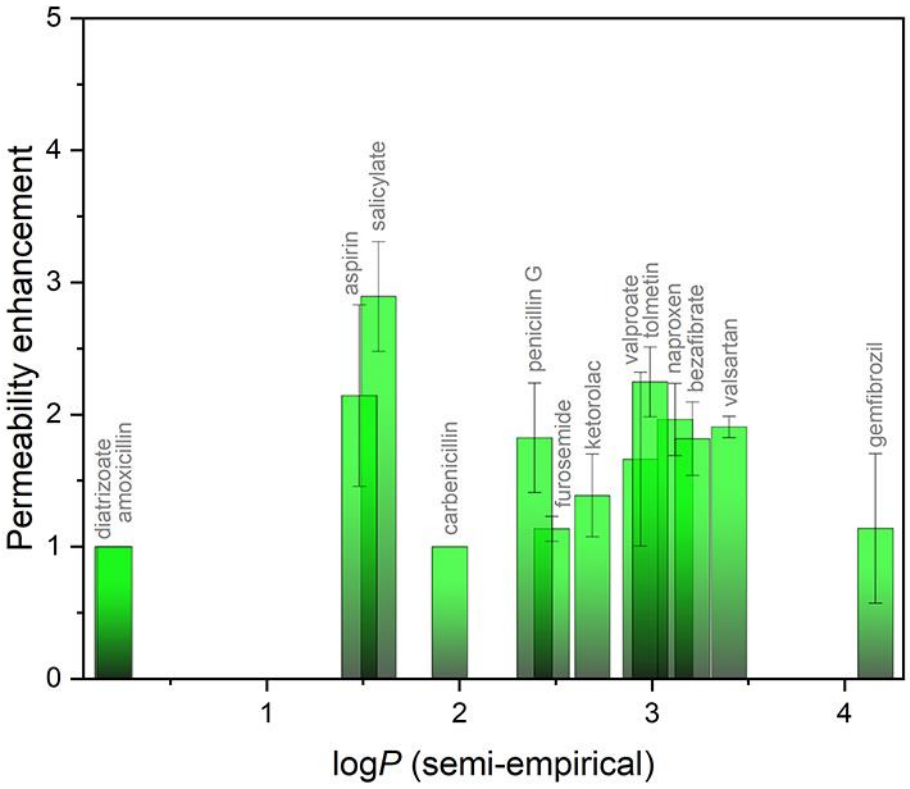

Figure S71. Enhancement of the permeability of different carboxylate drugs induced by compound **1**, as a function of the log*P* of the carboxylate drug.

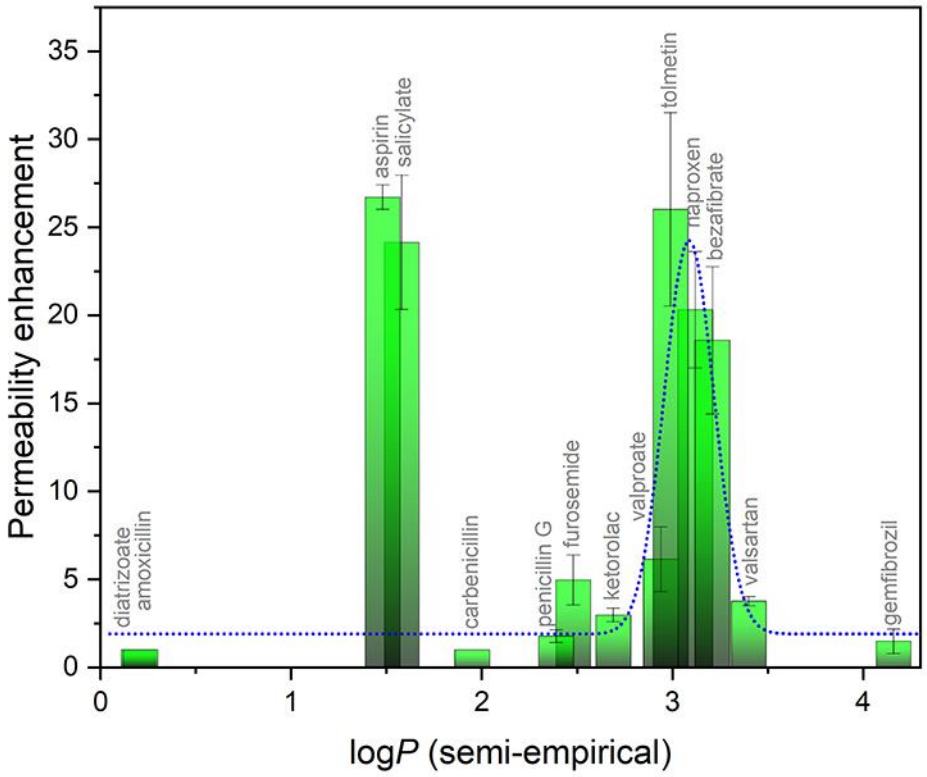

Figure S72. Enhancement of the permeability of different carboxylate drugs induced by compound **2**, as a function of the log*P* of the carboxylate drug.

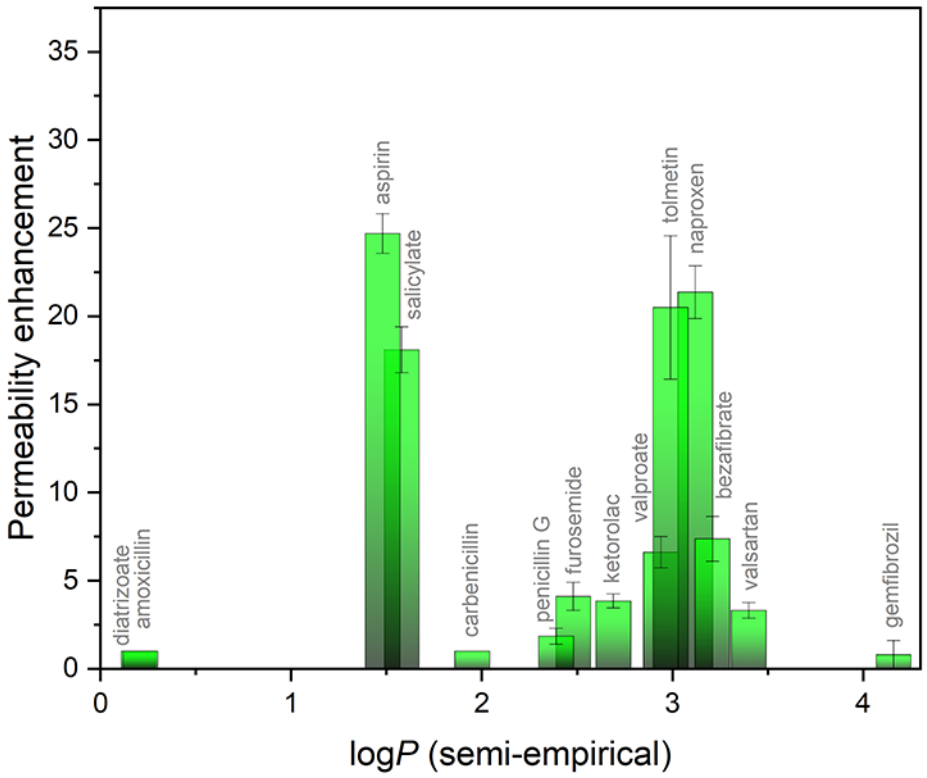

Figure S73. Enhancement of the permeability of different carboxylate drugs induced by compound **3**, as a function of the log*P* of the carboxylate drug.

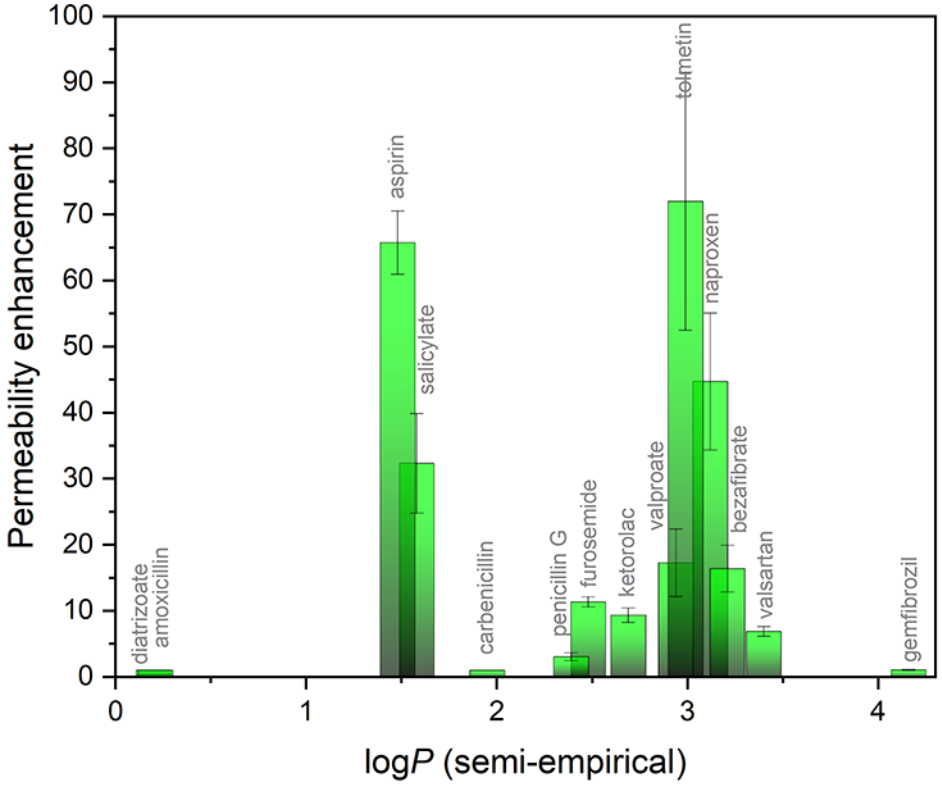

Figure S74. Enhancement of the permeability of different carboxylate drugs induced by compound **4**, as a function of the log*P* of the carboxylate drug.

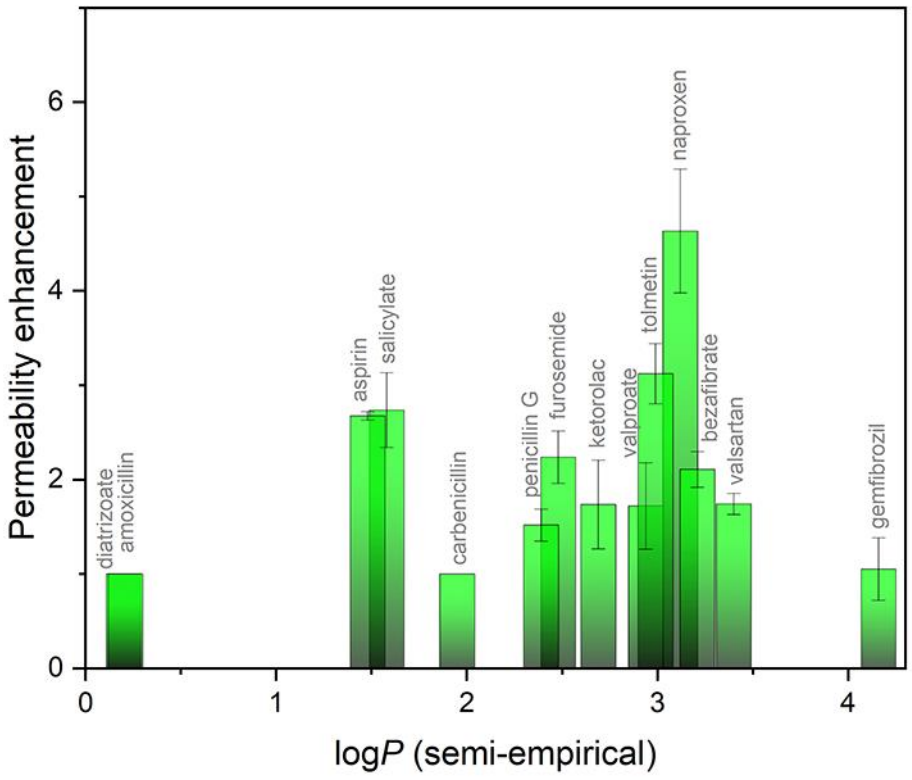

Figure S75. Enhancement of the permeability of different carboxylate drugs induced by compound **5**, as a function of the log*P* of the carboxylate drug.

S6. Valinomycin-mediated salicylate uniport

In the assays described above, the transport of the carboxylate drug causes a charge gradient across the membrane, that is presumably dissipated through the transport of nitrate anions out of the liposome (antiport). This antiport mechanism is unlikely to occur in biological systems, due to the low concentration of nitrate in cells.[11] It is more likely that the charge gradient created through transport of anionic drugs is compensate by the various ion channel proteins in the cell membrane. This requires that compounds **1**-**5** have to be able to perform electrogenic uniport of the carboxylate drugs in biological systems, whereby the charge gradient is dissipated through a separate uniport event induced by a separate ion transporter. To test this possibility, we performed a valinomycin-based assay similar to the assay established to assess chloride uniport.[12] In this assay, we employ the known K^+ uniport ability of valinomycin to help dissipate the charge gradient that would be created by carboxylate drug transport. Preparation of large unilamellar vesicles (LUVs), experimental procedure of the kinetic drug transport assay and data work-up were the same as described in Sections S3.1-S3.3, except that Na^+ was replaced with K^+, and NO_3^- with SO_4^{2-}. Thus, the employed buffer consisted of a K^+-based 10 mM HEPES buffer at pH 7.4, with 75 mM K_2SO_4. The assay was performed with potassium salicylate (25 mM) to study the uniport of salicylate as a model carboxylate drug. Transporter concentrations were the same as for the previous assays (5 mol% **1**, 5 mol% **2**, 0.01 mol% **3**, 0.05 mol% **4**, and 5 mol% **5**), and 5 mol% **3** and 5 mol% **4** were also tested. The concentration of valinomycin was set to 0.000025 mol% with respect to total lipid.

The results are shown in **Figure S76-Figure S80**. Each graph represents the uniport of salicylate by one transporter by comparing the salicylate permeability in the absence of transporter (DMF), in the presence of only urea-based transporters, in the presence of only valinomycin, and in the presence of both a urea-based transporter and valinomycin. Evidence of uniport is seen by the cooperative salicylate transport by a combination of a urea-based transporter and valinomycin (*i.e.* transport induce by a combination of urea-based transporter and valinomycin is greater than the sum of the transport induced by only urea-based transporter and only valinomycin). In all cases, the addition of urea-based transporter alone, or the addition of valinomycin alone caused a minimal increase in the permeability of salicylate. However, the combinations **2**-valinomycin, **3**-valinomycin, **4**-valinomycin and **5**-valinomycin caused a noticeable increase in salicylate membrane permeability, suggesting that transporters **2-5** are able to mediate electrogenic carboxylate drug uniport.

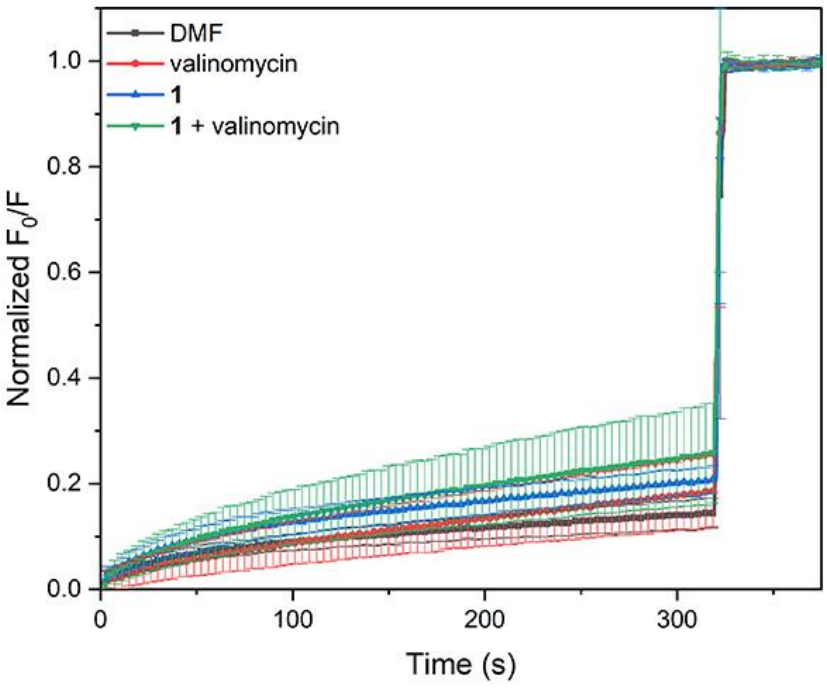

Figure S76. Uniport of salicylate mediated by compound **1**. Fraction of drug transported by 5 mol% **1**, 0.000025 mol% valinomycin, or the combination of 5 mol% **1** and 0.000025 mol% valinomycin across 100 nm 7:3 eggPC:cholesterol LUVs loaded with 1 mM lucigenin, 75 mM K_2SO_4, 10 mM HEPES buffer at pH 7.4. DMF was used as a blank run (no transporter). Results are the average of 3 independent repeats and error bars represent standard deviations.

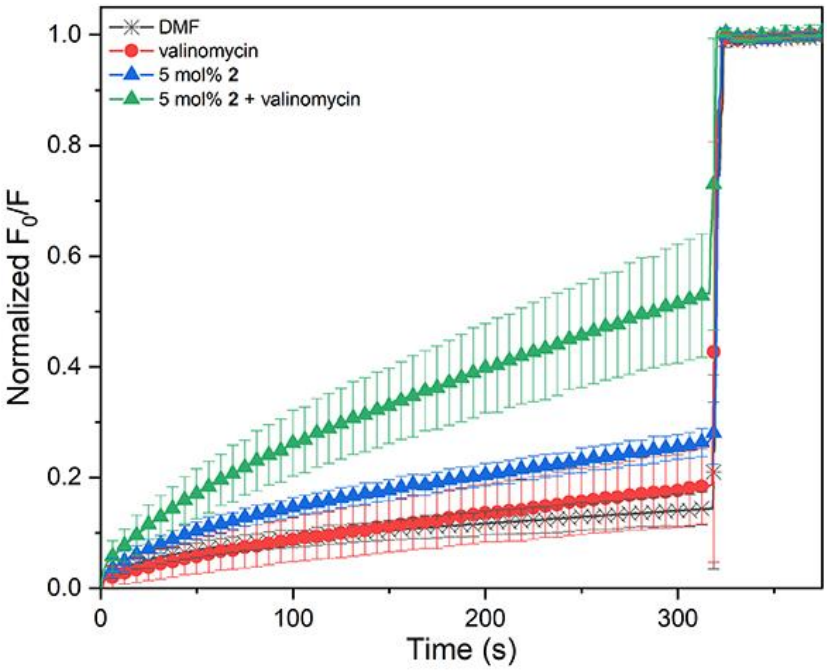

Figure S77. Uniport of salicylate mediated by compound **2**. Fraction of drug transported by 5 mol% **2**, 0.000025 mol% valinomycin, or the combination of 5 mol% **2** and 0.000025 mol% valinomycin across 100 nm 7:3 eggPC:cholesterol LUVs loaded with 1 mM lucigenin, 75 mM K_2SO_4, 10 mM HEPES buffer at pH 7.4. DMF was used as a blank run (no transporter). Results are the average of 3 independent repeats and error bars represent standard deviations.

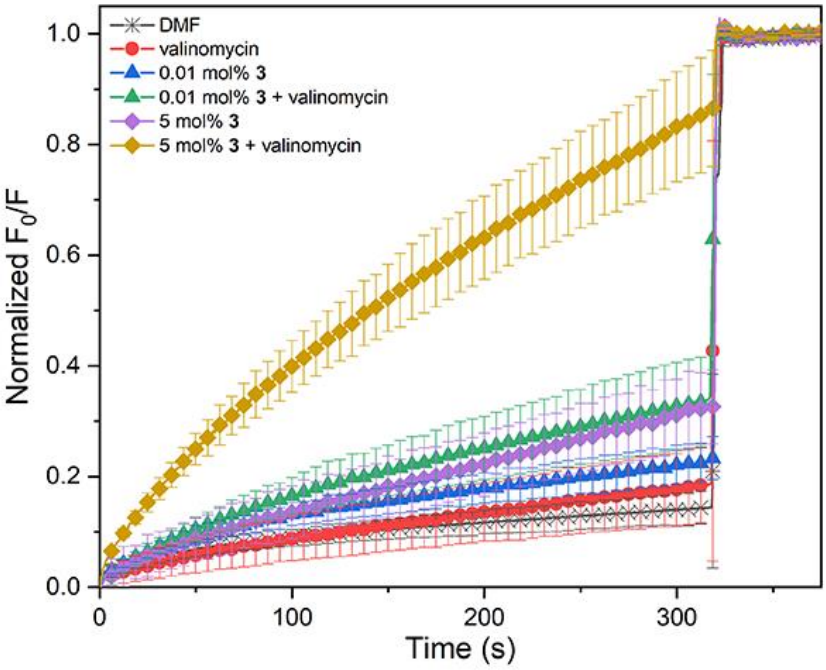

Figure S78. Uniport of salicylate mediated by compound **3**. Fraction of drug transported by 0.01 mol% **3,** 5 mol% **3**, 0.000025 mol% valinomycin, the combination of 0.01 mol% **3** and 0.000025 mol% valinomycin, or the combination of 5 mol% **3** and 0.000025 mol% valinomycin across 100 nm 7:3 eggPC:cholesterol LUVs loaded with 1 mM lucigenin, 75 mM K_2SO_4, 10 mM HEPES buffer at pH 7.4. DMF was used as a blank run (no transporter). Results are the average of 3 independent repeats and error bars represent standard deviations.

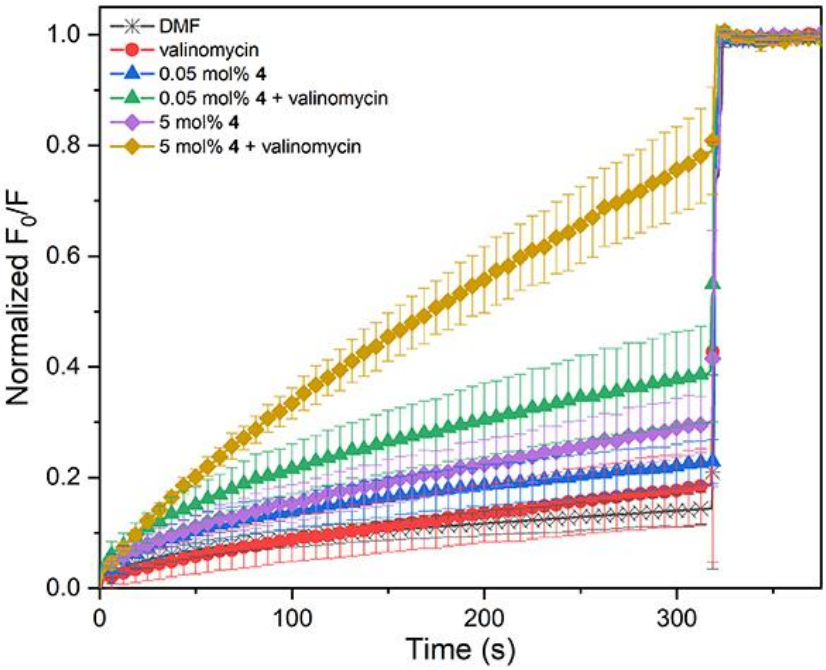

Figure S79. Uniport of salicylate mediated by compound **4**. Fraction of drug transported by 0.05 mol% **4**, 5 mol% **4**, 0.000025 mol% valinomycin, the combination of 0.05 mol% **4** and 0.000025 mol% valinomycin, or the combination of 5 mol% **4** and 0.000025 mol% valinomycin across 100 nm 7:3 eggPC:cholesterol LUVs loaded with 1 mM lucigenin, 75 mM K_2SO_4, 10 mM HEPES buffer at pH 7.4. DMF was used as a blank run (no transporter). Results are the average of 3 independent repeats and error bars represent standard deviations.

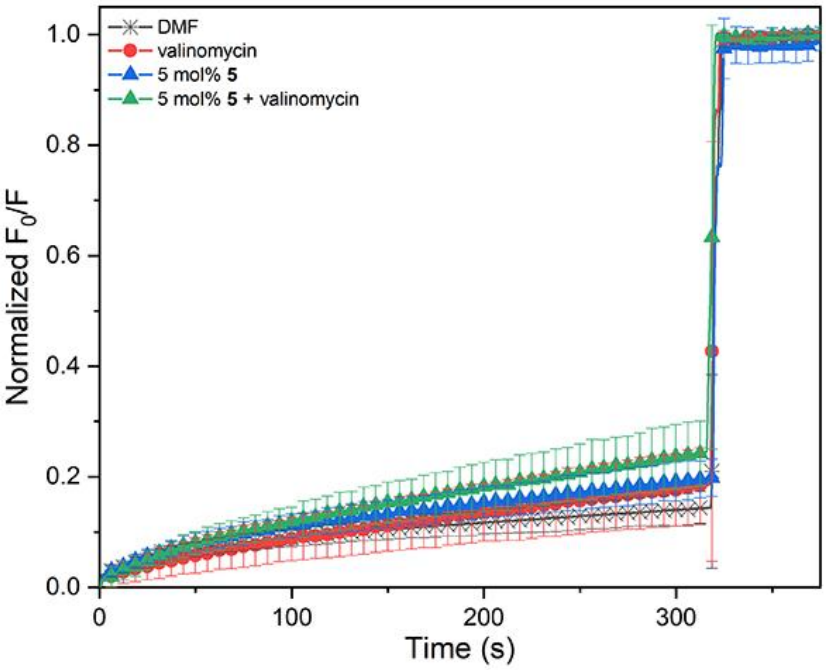

Figure S80. Uniport of salicylate mediated by compound **5**. Fraction of drug transported by 5 mol% **5**, 0.000025 mol% valinomycin, or the combination of 5 mol% **5** and 0.000025 mol% valinomycin across 100 nm 7:3 EggPC:cholesterol LUVs loaded with 1 mM lucigenin, 75 mM K_2SO_4, 10 mM HEPES buffer at pH 7.4. DMF was used as a blank run (no transporter). Results are the average of 3 independent repeats and error bars represent standard deviations.

S7. References

1. B. A. McNally, A. V. Koulov, B. D. Smith, J.-B. Joos and A. P. Davis, *Chem. Commun.*, 2005, 1087-1089.
2. G. van Meer, D. R. Voelker and G. W. Feigenson, *Nat. Rev. Mol. Cell Biol.*, 2008, **9**, 112-124.
3. J. L. Sampaio, M. J. Gerl, C. Klose, C. S. Ejsing, H. Beug, K. Simons and A. Shevchenko, *Proc. Natl. Acad. Sci. U. S. A.*, 2011, **108**, 1903.
4. M. J. Gerl, J. L. Sampaio, S. Urban, L. Kalvodova, J.-M. Verbavatz, B. Binnington, D. Lindemann, C. A. Lingwood, A. Shevchenko, C. Schroeder and K. Simons, *J. Cell Biol.*, 2012, **196**, 213-221.
5. S. R. Marshall, A. Singh, J. N. Wagner and N. Busschaert, *Chem. Commun.*, 2020, **56**, 14455-14458.
6. L. M. Lichtenberger, Z. M. Wang, J. J. Romero, C. Ulloa, J. C. Perez, M. N. Giraud and J. C. Barreto, *Nat. Med.*, 1995, **1**, 154-158.
7. C. Pereira-Leite, S. K. Jamal, J. P. Almeida, A. Coutinho, M. Prieto, I. M. Cuccovia, C. Nunes and S. Reis, *Mol. Pharmacol.*, 2020, **97**, 295.
8. E. Bignon, M. Marazzi, V. Besancenot, H. Gattuso, G. Drouot, C. Morell, L. A. Eriksson, S. Grandemange, E. Dumont and A. Monari, *Scientific Reports*, 2017, **7**, 8885.
9. S. Okazaki, A. Hirata, Y. Shogomori, M. Takemoto, T. Nagata, E. Hayashida and K. Takeshita, *J. Photochem. Photobiol., B*, 2021, **214**, 112090.
10. D. S. Wishart, C. Knox, A. C. Guo, S. Shrivastava, M. Hassanali, P. Stothard, Z. Chang and J. Woolsey, *Nucleic Acids Res.*, 2006, **34**, D668-672.
11. D. J. Stuehr and M. A. Marletta, *Proc. Natl. Acad. Sci. U. S. A.*, 1985, **82**, 7738.
12. X. Wu, Luke W. Judd, Ethan N. W. Howe, Anne M. Withecombe, V. Soto-Cerrato, H. Li, N. Busschaert, H. Valkenier, R. Pérez-Tomás, David N. Sheppard, Y.-B. Jiang, Anthony P. Davis and Philip A. Gale, *Chem*, 2016, **1**, 127-146.